DIGITALCOMMONS
—@WAYNESTATE—

Wayne State University

Wayne State University Dissertations

1-1-2011

Identification, state estimation, and adaptive control of type i diabetic patients

Ali Mohamad Hariri
Wayne State University,

Follow this and additional works at: http://digitalcommons.wayne.edu/oa_dissertations

Part of the Electrical and Computer Engineering Commons

Recommended Citation

IDENTIFICATION, STATE ESTIMATION, AND ADAPTIVE CONTROL OF TYPE 'I'
DIABETIC PATIENTS

by

ALI MOHAMAD HARIRI

DISSERTATION

Submitted to the Graduate School

of Wayne State University,

Detroit, Michigan

in partial fulfillment of the requirements

for the degree of

DOCTOR OF PHILOSOPHY

2012

MAJOR: ELECTRICAL ENGINEERING

Approved by:

_____

Advisor   Date

_____

_____

_____

_____

DEDICATION

To my parents

my wife

and my family

ACKNOWLEDGEMENTS

There are several people who deserve my heartfelt thanks for their generous contributions and support to this dissertation. First of all, I would like to express my sincere appreciation to my respectful advisor, Professor Le Yi Wang, for his directions, suggestions, corrections, supervision and support from the preliminary to the concluding level that enabled me to develop an understanding of the subject. Without his guidance, I do not believe this thesis would have been completed. Professor Wang's dedication and flexibility is what made it possible for me to succeed. He was always there when I needed his advice, even after hours and outside university. Also, I would like to thank my dissertation committee: Professor Ece Yaprak, Professor Harpreet Singh and Professor Pepe Siy for their helpful comments and encouragement. I must express my gratitude and deep appreciation to Dr. Eid Al-Radadi whose friendship, hospitality, knowledge have supported, enlightened, and entertained me over the many years of our friendship.

Many thanks go to my father and my brothers and sisters for their moral support and encouragement. My lovely daughters, Rana, Rola, Nour and Manar, also deserve a lot of appreciation for their patience and support.

Last but not least, I would like to thank my encouraging and supportive wife, Hikmat Hallal, whose faithful support during all phases of this PhD deserves my sincere appreciation for her patience and loving affirmative. Words fail me to express my appreciation to her whose dedication, love and persistent confidence in me, has taken the load off my shoulder. Without her support, it would have been impossible to complete this PhD.

TABLE OF CONTENTS

LIST OF TABLES

LIST OF FIGURES

CHAPTER 1

GENERAL INTRODUCTION

1.1   Introduction:

During the last few decades, control technology has been applied in a wide variety of systems such as medical, biomedical, industrial and other fields that require monitoring and adjusting the input of a system to get the desired output. Also, control technology has been utilized to improve the performance of different types of systems. Diabetes is one of the very important medical problems that needs to be addressed. The insulin infusion rate to the diabetic person can be administrated based on the glucose (sugar) level inside the body. Over the years, many mathematical models have been developed to describe the glucose insulin system of the human being. The most commonly used model is the minimal model introduced by Bergman. The minimal model consists of a set of three differential equations with unknown parameters. Since diabetic patients differ dramatically due to the deviation of their physiology and pathology characteristics, the parameters of the minimal model are significantly different among patients.

Most of the existing techniques assume the system to be time-invariant, and the original minimal model was modified by deleting some important parameters. The aim of this research is to design a new control scheme that uses the original minimal model to enhance the performance of the system and meet the design specifications. The other aim is to estimate the unknown parameters of the differential equations that describe the dynamic of a diabetic person. An automatic first order pump, P, will be added to automatically inject the required quantity of the insulin into the diabetic patient to bring down the glucose level to the neighborhood of the basal level.

1.2   Background of Diabetes:

Diabetes is a problem with the body's fuel system; it is caused by lack of insulin in the body. The human body maintains an appropriate level of insulin. There are two major types of diabetes, called type 'I' and type 'II' diabetes. Type 'I' diabetes is called Insulin Dependent Diabetes Mellitus (IDDM), or Juvenile Onset Diabetes Mellitus (JODM). Type 'II' diabetes is known as Non-Insulin Dependent Diabetes Mellitus (NIDDM) or Adult-Onset Diabetes (AOD) [1-7]. This study focuses on type 'I' diabetes. Type 'I' diabetes is a disease that develops when the pancreas stops producing the required amount of insulin that is needed to control the glucose level. Consequently, insulin must be provided through injection or continuous infusion to control glucose levels.

1.3   Problem Formulation:

Many mathematical models have been developed to describe the glucose-insulin system. The aim is to analyze and study the original nonlinear minimal model to bring the glucose level to the neighborhood of the basal level and to regulate the blood glucose level in type 'I' diabetic patients by controlling the insulin infusion rate, that is, produce an "artificial pancreas". A fourth differential equation will be added to the set of the minimal model equations to represent a first order pump 'P'. The role of pump 'P' is to inject the insulin into the system. The fourth differential equation is defined as

$$\dot{w}(t) = \frac{1}{a}\left(-w(t) + u(t)\right) \tag{1.1}$$

where $w(t)$ is the infusion rate, $u(t)$ is the input command, and a is the time constant of the pump.

1.4   Problem Statement:

The first goal of this research is to obtain the estimation of the unknown parameters of the four differential equations that describe the dynamic relationship between the glucose and the insulin. The Least Square method for nonlinear system with the Levenberg-Marquadrt Algorithm will be used. The second goal is to design feedback controller(s) to regulate(s) the infusion rate of the insulin inside the diabetic patient and to bring down the glucose level to neighborhood of the basal level with a short period of time using the nonlinear minimal model.

1.5   Dissertation Organization:

This dissertation is organized as the following

Chapter two: This research presents some background and literature overviews. These overviews will be about diabetes and the importance of this problem.

Chapter three: This chapter introduces the simplest physiologically based representation of diabetic patients and explains the mathematical model.

Chapter four: In this chapter, a simulation diagram is introduced to study and simulate the mathematical model that describes the dynamics of diabetic patients.

Chapter five: The Nonlinear Least Square Method with the Levenberg-Margaurdt Algorithm is introduced to estimate the unknown parameters of the differential equations that describe the diabetic patient.

Chapter six: This chapter explains the differential equation that represents the first order pump and introduces the proposed mathematical model and its implementation.

Chapter seven: This chapter presents a new technique called Low-Complexity Regime-Switching control scheme that uses adaptation strategy to enhance the system performance and meet the design specifications.

Chapter eight: This chapter investigates the patient model and presents a simplified control scheme using observer-based state feedback controller. Also, it shows that the new control scheme can eliminate the adaptation strategy.

Chapter nine: The conclusion is presented in this chapter. Also, this chapter has a summary of contributions and achieved results of this research.

CHAPTER 2

DIABETES LITERATURE OVERVIEW

2.1   Introduction:

Insulin is a hormone that is necessary for converting the blood sugar, or glucose, into usable energy. The human body maintains an appropriate level of insulin. The lifestyles of type 'I' diabetes are often severely affected by the consequences of the disease. Because the insulin producing B-cells of the pancreas is destroyed, patients typically regulate glucose manually. The patient is totally dependent on an external source of insulin to be infused at an appropriate rate to maintain blood glucose concentration. Mishandling this task potentially leads to a number of serious health problems. Deviations below the basal glucose levels (hypoglycaemic) deviations are considerably more dangerous in the short term than positive (hyperglycemic) deviations, although both types of deviations are undesirable [8, 9].

Type 'I' diabetes is a disease that develops when the pancreas stops producing the required amount of insulin that is needed to control the glucose level. In normal cases, the body maintains an appropriate level of insulin through the day. Long-term consequences of the glucose concentration inside a diabetic individual will lead to a severe decrease of health status and a dramatic increase of cost of rehabilitation. Large efforts are undertaken in pharmacology and biomedical engineering to control glucose concentration by proper insulin dosing [10].

2.2   Overview of Diabetes:

After eating, food is digested in the stomach, and carbohydrates are broken down into glucose. The glucose is then absorbed into the bloodstream, and the blood glucose level rises.

Normally, blood glucose levels are tightly controlled by insulin. The rise in blood sugar level normally signals special cells in the pancreas, called beta cells, to release the right amount of insulin to normalize the glucose level in the blood and lower it to the normal level. The glucose-insulin system inside a normal human body is shown in Figure 2.1, while Figure 2.2 shows the glucose-insulin system inside a diabetic patient. Typically, the normal range of the glucose level in a normal individual should fall between 3.9 – 7.7 millimole/liter, (mmol/l), or in metric system 70 – 140 milligram/deciliter, (mg/dl) [11, 12]. The conversion factor between mmol/l and mg/dl is given by the following 1 millimole/liter = 18.18 milligram/deciliter

In type 'I' diabetes, the pancreas undergoes an autoimmune attack by the body itself and is unable of making insulin. Type 'I' diabetes is caused by an autoimmune destruction of beta cells in the pancreas, which leads to an absolute insulin deficiency [13]. Abnormal antibodies have been found in the majority of patients with type 'I' diabetes. Antibodies are proteins in the blood that are part of the body's immune system. The patient with type 'I' diabetes must rely on insulin medication or injection for survival. In patients with diabetes, the absence or insufficient production of insulin causes high glucose. Without the insulin, the glucose remains in the blood, and the body does not receive fuel for energy. The human body cannot function without insulin. High glucose is unsafe, and if left untreated, can cause a life–threatening complication known as diabetic ketoacidosis [14, 15]. Over time, high glucose level can lead to blindness, risk of heart attack, stroke and possible amputation, nerve damage and kidney failure. Also, diabetes can complicate pregnancy and put a mother at risk for having a baby with birth defects [16, 17].
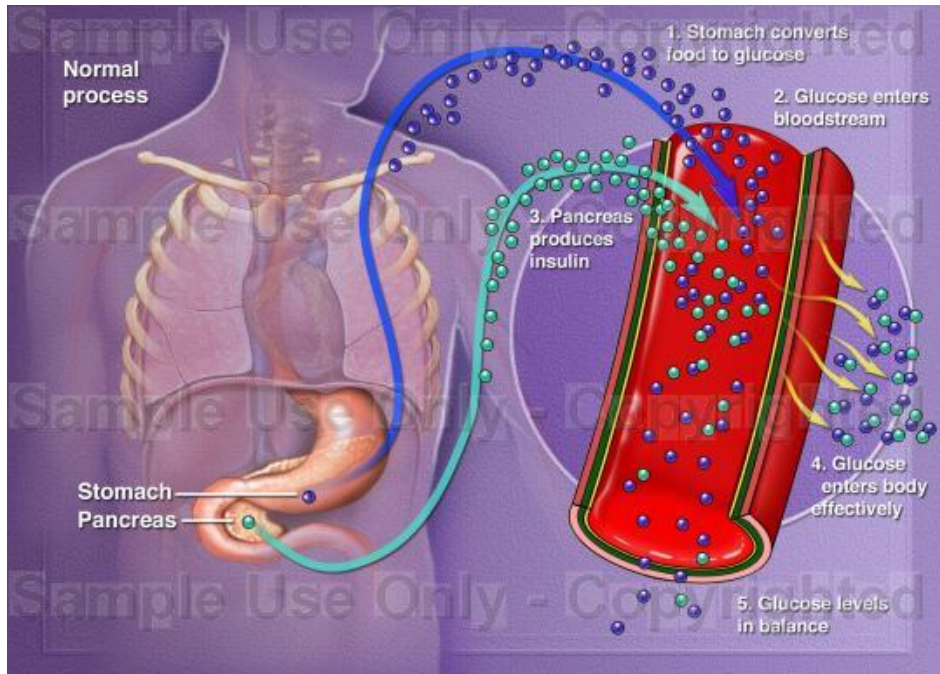
Figure 2.1 Glucose-insulin system inside a normal human body
(By Courtesy of Diabetes Treatment 365.com)
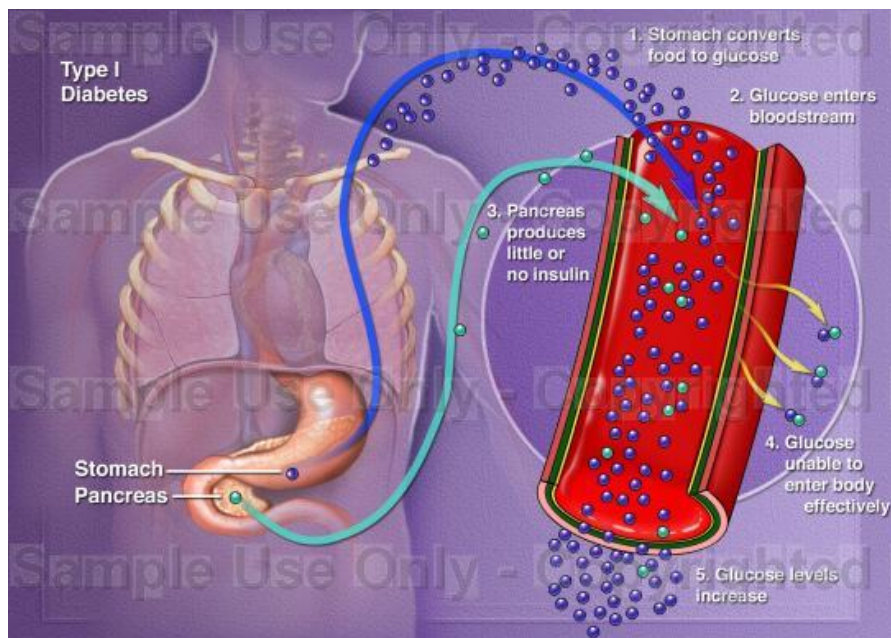
Figure 2.2 Glucose-insulin system inside a diabetic patient body.
(By Courtesy of Diabetes Treatment 365.com)

The normal range of blood glucose concentration should be maintained within narrow limits throughout the day. The average is 70–140 mg/dl, lower in the morning and higher after the meals [11, 12].

Person's Category	Fasting State		Postprandial
	Glucose minimum value (mg/dl)	Glucose maximum value (mg/dl)	2-3 hours after eating (mg/dl)
Hypoglycemia	-	< 59	< 60
Early Hypoglycemia	60	79	60 - 70
Normal	80	100	< 140
Early diabetes	101	126	140-200
Diabetic	> 126	-	> 200

Table 2.1 Blood glucose levels chart

For most normal persons, the glucose levels are between 80 mg/dl and 100 mg/dl in a fasting state that occurs when a person has not eaten or drunk anything for at least eight hours. Table 2.1 shows the glucose levels for different people categories with the minimum and maximum value of the glucose level for each category. After eating, the glucose level rises above the normal level and should fall back to the original starting point within two to three hours. If the glucose level does not fall, the person is classified as diabetic or at the early diabetes stage. However, the glucose level should not fall below 60 mg/dl as this is typically the symptom of hypoglycemia.

There are total of 25.8 million children and adults in the United States, or 8.3% of the populations have diabetes. Also, there is an estimated 79 million people who are classified as pre-diabetes patients in the United States. Worldwide there are about 346 million people who are diabetics. The number is expected to rise to about 438 million by year 2030 [18]. Diabetes is the

seventh-leading cause of death worldwide. The condition and its complication cost an estimated $132 billion annually in the United State alone and about $376 billion worldwide, in terms of healthcare expenses and lost productivity [19]. Based on the death data, diabetes was a contributing cause of a total of 231,404 deaths in year 2007 in the United State only [20]. The following statistics show the rate of heart disease and stroke due to diabetes [18]

- In 2004, heart disease was noted on 68% of diabetes-related death certificates among people aged 65 years or older.

- In 2004, stroke was noted on 16% of diabetes-related death certificates among people aged 65 years or older.

- Adults with diabetes have heart disease death rates about two to four times higher than adults without diabetes.

- The risk for stroke is two to four times higher among people with diabetes.

2.3   Automation in Diabetes Control:

Insulin injection is a process in which the level of glucose is monitored to indicate the adequate amount of insulin. From the technical point of view, it is highly beneficent to investigate the application of control engineering techniques to automate the infusion of the insulin. In recent years, many researchers focused on the diabetes problem, and the minimal model was widely used. The concept and implementation of controlling the insulin infusion for diabetic individuals has been investigated for a few decades via numerous attempts. Various types of controllers were designed based on a linear model where the output is adequate in the neighborhood of the equilibrium points. As an overall remark, the mathematical model that describes the glucose-insulin system of the human beings is a nonlinear model. It is believed that

with deeper investigation of modern nonlinear control techniques, algorithm and methods that can be applied to studies of diabetes. A closed loop system would accurately manage and regulate the infusion rate of the insulin to the diabetic patients.

2.4   Nonlinear System Identification:

The knowledge of the mathematical model of the system is an essential task for closed loop control. The accuracy of the model is required for the system to work properly. Since the level of glucose inside the human being body changes significantly up or down based on the amount and the kind of food, it is a nonlinear model. One major key problem in nonlinear system identification is to estimate the unknown parameters. System identification is the experimental approach to process modeling. System identification includes the following

- Experimental planning

- Selection of model structure

- Criteria

- Parameter estimation

- Model validation

Experimental planning is normally to get some experimental data from a medical clinic. The model structure can be derived based on prior knowledge of the process. When formulating an identification problem, a criterion is postulated to indicate how well a model fits the experimental data. By making some statistical assumptions, it is feasible to derive criteria from probabilistic argument. Estimating the unknown parameters of a mathematical model requires the input-output data and the class of model. The parameters estimation problem can be formulated as an optimization problem where the best model is the model that best fits the data

according to the given criterion. Nonlinear model is defined as an equation that is nonlinear in the coefficients or a combination of linear and nonlinear in the coefficients. The nonlinear estimation is the process of fitting a mathematical model to experimental data to determine unknown parameters of that model. The parameters are chosen or guessed so that the output of the model is the best match with respect to the experimental data. Nonlinear models require iterative methods that start with an initial guess of the unknown parameters. The iteration alters the current guess until the algorithm converges.

CHAPTER 3

DIABETES MATHEMATICAL MODEL

3.1   Introduction:

The minimal model of glucose and insulin was formulated to be the easiest model with which to deal. This has been shown to be the simplest physiologically based representations that can respectively account for the observed glucose kinetics when the plasma insulin values are supplied and for the observed insulin kinetics when the plasma glucose values are supplied. The minimal model is capable of describing the dynamics of the diabetic patient. The insulin enters or exits the interstitial insulin compartment at a rate that is proportional to the difference $i(t) - i_b$ of plasma insulin $i(t)$ and the basal insulin level i_b [21, 22]. If the level of insulin in the plasma is below the insulin basal level, insulin exits the interstitial insulin compartment. When the level of insulin in the plasma is above the insulin basal level, insulin enters the interstitial insulin compartment. Insulin also can flee the interstitial insulin compartment through another route at a rate that is proportional to the insulin amount inside the interstitial insulin compartment. On the other hand, glucose enters or exits the plasma compartment at a rate that is proportional to the difference $g(t) - g_b$ of the plasma glucose level $g(t)$ and the basal glucose level g_b. When the level of glucose in the plasma is below the glucose basal level, the glucose exits the plasma compartment. When the level of glucose in the plasma is above the glucose basal level, glucose enters the glucose compartment. Glucose also can flee the plasma compartment through another route at a rate that is proportional to the glucose amount inside the interstitial insulin compartment. The normal range of blood glucose concentration should be maintained within

narrow limits throughout the day, 70–140 mg/dl, lower in the morning and higher after the meals [11, 12].

3.2 Minimal Model Structures:

The level of glucose inside the human being body changes significantly in response to food intake and other physiological and environment conditions. It is necessary to derive mathematics models to capture such dynamics for control design [11-12, 21-26]. Over the years, many mathematical models have been developed to describe the dynamic behavior of the human glucose/insulin system. Such models are highly nonlinear and usually very complex. The most commonly used and simplified model is the minimal model introduced by Bergman [6, 26-32]. The minimal model consists of a set of three differential equations with unknown parameters. Since diabetic patients differ dramatically due to variations of their physiology and pathology characteristics, the parameters of the minimal model are significantly different among patients. Based on such models, a variety of control technologies have been applied to glucose/insulin control problems.

The minimal model has been developed and tested on healthy subjects whose insulin is released by the pancreas depending on the actual blood glucose concentration [21]. The minimal model consists of two parts [27-29]: the minimal model of glucose disappearance (g and v) and the minimal model of insulin kinetics (i). The mathematical minimal model is stated below

$$\dot{g}(t) = -\left[P_1 + v(t)\right]g(t) + P_1 g_b \tag{3.1}$$

$$\dot{v}(t) = -P_2 v(t) + P_3\left[i(t) - i_b\right] \tag{3.2}$$

$$\dot{i}(t) = -n\, i(t) + \gamma\left[g(t) - h\right]t \tag{3.3}$$

where

$g(t)$ (mg/dl) is the blood glucose level in plasma.

$i(t)$ (µU/ml) is the insulin concentration level in plasma.

$v(t)$ (min^{-1}) is the variable which is proportional to the insulin in the remote compartment.

g_b (mg/dl) is the basal blood glucose level in plasma.

i_b (µU/ml) is the basal insulin level in plasma.

t (min) is the time interval from the glucose injection.

The initial conditions of the above differential equations are: $g(0) = g_0$, $v(0) = 0$, $i(0) = i_0$.

The model parameters carry some physiological meanings [27-29, 33] that can be summarized as follows

P_1 (min^{-1}) describes the "glucose effectiveness" which represents the ability of blood glucose to enhance its own disposal at the basal insulin level.

P_2 (min^{-1}) describes the decreasing level of insulin action with time.

P_3 $(\text{min}^{-2}(\mu U/ml)^{-1})$ describes the rate in which insulin action is increased as the level of insulin deviates from the corresponding baseline.

γ $((\mu U/ml)(mg/dl)^{-1} \text{min}^{-1})$ denotes the rate at which insulin is produced as the level of glucose rises above a "target glycerin" level.

n (min^{-1}): represents fractional insulin clearance.

h (mg/dl) is the pancreatic "target glycemia" level.

g_0 (mg/dl) is the theoretical glucose concentration in plasma extrapolated to the time of glucose injection $t = 0$.

i_0 (µU/ml) is the theoretical plasma insulin concentration at $t = 0$.

μU/ml is the conventional unit to measure the insulin level and has the following conversion

1 micro-unit/milliliter = 6 picomole/liter (1 μU/ml = 6 pmol/l) [34 35].

A fourth differential equation will be added to the set of the minimal model equations to represent a first-order pump dynamics

$$\dot{w}(t) = \frac{1}{a}\left(-w(t) + u(t)\right) \tag{3.4}$$

where

   $w(t)$ is the infusion rate.

   $u(t)$ is the input command.

   a is time constant of the first-order pump.

3.3   Literature Surveys:

Many methods and techniques have been investigated, tested, and studied for controlling the glucose level in type 'I' diabetes patients. Research in this field has always been model-based and has moved from the development of the structure of a model of glucose and insulin dynamics stepping towards model parameter estimation and model personalization to each single patient's requirements.

Lynch and Bequette [36] tested the glucose minimal model of Bergman to design a Model Predictive Control (MPC) to control the glucose level in a diabetic patient. The insulin secretion term $\left(\gamma * (g - h) * t\right)$ of the differential equation of the minimal model was replaced by a constant term which makes the infusion of the insulin to be constant and independent of the glucose level.

Fisher [37] used the glucose insulin minimal model of Bergman to design a semi-closed loop insulin infusion algorithm based on plasma glucose samplings taken over a three hours time span. The study concentrates on the glucose level and did not take into consideration some important factors such as free plasma insulin concentration and the rate (γ) at which insulin is produced as the level of glucose rises.

Furler [38] modified the glucose insulin minimal model of Bergman by removing the insulin secretion and adding insulin antibodies to the model. The algorithm calculates the insulin infusion rate as a function of the measured plasma glucose concentration. The linear interpolation was used to find the insulin rate. The algorithm neglected some important variations in insulin concentration and other model variables. Also, it took more than two hours to bring the glucose level to the neighborhood of the glucose basal level.

Ibbini, Masadeh and Amer [39] tested the glucose minimal model of Bergman to design a semi closed-loop optimal control system to control the glucose level in diabetes patients. Also, in that study, the term (γt) of the minimal model has been eliminated which makes the linearized version of the minimal model to be a time-invariant system.

3.4   Experimental Data:

A new approach was developed by Bergman [27-29] to compute the pancreatic responsiveness and insulin sensitivity in the intact organism. This approach uses computer modeling to investigate the plasma glucose and insulin dynamics during a **F**requently **S**ampled **I**ntravenous **G**lucose **T**olerance (FSIGT). The FSIGT test was performed after an overnight fast. An amount of glucose of 0.3g of glucose per 1 kg of patient body weight was injected at t = 0 over a period of time equal to 60 seconds [27-29][40]. The blood samples were taken at regular

intervals of time and then analyzed for glucose and insulin content. Glucose was measured in triplicate by the glucose oxidize technique on an automated analyzer. The coefficient of variation of a single glucose determination was about ± 1.5%. Insulin was measured in duplicate by radioimmunoassay, with dextrin-charcoal separation using a human insulin standard. Table 1 shows the FSIGT test data for a normal individual.

Sampling time (minutes)	Glucose level (mg/dl)	Insulin level (μU/ml)
0	92	11
2	350	26
4	287	130
6	251	85
8	240	51
10	216	49
12	211	45
14	205	41
16	196	35
19	192	30
22	172	30
27	163	27
32	142	30
42	124	22
52	105	15
62	92	15
72	84	11
82	77	10
92	82	8
102	81	11
122	82	7
142	82	8
162	85	8
182	90	7

Table 3.1 FSIGT test data for a normal individual.

The plot of the glucose $g(t)$ and the insulin $i(t)$ levels versus time, t, during the FSIGT test are plotted in Figure 3.1 and 3.2 respectively.
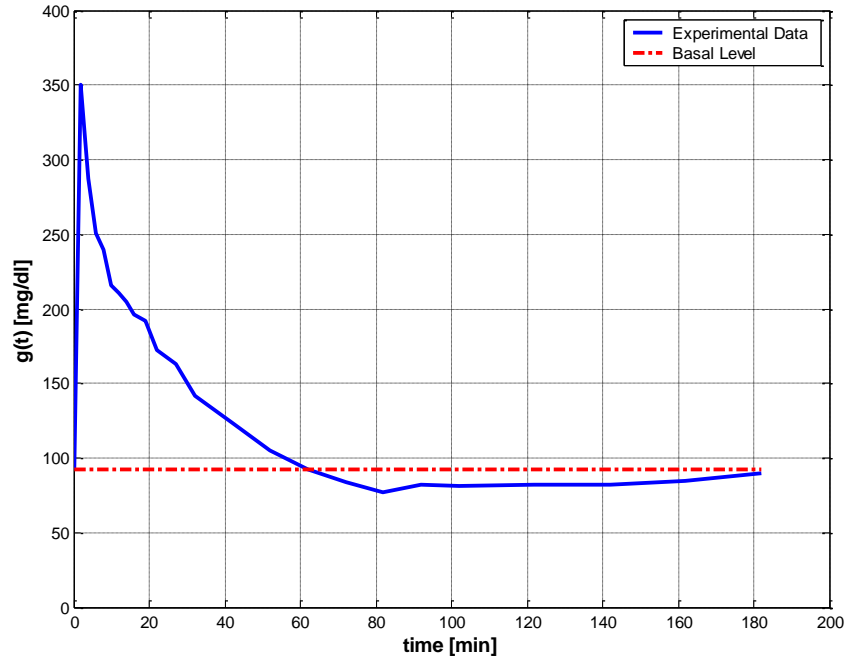
Figure 3.1 Glucose level *g(t)* during the FSIGT test
for a normal individual
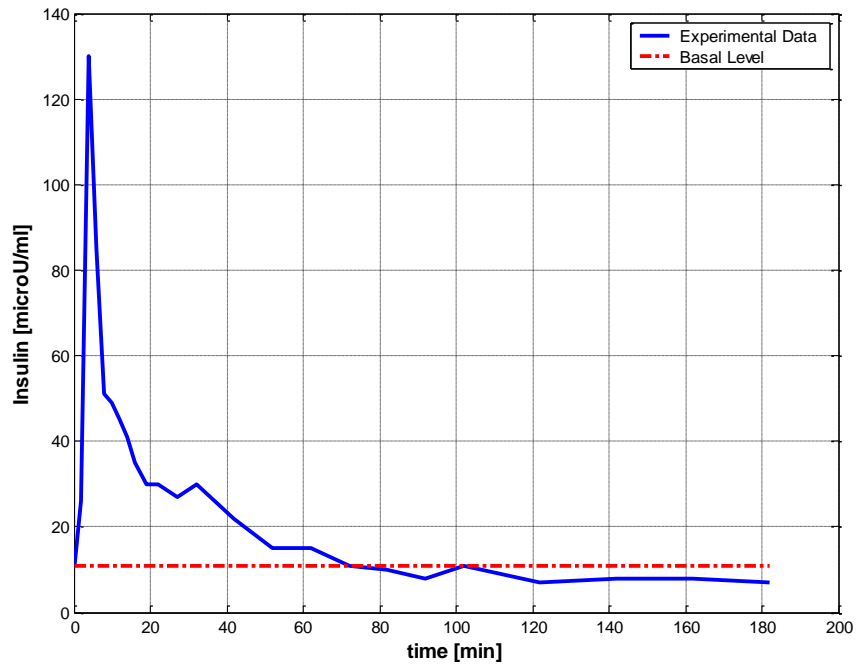
Figure 3.2 Insulin level *i(t)* during the FSIGT test
for a normal individual

CHAPTER 4

SIMULATION OF MINIMAL MODEL

4.1   Introduction:

The implementation of the minimal model can be achieved by using computer simulation software. Computer simulation is a computer program that attempts to simulate an abstract model of a particular system. Computer simulations have become a useful part of mathematical modeling of many natural systems in physics, chemistry, biology, medical, biomedical and engineering to gain insight into the operation of those systems. Traditionally, the formal modeling of systems has been via a mathematical model, which attempts to find analytical solutions to problems which enable the prediction of the behavior of the system from a set of parameters and initial conditions.

4.2   Simulation of the Glucose Kinetics Model:

Implementation of the minimal model can be achieved by using computer simulation tools. The mathematical minimal model is stated in chapter 3 and repeated here for convenience

$$\dot{g}(t) = -\left[P_1 + v(t)\right]g(t) + P_1 g_b \tag{4.1}$$

$$\dot{v}(t) = -P_2 v(t) + P_3\left[i(t) - i_b\right] \tag{4.2}$$

$$\dot{i}(t) = -n\, i(t) + \gamma\left[g(t) - h\right]t \tag{4.3}$$

The two differential equations (4.1) and (4.2) correspond to the glucose kinetics are modeled here by using the MATLAB/Simulink software. In this model, the insulin *i(t)* is considered as an

input and the glucose $g(t)$ as an output. The values of the input $i(t)$ at a time interval are given in Table 3.1. The simulation diagram of the minimal model for the glucose kinetics is shown in Figure 4.1. The output of the system, glucose $g(t)$, is shown in Figure 4.2 for a normal individual with the following parameters [27-29]

$P_1 = 3.082$ x 10^{-2}

$P_2 = 2.093$ x 10^{-2}

$P_3 = 1.062$ x 10^{-5}

$g_0 = 350$

$g_b = 92$

$i_b = 11$
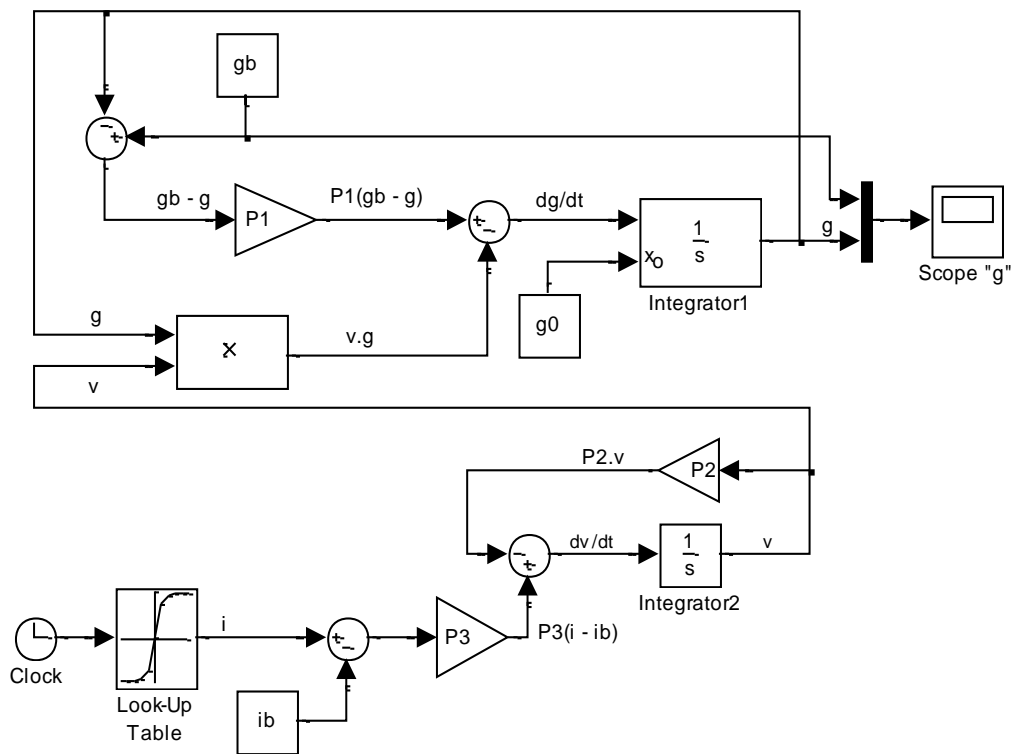
Figure 4.1 Simulation diagram of the glucose kinetics model
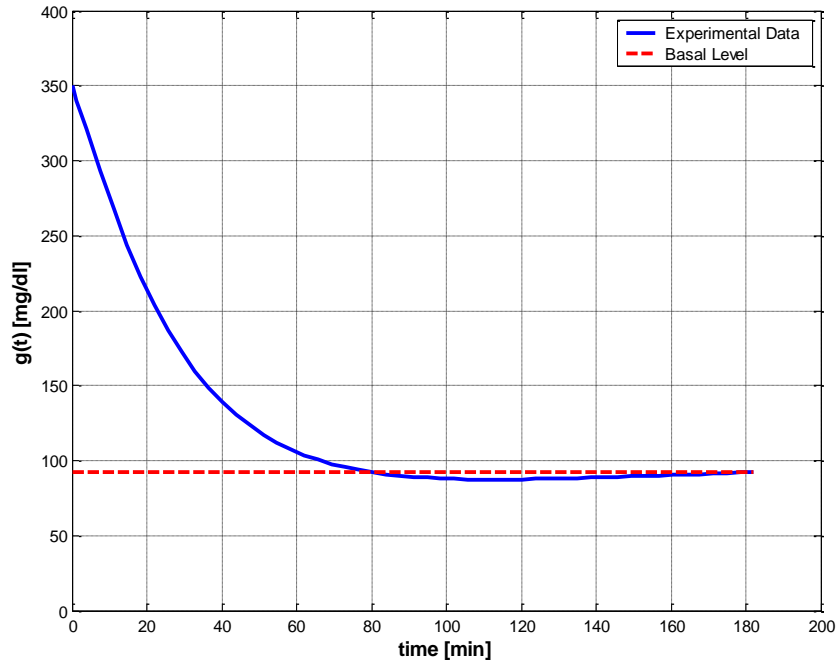
Figure 4.2 The simulated output *g(t)* of the glucose kinetics model

4.3   Simulation of the Minimal Model:

The minimal model consists of two equations that represent the glucose kinetics and one equation that represents the insulin kinetics. The three equations are combined together as one set and a simulation diagram is constructed. The simulation diagrams of the glucose kinetics model and the insulin kinetics model are shown in Figures 4.3 and 4.4 respectively. The models can be combined together to form the minimal model. The schematic diagram of the minimal model is shown in Figure 4.5.
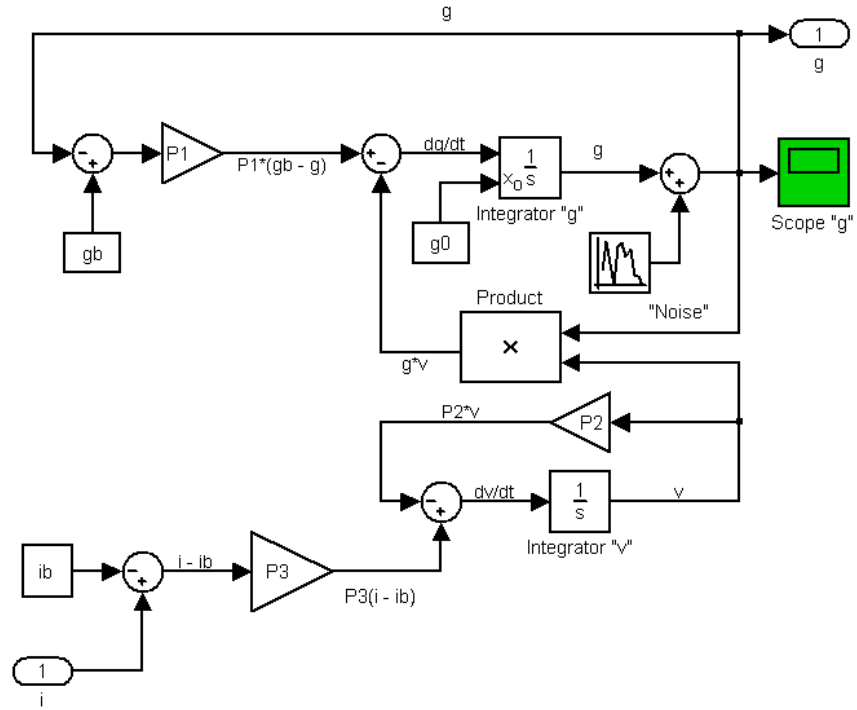
Figure 4.3 Simulation diagram of minimal model (glucose kinetics part)
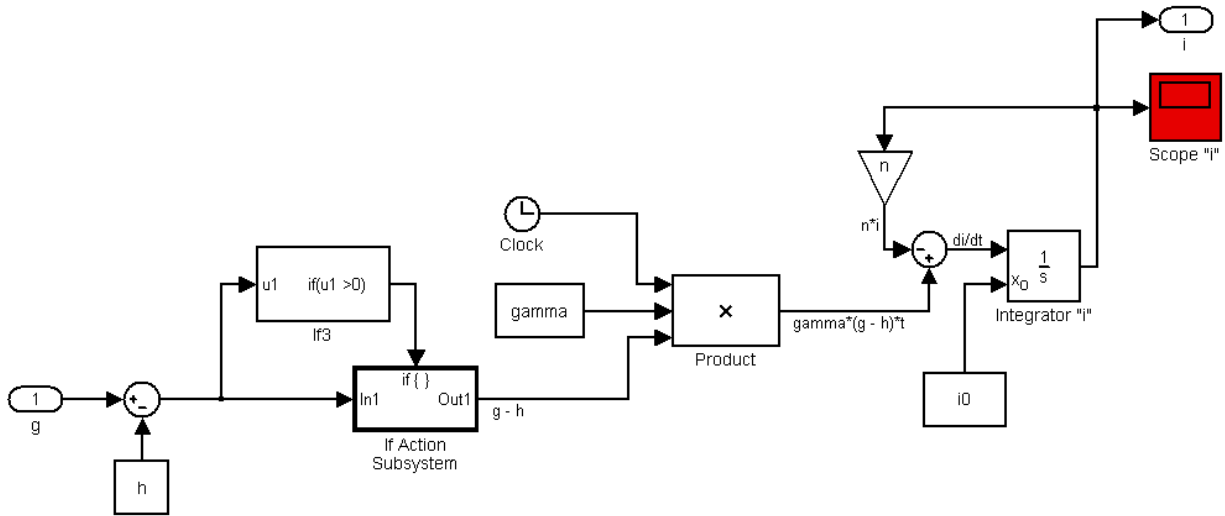
Figure 4.4 Simulation diagram of minimal model (insulin kinetics part)
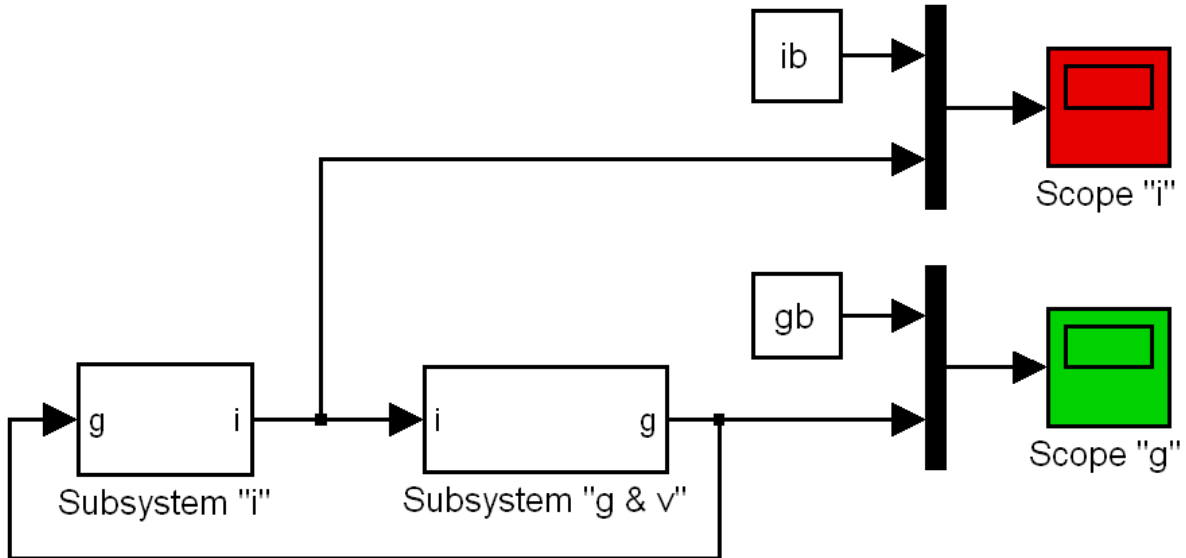
Figure 4.5 Simulation diagram of minimal model

The minimal model simulation diagram shown on Figure 4.5 is tested on a normal individual with the following parameters [29]

$P_1 = 2.6 \times 10^{-2}$

$P_2 = 2.5 \times 10^{-2}$

$P_3 = 1.25 \times 10^{-5}$

$g_b = 92$

$i_b = 11$

$g_0 = 279$

$i_0 = 363.7$

$n = 0.287$

$h = 83.7$

$\gamma = 0.0041$

The graph of the output of the system, the glucose level *g(t)*, is shown in Figure 4.6. The glucose level reaches the glucose basal level of a normal individual within 65 minutes. That observation leads to conclude the minimal model simulation diagram is achieving the goal.
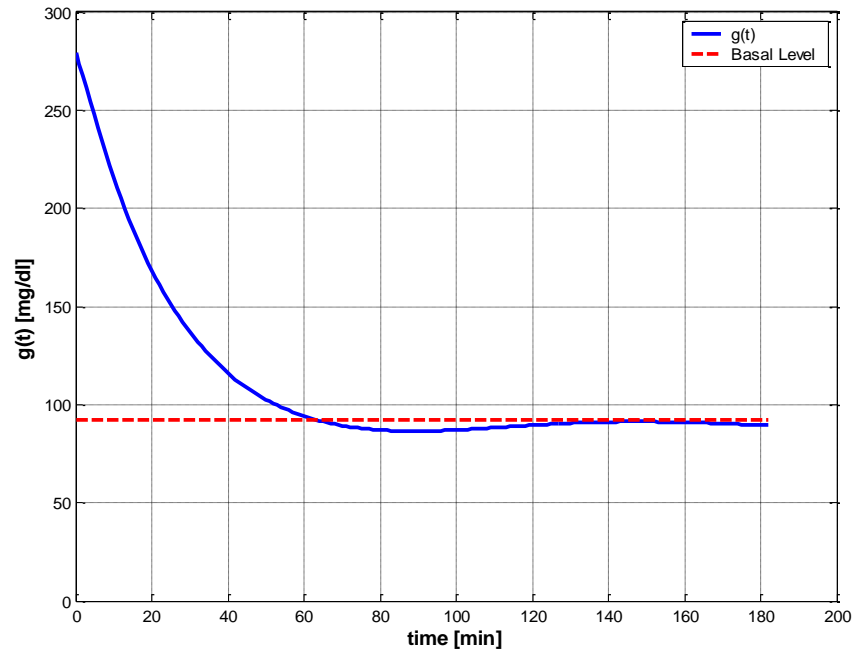
Figure 4.6 Graph of glucose level of the minimal model for normal patient

CHAPTER 5

PARAMETERS ESTIMATION

5.1 Introduction:

Parameter estimation is a common problem in many areas of process modeling. The goal is to determine values of model parameters that provide the best fit to measured data, generally based on some type of least squares or maximum likelihood criterion. Parameter estimation can be described as a method that is able to take control of a model running it as many times as it needs while adjusting its parameters until the discrepancies between selected model outputs and a set of data or laboratory measurements are reduced to a minimum in the weighted least square sense.

5.2 Least Squares Parameter Estimation:

The method of least squares assumes that the best-fit curve of a given set of data is the curve that has the minimal sum of the deviations squared (*least squares error*) from a given set of data [42-44]. Assume a set of data given as: $(x_1, y_1), (x_2, y_2), (x_3, y_3), \ldots, (x_N, y_N)$, where the independent variable is x and the dependent variable is y. The curve *f(x)* is the fitting curve that has the deviation or what is called the error *d*. The error *d* is basically the horizontal (or vertical) distance between the points and the fitted graph. The error *d* can be defined as the following

$$d_1 = y_1 - f(x_1)$$
$$d_2 = y_2 - f(x_2)$$
$$d_3 = y_3 - f(x_3) \tag{5.1}$$
$$\vdots \quad \vdots \quad \vdots$$
$$d_N = y_N - f(x_N)$$

As per the principle of the least square method, the best fitting curve has the following property

$$\Pi = d_1^2 + d_2^2 + d_3^2 + \ldots\ldots d_N^2 = \sum_{i=1}^{N} d_i^2 \tag{5.2}$$

where the symbol (Π) represents the minimum least square error. Now substituting equation (5.1) into equation (5.2), we obtain

$$\Pi = \sum_{i=1}^{N} \left[y_i - f(x_i) \right]^2 \tag{5.3}$$

When the function is to the m-th degree polynomial form

$$f(x) = a_0 + a_1 x + a_2 x^2 + a_3 x^3 + \ldots a_m x^m \tag{5.4}$$

The minimum Least Squares Error becomes

$$\Pi = \sum_{i=1}^{N} \left[y_i - f(x_i) \right]^2$$
$$= \sum_{i=1}^{N} \left[y_i - (a_0 + a_1 x_i + a_2 x_i^2 + a_3 x_i^3 + \ldots a_m x_i^m) \right]^2 \tag{5.5}$$

The unknown coefficients a_0, a_1, a_2, a_3,....., a_m can be estimated to yield a minimum least squares error. This can be done by taking the partial derivatives with respect to unknown coefficients and set the derivative equation to zero as the following

$$\frac{\partial \Pi}{\partial a_0} = \frac{\partial}{\partial a_0} \sum_{i=1}^{N} \left[y_i - (a_0 + a_1 x_i + a_2 x_i^2 + a_3 x_i^3 + \ ..... \ a_m x_i^m) \right]^2 = 0$$

$$\frac{\partial \Pi}{\partial a_1} = \frac{\partial}{\partial a_1} \sum_{i=1}^{N} \left[y_i - (a_0 + a_1 x_i + a_2 x_i^2 + a_3 x_i^3 + \ ..... \ a_m x_i^m) \right]^2 = 0$$

$$\frac{\partial \Pi}{\partial a_2} = \frac{\partial}{\partial a_2} \sum_{i=1}^{N} \left[y_i - (a_0 + a_1 x_i + a_2 x_i^2 + a_3 x_i^3 + \ ..... \ a_m x_i^m) \right]^2 = 0 \qquad (5.6)$$

$$\vdots \qquad \qquad \vdots \qquad \qquad \vdots$$

$$\frac{\partial \Pi}{\partial a_m} = \frac{\partial}{\partial a_m} \sum_{i=1}^{N} \left[y_i - (a_0 + a_1 x_i + a_2 x_i^2 + a_3 x_i^3 + \ ..... \ a_m x_i^m) \right]^2 = 0$$

Taking the partial derivative of equation (5.6) yields

$$\frac{\partial \Pi}{\partial a_0} = 2\sum_{i=1}^{N} \left[y_i - (a_0 + a_1 x_i + a_2 x_i^2 + a_3 x_i^3 + \ ..... \ a_m x_i^m) \right] = 0$$

$$\frac{\partial \Pi}{\partial a_1} = 2\sum_{i=1}^{N} \left\{ \left[y_i - (a_0 + a_1 x_i + a_2 x_i^2 + a_3 x_i^3 + \ ..... \ a_m x_i^m) \right] \times [x_i] \right\} = 0$$

$$\frac{\partial \Pi}{\partial a_2} = 2\sum_{i=1}^{N} \left\{ \left[y_i - (a_0 + a_1 x_i + a_2 x_i^2 + a_3 x_i^3 + \ ..... \ a_m x_i^m) \right] \times [x_i^2] \right\} = 0 \qquad (5.7)$$

$$\vdots \qquad \qquad \vdots \qquad \qquad \vdots$$

$$\frac{\partial \Pi}{\partial a_m} = 2\sum_{i=1}^{N} \left\{ \left[y_i - (a_0 + a_1 x_i + a_2 x_i^2 + a_3 x_i^3 + \ ..... \ a_m x_i^m) \right] \times [x_i^m] \right\} = 0$$

Equation (5.7) can be rearranged as

$$\sum_{i=1}^{N} y_i = \sum_{i=1}^{N} \left(a_0 + a_1 x_i + a_2 x_i^2 + a_3 x_i^3 + \ ..... \ a_m x_i^m \right)$$

$$\sum_{i=1}^{N} x_i y_i = \sum_{i=1}^{N} \left[(x_i) \times \left(a_0 + a_1 x_i + a_2 x_i^2 + a_3 x_i^3 + \ ..... \ a_m x_i^m \right) \right]$$

$$\sum_{i=1}^{N} x_i^2 y_i = \sum_{i=1}^{N} \left[(x_i^2) \times \left(a_0 + a_1 x_i + a_2 x_i^2 + a_3 x_i^3 + \ ..... \ a_m x_i^m \right) \right] \qquad (5.8)$$

$$\vdots \qquad \qquad \vdots \qquad \qquad \vdots$$

$$\sum_{i=1}^{N} x_i^m y_i = \sum_{i=1}^{N} \left[(x_i^m) \times \left(a_0 + a_1 x_i + a_2 x_i^2 + a_3 x_i^3 + \ ..... \ a_m x_i^m \right) \right]$$

Expanding equation (5.8) as

$$\sum_{i=1}^{N} y_i = a_0 \sum_{i=1}^{N} 1 + a_1 \sum_{i=1}^{N} x_i + a_2 \sum_{i=1}^{N} x_i^2 + \cdots + a_m \sum_{i=1}^{N} x_i^m$$

$$\sum_{i=1}^{N} x_i y_i = a_0 \sum_{i=1}^{N} x_i + a_1 \sum_{i=1}^{N} x_i^2 + a_2 \sum_{i=1}^{N} x_i^3 + \cdots + a_m \sum_{i=1}^{N} x_i^{m+1}$$

$$\sum_{i=1}^{N} x_i^2 y_i = a_0 \sum_{i=1}^{N} x_i^2 + a_1 \sum_{i=1}^{N} x_i^3 + a_2 \sum_{i=1}^{N} x_i^4 + \cdots + a_m \sum_{i=1}^{N} x_i^{m+2} \qquad (5.9)$$

$$\vdots \qquad \qquad \vdots \qquad \qquad \vdots$$

$$\sum_{i=1}^{N} x_i^m y_i = a_0 \sum_{i=1}^{N} x_i^m + a_1 \sum_{i=1}^{N} x_i^{m+1} + a_2 \sum_{i=1}^{N} x_i^{m+2} + \cdots + a_m \sum_{i=1}^{N} x_i^{2m}$$

Writing equation (5.9) in the matrix format

$$
\begin{bmatrix} \sum_{i=1}^{N} y_i \\ \sum_{i=1}^{N} x_i y_i \\ \sum_{i=1}^{N} x_i^2 y_i \\ \vdots \\ \sum_{i=1}^{N} x_i^m y_i \end{bmatrix}
=
\begin{bmatrix}
\sum_{i=1}^{N} 1 & \sum_{i=1}^{N} x_i & \sum_{i=1}^{N} x_i^2 \cdots\cdots \sum_{i=1}^{N} x_i^m \\
\sum_{i=1}^{N} x_i & \sum_{i=1}^{N} x_i^2 & \sum_{i=1}^{N} x_i^3 \cdots\cdots \sum_{i=1}^{N} x_i^{m+1} \\
\sum_{i=1}^{N} x_i^2 & \sum_{i=1}^{N} x_i^3 & \sum_{i=1}^{N} x_i^4 \cdots\cdots \sum_{i=1}^{N} x_i^{m+2} \\
\vdots & \vdots & \vdots \\
\sum_{i=1}^{N} x_i^m & \sum_{i=1}^{N} x_i^{m+1} & \sum_{i=1}^{N} x_i^{m+1} \cdots\cdots \sum_{i=1}^{N} x_i^{m+2}
\end{bmatrix}
\begin{bmatrix} a_0 \\ a_1 \\ a_2 \\ \vdots \\ a_m \end{bmatrix}
\qquad (5.10)
$$

The coefficients a_0, a_1, a_2, a_3,....., a_m can be found using the following equation

$$
\begin{bmatrix} a_0 \\ a_1 \\ a_2 \\ \vdots \\ a_m \end{bmatrix} = \begin{bmatrix} \sum_{i=1}^{N}1 & \sum_{i=1}^{N}x_i & \sum_{i=1}^{N}x_i^2 \cdots\cdots\cdots \sum_{i=1}^{N}x_i^m \\ \sum_{i=1}^{N}x_i & \sum_{i=1}^{N}x_i^2 & \sum_{i=1}^{N}x_i^3 \cdots\cdots\cdots \sum_{i=1}^{N}x_i^{m+1} \\ \sum_{i=1}^{N}x_i^2 & \sum_{i=1}^{N}x_i^3 & \sum_{i=1}^{N}x_i^4 \cdots\cdots\cdots \sum_{i=1}^{N}x_i^{m+2} \\ \vdots & & \vdots & \vdots \\ \sum_{i=1}^{N}x_i^m & \sum_{i=1}^{N}x_i^{m+1} & \sum_{i=1}^{N}x_i^{m+1} \cdots\cdots \sum_{i=1}^{N}x_i^{m+2} \end{bmatrix}^{-1} \begin{bmatrix} \sum_{i=1}^{N}y_i \\ \sum_{i=1}^{N}x_i y_i \\ \sum_{i=1}^{N}x_i^2 y_i \\ \vdots \\ \sum_{i=1}^{N}x_i^m y_i \end{bmatrix} \tag{5.11}
$$

5.3   The Levenberg –Marquardt Algorithm:

Nonlinear model is defined as an equation that is nonlinear in the coefficients or a combination of linear and nonlinear in the coefficients. The nonlinear estimation is the process of fitting a mathematical model to experimental data to determine unknown parameters of that model. The parameters can be obtained iteratively to reduce computational complexity. In general, the nonlinear models are more difficult to fit than linear models because the unknown parameters or coefficients cannot be estimated using a simple matrix technique that normally is used to solve linear equations. Nonlinear models require an iterative method that starts with an initial guess of the unknown parameters. Each iteration updates the current estimate based on new observation. Suppose there are m base functions $f_1, f_2,....f_m$ of n parameters $p_1, p_2,....p_n$. The functions and the parameters can be represented as follows

$$
\begin{aligned} f^T &= (f_1, f_2, \ ..., f_m) \\ p^T &= (p_1, p_2, \ ..., p_n) \end{aligned} \tag{5.12}
$$

The least squares method is to find the values of the unknown parameters $p_1, p_2,....p_n$ for which the cost function is minimum, i.e.

$$S(p) = \frac{1}{2} f^T f = \frac{1}{2} \sum_{i=1}^{m} \left[f_i(p) \right]^2 \qquad (5.13)$$

The Levenberg-Marquardt algorithm is an iterative technique that seeks the minimum of a multivariate function that is expressed as the sum of squares of nonlinear real-valued functions [41]. It has become a standard technique for nonlinear least-squares problems. Levenberg-Marquardt can be thought of as a combination of steepest descent and the Gauss-Newton method. When the current solution is far from the correct one, the algorithm behaves like a steepest descent method which is guaranteed to converge. When the current solution is close to the correct solution, it becomes a Gauss-Newton method.

The Levenberg-Marquardt algorithm is an iterative procedure. Let $\hat{x} = f(p)$ be the parameterized model function. The minimization starts after an initial guess for the parameters when vector p is provided. The algorithm is locally convergent; namely, it converges when the initial guess is close to the true values. In each iteration step, the parameter vector p is updated by a new estimate $p + \varepsilon_p$ where ε_p is a small correction term that can be determined by a Taylor Series expansion which leads to the following approximation

$$f(p + \varepsilon_p) \approx f(p) + J \varepsilon_p \qquad (5.14)$$

where, J is the Jacobian of f at p

$$J = \frac{\partial f(p)}{\partial p} \qquad (5.15)$$

Levenberg-Marquardt iterative initiates at the starting point p_0 and produces a series of vectors p_1, p_2, p_3, etc, that converge towards a local minimizer p^+ of f [45]. At each step, it is required to find the small correction factor ε which minimizes the value of

$$\left\| x - f(p + \varepsilon_p) \right\| \approx \left\| x - f(p) - J \varepsilon_p \right\|$$

That gives the following

$$\left\| x - f\left(p + \varepsilon_p \right) \right\| \approx \left\| x - \hat{x} - J \delta p \right\| = \left\| e - J \varepsilon_p \right\| \tag{5.16}$$

where ε_p is the solution to a linear least squares problem. The minimum is achieved when the

term $J \varepsilon_p - e$ is orthogonal to column space J. Based on that, the following can be concluded

$$J^T (J \varepsilon_p - e) = 0 \tag{5.17}$$

equation (5.17) can be rearranged as the following

$$J^T J \varepsilon_p = J^T e \tag{5.18}$$

The Levenberg-Marquardt algorithm solves a slight variation of equation (5.18), which is known

as the augmented normal equation

$$N \varepsilon_p = J^T e \tag{5.19}$$

where the diagonal elements of N are computed as $N_{ii} = \eta + \left[J^T J \right]_{ii}$ for $\eta > 0$ [45], while the

other elements of the matrix N are identical to those of the matrix $\left[J^T J \right]$. η is called the

damping parameter. If the updated parameter vector, $p + \varepsilon_p$, where ε_p is computed from

equation (5.19), yields a reduction in the residual value or error e, then the update is valid and the

process repeats with a decreased damping parameter η. Otherwise, the damping parameter is

increased and the augmented normal equation (5.19) is solved again. Then the process iterates

until a value of ε_p that reduces error is found. A flow chart that summarizes the least squares

method is shown in Figure 5.1. The MATLAB Software has the Optimization Toolbox which

has a command called *Lsqnonlin* for this algorithm.
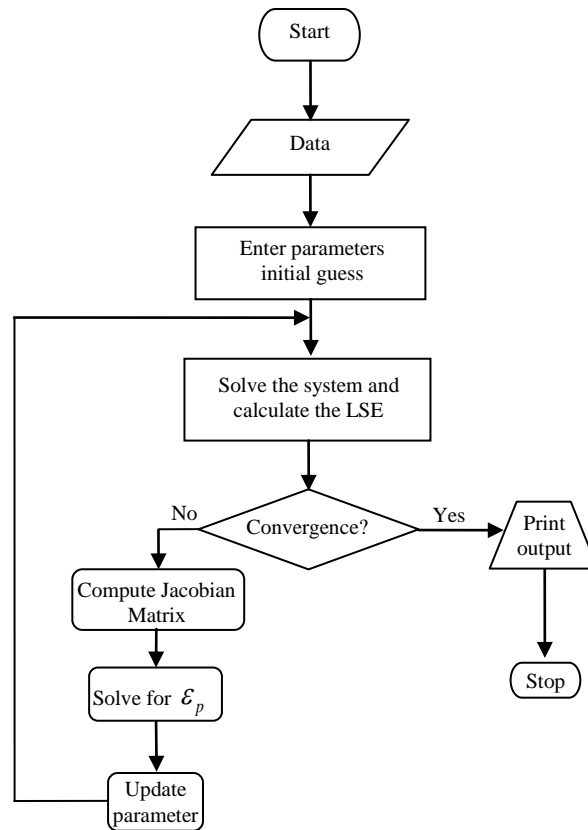
Figure 5.1 Flowchart for the least squares method

5.4 Minimal Model Parameters Estimation:

A glucose level test was conducted on two normal individuals that took three hours [27-28, 40]. The FSIGT test was performed after an overnight fast, an amount of 298 mg/dl of glucose was injected in the first normal individual. Another amount of 320 mg/dl of glucose was injected in the second normal individual. The injection starts at t = 0 and lasts for 60 seconds. Then blood samples were collected from the two individuals and the glucose levels were measured. The result is shown in tables 5.2. The two individuals have different weight and their glucose basal level was 94 mg/dl.

Sampling time During test (minutes)	Normal Patient #1 Glucose level (mg/dl)	Normal Patient #2 Glucose level (mg/dl)
0	94	94
2	298	320
4	284	303
6	272	289
8	253	272
10	248	258
12	235	244
14	217	223
16	208	205
19	205	194
22	191	182
27	172	169
32	164	152
42	141	139
52	132	122
62	120	112
72	116	105
82	108	100
92	106	98
102	104	97
122	105	97
142	109	95
162	107	94
182	110	93

TABLE 5.1 FSIGT test data for a two normal individuals

The mathematical minimal model is stated in chapter 3 and repeated here for convenience

$$\dot{g}(t) = -\left[P_1 + v(t) \right] g(t) + P_1 g_b \tag{5.20}$$

$$\dot{v}(t) = -P_2 v(t) + P_3 \left[i(t) - i_b \right] \tag{5.21}$$

$$\dot{i}(t) = -n\, i(t) + \gamma \left[g(t) - h \right] t \tag{5.22}$$

This algorithm is applied to the problem here. The FSIGT data sample in Table 5.1 consists of 24 samples. The unknown parameters of the minimal model equations (5.20), (5.21) and (5.22) were estimated by utilizing the Levenberg-Marquadrt Algorithm. The parameters to be estimated were given an initial guess, and then the algorithm was used to update the parameters using the sequential data in Table 5.1. A MATLAB program was written to estimate the unknown parameters. The estimated values of those parameters are shown in Table 5.2.

Parameters	Normal Individual #1	Normal Individual #2
P_1	0.032299	0.049519
P_2	0.0092644	41.5953
P_3	5.3004e-006	1.8577e-004
n	0.29858	0.14653
γ	0.0068676	1.0113e-005
h	90.3709	196.0531
g_0	295.6801	318.84
i_0	401.7177	203.2434

Table 5.2 Estimated minimal model parameters for two normal individuals

The values of the parameters shown in Table 5.2 were implemented in the minimal model simulation diagram that was shown on Figure 4.5 of section 4.3. The values of the glucose levels of both individuals are shown in Table 5.3.

Sampling time during the test (minutes)	Normal individual #1 Glucose level (mg/dl)	Normal individual #2 Glucose level (mg/dl)
0	94	94
2	295.6801	318.84
4	282.1308	297.2223
6	268.2993	277.7749
8	254.8580	260.2561
10	242.1020	244.4545
12	230.1353	230.1878
14	218.9702	217.2973
16	208.5776	205.6436
19	198.9116	195.1034
22	185.6659	181.1443
27	173.7810	169.1246
32	156.6159	152.6775
42	142.2917	139.8434
52	120.5167	122.0036
62	105.8327	111.1272
72	96.35277	104.4947
82	90.67314	100.4500
92	87.73594	97.98329
102	86.65621	96.47894
122	86.77255	95.56149
142	89.03143	94.66075
162	92.55181	94.32573
182	95.65837	94.20113

Table 5.3 Simulated glucose levels for two normal individuals

The graphs of both experimental data (Table 5.1) and simulated data (Table 5.3) for normal individuals #1 and #2 are shown in Figures 5.2 and 5.3 respectively.
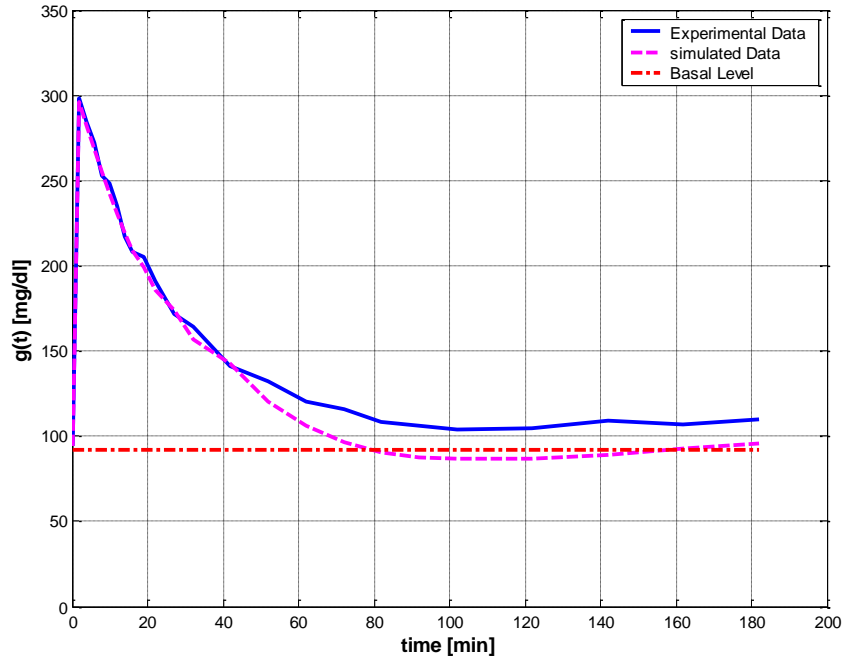
Figure 5.2 Plot of glucose level *g(t)* for normal individual #1
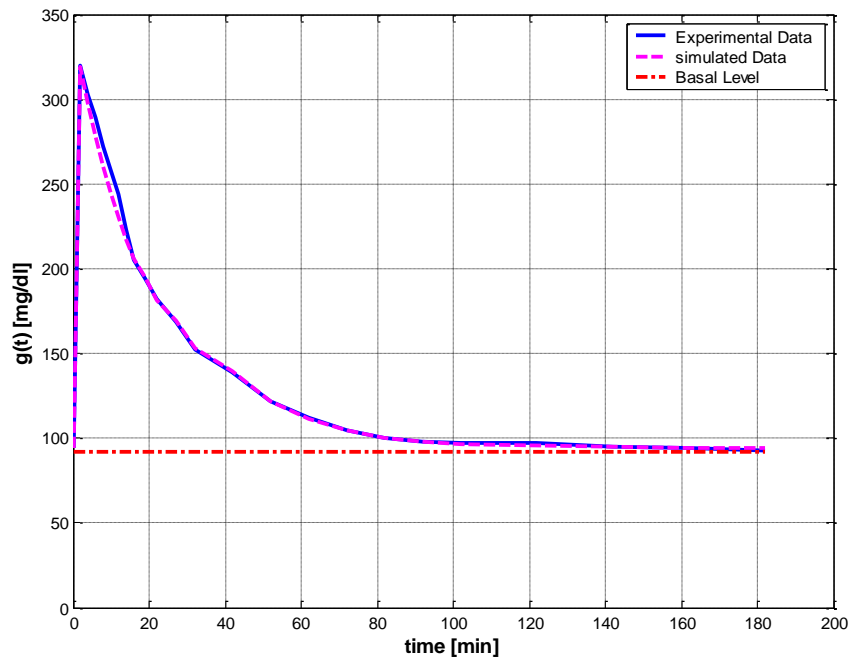
Figure 5.3 Plot of glucose level *g(t)* for normal individual #2

Figures 5.2 and 5.3 show that the two graphs (experimental and simulated) are close to each other. That leads to the conclusion that the estimated values of parameters are close to the actual values.

5.5   Square Relative Error:

In general, the **R**elative **E**rror, (RE) indicates how good an estimate is, in relative to the true values. Although absolute errors are useful, they do not necessarily give an indication of the importance of an error. If the experimental value is denoted by g, and the estimated (or simulated) value is denoted by $\hat{g}$, then the relative error is defined as

$$RE = \frac{g - \hat{g}}{g} \tag{5.23}$$

And the **S**quare **R**elative **E**rror, (SRE) can be expressed as

$$SRE = \left(\frac{g_i - \hat{g}_i}{g_i} \right)^2 \tag{5.24}$$

When the data is sampled over a certain period of time, the **M**ean **S**quare **R**elative **E**rror (MSRE) can be used. The MSRE is defined as

$$MSRE = \frac{1}{n} \sum_{i=1}^{n} \left(\frac{g_i - \hat{g}_i}{g_i} \right)^2, \quad \text{for } i = 1, 2, \ldots, n \tag{5.25}$$

where g_i is the experimental value at sample i, $\hat{g}_i$ is the estimated value at sample i, and where n is the number of samples of a data set.

The SRE between the experimental data and the simulated data of the glucose level for normal individuals #1 and # 2 are calculated based on equation 5.24 and shown in Table 5.4.

Normal individual #1

Normal individual #2

Experimental data, $g(t)$	Simulated data, $\hat{g}(t)$	SRE
94	94	0
298	295.6801	6.060466e-005
284	282.1308	4.3317e-005
272	268.2993	0.0001851148
253	254.8580	5.393524e-005
248	242.1020	0.0005656016
235	230.1353	0.0004285321
217	218.9702	8.243416e-005
208	208.5776	7.710311e-006
205	198.9116	0.0008820624
191	185.6659	0.0007799362
172	173.7810	0.0001072176
164	156.6159	0.002027272
141	142.2917	8.391868e-005
132	120.5167	0.007568141
120	105.8327	0.01393832
116	96.35277	0.0286871
108	90.67314	0.02573902
106	87.73594	0.02968814
104	86.65621	0.02781129
105	86.77255	0.03013514
109	89.03143	0.03356148
107	92.55181	0.01823304
110	95.65837	0.01699855

Experimental data, $g(t)$	Simulated data, $\hat{g}(t)$	SRE
94	94	0
320	318.84	1.314063e-005
303	297.2223	0.0003635986
289	277.7749	0.001508629
272	260.2561	0.001864179
258	244.4545	0.002756472
244	230.1878	0.003204405
223	217.2973	0.0006539557
205	205.6436	9.857924e-006
194	195.1034	3.235126e-005
182	181.1443	2.210359e-005
169	169.1246	5.439401e-007
152	152.6775	1.986409e-005
139	139.8434	3.681781e-005
122	122.0036	8.715616e-010
112	111.1272	6.073247e-005
105	104.4947	2.315634e-005
100	100.4500	2.024906e-005
98	97.98329	2.909034e-008
97	96.47894	2.88559e-005
97	95.56149	0.0002199282
95	94.66075	1.275242e-005
94	94.32573	1.200794e-005
93	94.20113	0.0001668063

Table 5.4 SRE data for between the experimental and simulated glucose level for normal individuals #1 and #2

The graphs of the SRE for both individuals are show in the figures below
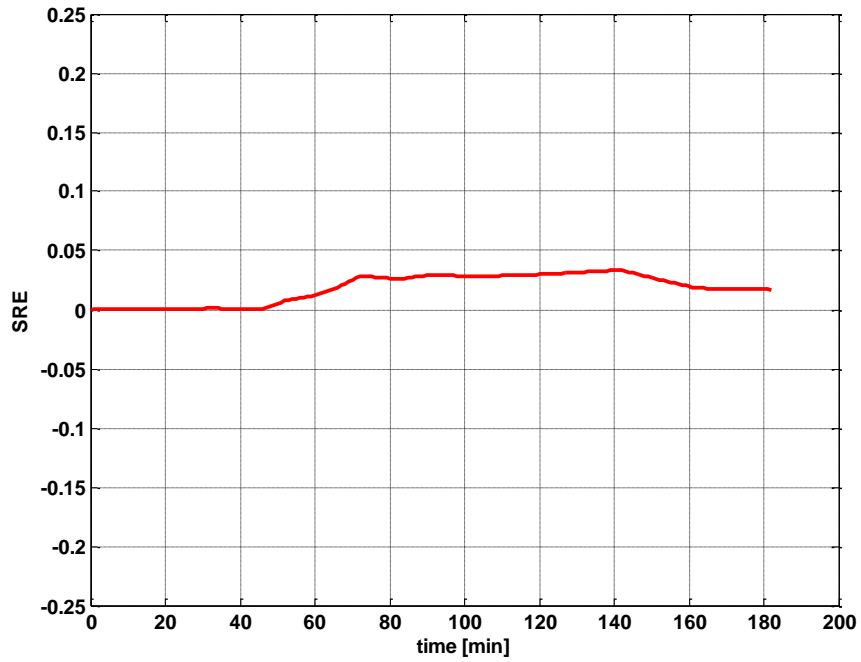
Figure 5.4 Plot of SRE for normal individual #1
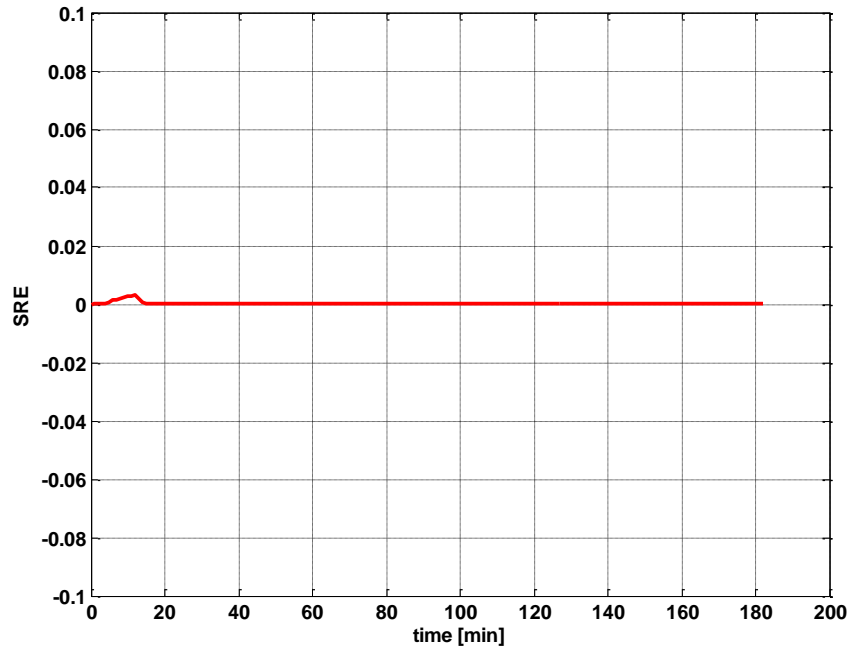
Figure 5.5 Plot of SRE for normal individual #2

Normally, the Mean Square Relative Error is expressed in percentage format. As per equation (5.25), the percentages MSRE for both individuals are listed below

- The percentage MSRE for individual # 1 = 1.79%.

- The percentage MSRE for individual # 2 = 0.0149%.

CHAPTER 6

PROPOSED MATHEMATICAL
MODEL AND IMPLEMENTATION

6.1   Introduction:

As stated in the previous chapters, the proposed mathematical model consists of three differential equations that describe the dynamic of a diabetic patient known as minimal model, and a fourth differential equation that represents a first order infusion pump 'P'. The role of pump 'P' is to inject the insulin into the system when the glucose level goes above the normal basal level.

6.2   Proposed Mathematical Model Analysis:

The differential equation represents the first order infusion pump 'P' is represented schematically in Figure 6.1
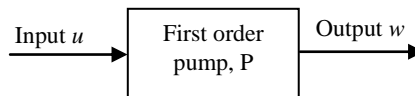
Figure 6.1 Block diagram of the infusion pump

The dynamic of the first order infusion pump is represented by the following equation

$$P(s) = \frac{1}{1 + as} \tag{6.1}$$

where "a" is the pump constant.

The relation between the input of the pump and its output can be written as

$$w = Pu \tag{6.2}$$

Substituting equation 6.1 into equation 6.2 will yield the following

$$w = \frac{1}{1+as}u \tag{6.3}$$

The above equation can be expressed as the following

$$w + asw = u \tag{6.4}$$

Taking the inverse laplace transform for both sides of the above equation yields the following

$$w(t) + a\left(\dot{w}(t) - w(0)\right) = u(t) \tag{6.5}$$

Since $w(0) = 0$, the above equation can be rearranged and written in the form of differential equation

$$\dot{w}(t) = \frac{1}{a}\left[-w(t) + u(t)\right] \tag{6.6}$$

The proposed mathematical model represented in the form of cascade block diagram is shown in the following figure
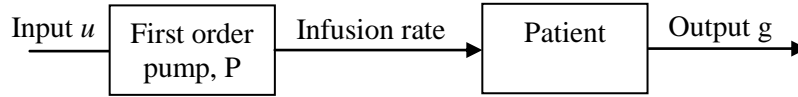
Figure 6.2 Schematic diagram of the proposed mathematical model

The proposed mathematical model that will be used consists of the following four differential equations

$$
\begin{aligned}
\dot{g}(t) &= -\left[P_1 + v(t)\right]g(t) + P_1 g_b \\
\dot{v}(t) &= -P_2 v(t) + P_3\left[i(t) - i_b\right] \\
\dot{i}(t) &= -n\,i(t) + \gamma\left[g(t) - h\right]t + w(t) \\
\dot{w}(t) &= \frac{1}{a}\left[-w(t) + u(t)\right]
\end{aligned}
\tag{6.7}
$$

The simulation diagram of the glucose kinetics model is shown in Figure 4.3 in chapter 4. The simulation diagram of the insulin kinetics model with the first order infusion part is shown in Figure 6.3.
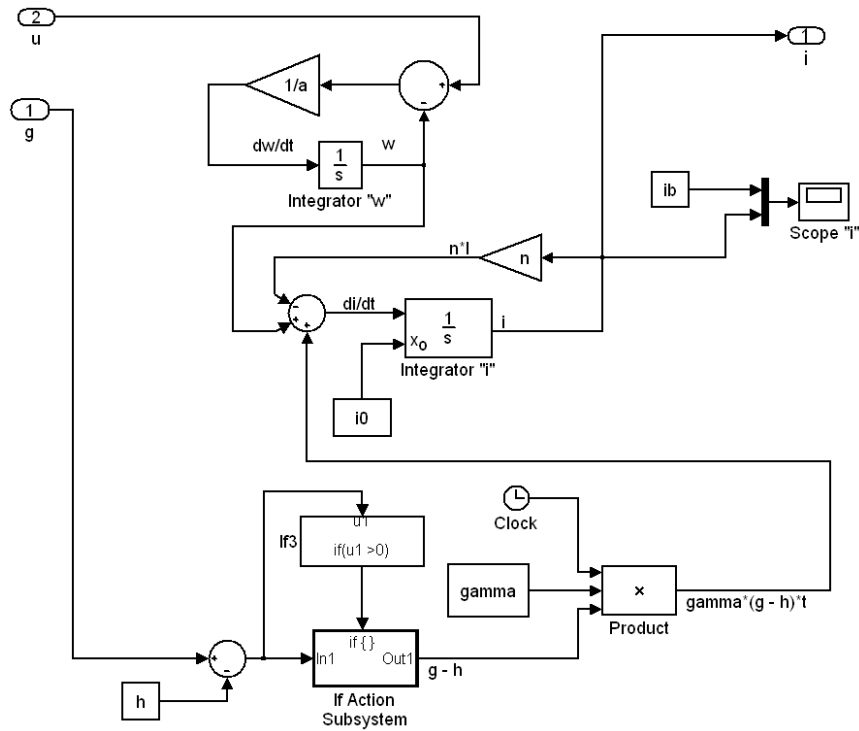
Figure 6.3 Insulin kinetics simulation diagram with first order infusion pump

The initial conditions of the above four differential equations are

$g(0) = g_0,\ v(0) = 0,\ i(0) = i_0,\ u(0) = 0.$

Define the following

$x_1(t) = g(t),\ x_2(t) = v(t),\ x_3(t) = i(t),\ x_4(t) = w(t)$

Then equation 6.7 can be rearranged as

$$\dot{x}_1(t) = -P_1 x_1(t) - x_1(t) x_2(t) + P_1 g_b$$

$$\dot{x}_2(t) = -P_2 x_2(t) + P_3 x_3(t) - P_3 i_b$$

$$\dot{x}_3(t) = -n x_1(t) - n x_3(t) + x_4(t) - \gamma ht \qquad (6.8)$$

$$\dot{x}_4(t) = -\frac{1}{a} x_4(t) + \frac{1}{a} u(t)$$

6.3 Linearization Overview:

Most components that are found in physical systems have nonlinear characteristics. In practice, some devices have moderate nonlinear characteristics, or nonlinear properties, that would occur if they were driven into certain operating regions. For these devices, the modeling by linear system give quite accurate analytical results over a relatively wide range of operating conditions. When a nonlinear system is linearized at an operating point, the linear model may contain time-variant elements [45]. If we are interested in values of the function close to some point, then often we can replace the given function by its first Taylor polynomial, which is a linear function. That is why the first Taylor polynomial is often called the local linearization. The use of linearization makes it possible to use tools for studying linear systems to analyze the behavior of a nonlinear function near a given point. The linearization of a function is the first order term of its Taylor expansion around the point of interest. To study the behavior of a nonlinear dynamical system near an equilibrium point, we can linearize the system.

The following is a brief discussion of the linearization of nonlinear first order equations by using the Taylor Series expansion and the Jacobian Matrix. Consider the following first order nonlinear equations

$$\dot{x}_1 = f_1\left(x_1, x_2, x_3, \ldots\ldots x_n, u_1, u_2, u_3, \ldots\ldots u_n\right)$$

$$\dot{x}_2 = f_2\left(x_1, x_2, x_3, \ldots\ldots x_n, u_1, u_2, u_3, \ldots\ldots u_n\right)$$

$$\dot{x}_3 = f_3\left(x_1, x_2, x_3, \ldots\ldots x_n, u_1, u_2, u_3, \ldots\ldots u_n\right) \qquad (6.9)$$

$$\vdots$$
$$\vdots$$

$$\dot{x}_n = f_m\left(x_1, x_2, x_3, \ldots\ldots x_n, u_1, u_2, u_3, \ldots\ldots u_n\right)$$

The above equation can be represented in the vector format as shown below

$$\dot{x} = f\left(x, u\right) \qquad (6.10)$$

where

$$\dot{x} = \begin{bmatrix} \dot{x}_1 \\ \dot{x}_2 \\ \dot{x}_3 \\ \vdots \\ \vdots \\ \dot{x}_n \end{bmatrix}, \quad x = \begin{bmatrix} x_1 \\ x_2 \\ x_3 \\ \vdots \\ x_n \end{bmatrix} \quad and \quad u = \begin{bmatrix} u_1 \\ u_2 \\ u_3 \\ \vdots \\ u_n \end{bmatrix} \qquad (6.11)$$

The Taylor Series expansion of equation (6.10) is

$$f\left(x\right) = f_0 + a_1\left(x - x_0\right) + b_1\left(u - u_0\right) + \text{h.o.t} \qquad (6.12)$$

where

$$f_0 = f\left(x_0, u_0\right)$$

$$a_1 = \left.\frac{df\left(x, u\right)}{dx}\right|_{x=x_0,\, u=u_0}$$

$$b_1 = \left.\frac{df\left(x, u\right)}{du}\right|_{x=x_0,\, u=u_0}$$

h.o.t is the Higher Order Term.

The point (x_0, u_0) is the equilibrium point which can be found by setting up the function $f(x, u)$ equals to zero, then $f(x_0, u_0) = 0$. The Jacobian Matrix is the matrix of all first-order partial derivatives of a vector-valued function. If a function is differentiable at a point, its derivative is given in coordinates by the Jacobian, but a function does not need to be differentiable for the Jacobian to be defined, since only the partial derivatives are required to exist. Its importance lies in the fact that it represents the best linear approximation to a differentiable function near a given point. In this sense, the Jacobian is the derivative of a multivariate function. For a function of n variables, $n > 1$, the derivative of a numerical function must be matrix-valued, or a partial derivative. The partial derivatives of all the functions $f_1(x, u), f_2(x, u), f_3(x, u), \ldots, f_m(x, u)$ (if they exist) can be organized in an m-by-n matrix, the Jacobian Matrices (J_x and J_u), of the function f with respect to x and u, as follows

$$J_x = \frac{df(x,u)}{dx}\bigg|_{x=x_0,\, u=u_0} = \begin{bmatrix} \frac{\partial f_1}{\partial x_1} & \frac{\partial f_1}{\partial x_2} & \frac{\partial f_1}{\partial x_3} & \cdots & \frac{\partial f_1}{\partial x_n} \\[2mm] \frac{\partial f_2}{\partial x_1} & \frac{\partial f_2}{\partial x_2} & \frac{\partial f_2}{\partial x_3} & \cdots & \frac{\partial f_2}{\partial x_n} \\[2mm] \frac{\partial f_3}{\partial x_1} & \frac{\partial f_3}{\partial x_2} & \frac{\partial f_3}{\partial x_3} & \cdots & \frac{\partial f_3}{\partial x_n} \\[2mm] \vdots & \vdots & \vdots & \ddots & \vdots \\[2mm] \frac{\partial f_m}{\partial x_1} & \frac{\partial f_m}{\partial x_2} & \frac{\partial f_m}{\partial x_3} & \cdots & \frac{\partial f_m}{\partial x_n} \end{bmatrix}_{x=x_0,\, u=u_0} \qquad (6.13)$$

$$\mathbf{J}_u = \frac{df(x,u)}{du}\bigg|_{x=x_0,\,u=u_0} = \begin{bmatrix} \dfrac{\partial f_1}{\partial u_1} & \dfrac{\partial f_1}{\partial u_2} & \dfrac{\partial f_1}{\partial u_3} & \cdots\cdots & \dfrac{\partial f_1}{\partial u_n} \\[2mm] \dfrac{\partial f_2}{\partial u_1} & \dfrac{\partial f_2}{\partial u_2} & \dfrac{\partial f_2}{\partial u_3} & \cdots\cdots & \dfrac{\partial f_2}{\partial u_n} \\[2mm] \dfrac{\partial f_3}{\partial u_1} & \dfrac{\partial f_3}{\partial u_2} & \dfrac{\partial f_3}{\partial u_3} & \cdots\cdots & \dfrac{\partial f_3}{\partial u_n} \\[2mm] \vdots & \vdots & \vdots & \ddots & \vdots \\[2mm] \dfrac{\partial f_m}{\partial u_1} & \dfrac{\partial f_m}{\partial u_2} & \dfrac{\partial f_m}{\partial u_3} & \cdots\cdots & \dfrac{\partial f_m}{\partial u_n} \end{bmatrix}_{x=x_0,\,u=u_0} \tag{6.14}$$

The linearized form of the nonlinear system can be written in the state space form as the following

$$\dot{x} = J_x x + J_u u \tag{6.15}$$

6.4 Proposed Mathematical Model Linearization:

The proposed mathematical model is a nonlinear model due to the presence of the term $x_1(t)x_2(t)$ which is a nonlinear term. The Jacobian Matrices (J_x and J_u) are calculated by differentiating equation (6.8) with respect to the state variables $x_1,\ x_2,\ x_3,\ x_4$ and the input u, and substitute in the equations (6.13) and (6.12) we get the following

$$\mathbf{J}_x = \begin{bmatrix} -P_1 - x_2 & -x_1 & 0 & 0 \\ 0 & -P_2 & P_3 & 0 \\ \gamma t & 0 & -n & 1 \\ 0 & 0 & 0 & -\dfrac{1}{a} \end{bmatrix}_{x=x_0,\,u=u_0} \quad \text{and } \mathbf{J}_u = \begin{bmatrix} 0 \\ 0 \\ 0 \\ \dfrac{1}{a} \end{bmatrix}_{x=x_0,\,u=u_0} \tag{6.16}$$

where the point $(x_0,\ u_0)$ is the equilibrium point. The equilibrium point can be calculated by setting the state equation to zero and solve as shown below

$$-P_1 x_{10} - x_{10}x_{20} + P_1 g_b = 0 \tag{6.17}$$

$$-P_2 x_{20} + P_3 x_{30} - P_3 i_b = 0 \tag{6.18}$$

$$\gamma t x_{10} - n x_{30} - \gamma h t + x_{40} = 0 \tag{6.19}$$

$$-\frac{1}{a} x_{40} + \frac{1}{a} u_0 = 0 \tag{6.20}$$

where, x_{10}, x_{20}, x_{30}, x_{40} and u_0 are the values of the state variables and the input at the operating

point (i.e. the equilibrium point).

At the equilibrium point, $u_0 = 0$, then equation (6.20) becomes as $-\frac{1}{a} x_{40} = 0$, that gives

$$x_{40} = 0 \tag{6.21}$$

Substituting the value of x_{40} in equation (6.19) results $\gamma t x_{10} - n x_{30} - \gamma h t = 0$ and

$$x_{30} = \frac{(x_{10} - h)\gamma t}{n} \tag{6.22}$$

The value of X_{30} can be substituted in equation (6.18) as $-P_2 x_{20} + P_3 \dfrac{(x_{10} - h)\gamma t}{n} - P_3 i_b = 0$ to

obtain

$$x_{20} = \frac{P_3 \gamma t x_{10}}{P_2 n} - \frac{P_3 \gamma t h}{P_2 n} - \frac{P_3 i_b}{P_2} \tag{6.23}$$

Now, by substituting the value of x_{20} in equation (6.17), we have

$$-\frac{P_3 \gamma t}{P_2 n}(x_{10})^2 + \left(-P_1 + \frac{P_3 \gamma t h}{P_2 n} + \frac{P_3 i_b}{P_2}\right) x_{10} + P_1 g_b = 0 \tag{6.24}$$

The above equation is a 2nd order equation of the form $ax^2 + bx + c = 0$ and can be solved by

using the quadratic formula

$$x_{10} = \frac{-b \pm \sqrt{b^2 - 4ac}}{2a} \tag{6.25}$$

where $a = -\dfrac{P_3 \gamma t}{P_2 n}$, $b = -P_1 + \dfrac{P_3 \gamma t h}{P_2 n} + \dfrac{P_3 i_b}{P_2}$, $c = P_1 g_b$.

There are two possible values (solutions) of x_{10}. Since x_{20} and x_{30} are expressed in term of x_{10}, there will be two values for each. Based on that, the controllability test will be studied to check which value of x_{10} is accepted.

6.5   Proposed Mathematical Model Experimental Study:

The following are the parameters values of the mathematical minimal model that represent the dynamic of a diabetic patient [27-29]

$P_1 = 0$

$P_2 = 0.81/100$

$P_3 = 4.01/1000000$

$i_0 = 192$

$g_0 = 337$

$\gamma = 2.4/1000$

$h = 93$

$n = 0.23$

$g_b = 99$

$i_b = 8$

$a = 2$

These values of the parameters are substituted in the patient dynamic system and the simulation is run using the minimal model simulation diagram that is shown in Figure 4.5. The result of the simulation is shown in Figure 6.4.

By examining Figure 6.4, it can be clearly seen that the glucose level does not come down to the basal level after injecting an amount of 337 mg/dl of glucose inside a diabetic patient. The graph shows that the level of glucose inside a diabetic patient decreases for almost the first 100 minutes and starts increasing afterward and reaches the value of almost 310 mg/dl after 3 hours from the time the glucose was injected [46]. The goal is to lower the value of glucose inside a diabetic patient to the normal level or at least to the neighborhood of the basal level.
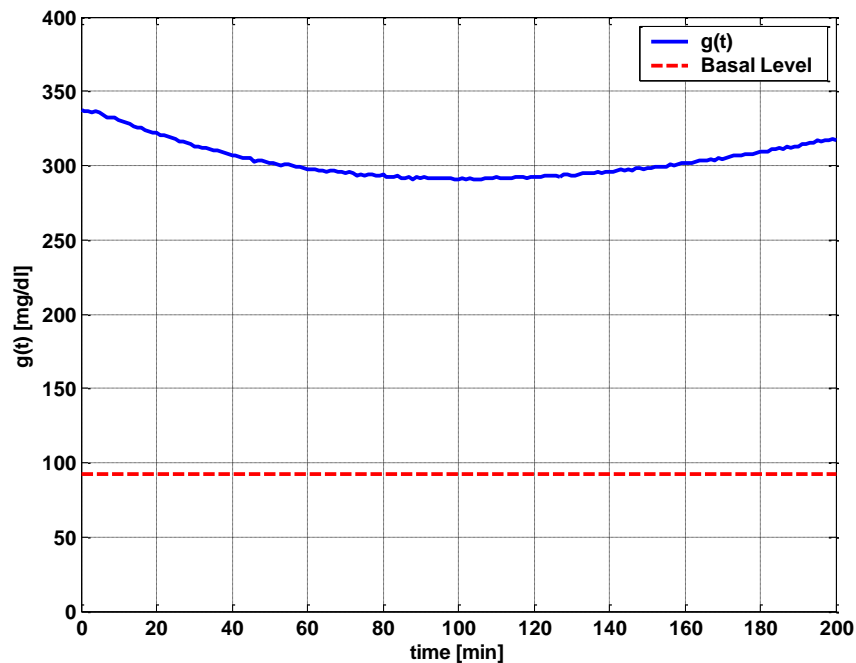
Figure 6.4 Simulated glucose level *g(t)* for diabetic patient

6.6   State Space Representations:

The state space method is based on the description of the system equation in terms of *n* first order difference equations or differential equations, which may be combined into a first order vector matrix difference equations or differential equations [47]. Let us define some terms of the state space system.

- State Variables: The variables making up the smallest set of variables that determine the state of the dynamic system.

- State Vector: If n state variables are needed to completely describe the behaviour of a given system, then the n state variable can be considered the n component if the vector.

- State Space Equation: There are three types of variable that are involved in the modeling of dynamic systems

    i. Input Vector.

    ii. Output Vector.

    iii. State Variable.

The general form of the state space is defined as

$$\dot{x} = Ax + Bu$$
$$y = Cx + Du$$

(6.26)

where

x is the state vector.

y is the output vector.

u is the control vector.

A is the state matrix.

B is the control matrix.

C is the output matrix.

D is the direct transmission matrix.

The proposed mathematical model at the equilibrium point $(x_0,\ u_0)$ can be written in the state space form as shown below

$$\dot{x} = \begin{bmatrix} -P_1 - x_{20} & -x_{10} & 0 & 0 \\ 0 & -P_2 & P_3 & 0 \\ \gamma t & 0 & -n & 1 \\ 0 & 0 & 0 & -\dfrac{1}{a} \end{bmatrix} x + \begin{bmatrix} 0 \\ 0 \\ 0 \\ \dfrac{1}{a} \end{bmatrix} u \tag{6.27}$$

$$y = \begin{bmatrix} 1 & 0 & 0 & 0 \end{bmatrix} x$$

where u is the input and y is the output of the system. The data of a diabetic person shown in section 6.5 was used, and the equilibrium point (x_0, u_0) was calculated as time varied from $t = 1$ min to $t = 182$ min. The two values for x_{10} were calculated using equation (6.25), and it was found that only one of these values, (the one obtained from the $\dfrac{-b - \sqrt{b^2 - 4ac}}{2a}$), makes the system controllable; hence, only this value is used in the subsequent development.

6.7   Transfer Function and State Space Representations:

A dynamic system can be expressed either in the state space representation or in the transfer function representation. The transfer function of a continuous time-invariant state space model can be derived by taking the laplace transform of the sate space equation (see equation 6.26).

The laplace transform of

$$\dot{x} = Ax + Bu$$
$$y = Cx + Du$$

yields

$$sX(s) = AX(s) + BU(s)$$
$$Y(s) = CX(s) + DU(s) \tag{6.28}$$

Solve the above equation for $X(s)$ as

$$X(s) = (sI - A)^{-1} BU(s) \tag{6.29}$$

Substitute $X(s)$ in the oputput of the system as

$$Y(s) = C\left((sI - A)^{-1} BU(s)\right) + DU(s) \tag{6.30}$$

Rearrange equation (6.30) yields

$$Y(s) = \left(C(sI - A)^{-1} B + D\right)U(s) \tag{6.31}$$

Since the transfer function of a dynamic system is defined as the ratio of the output to the input

of a system, then

$$G(s) = \frac{Y(s)}{U(s)} = C(sI - A)^{-1} B + D \tag{6.32}$$

CHAPTER 7

LOW-COMPLEXITY REGIME-SWITCHING

INSULIN CONTROL OF TYPE 'I' DIABETIC PATIENTS

7.1   Overview:

This chapter studies the benefits of using simplified adaptation control strategies in improving performance of insulin control for type 'I' diabetic patients. Typical dynamic models of glucose levels in diabetic patients are nonlinear. Using a linear time-invariant controller based on an operating condition is a common method to simplify control design. On the other hand, adaptive control can potentially improve system performance, but it increases control complexity and may create further stability issues. This research investigates patient model identification and presents a simplified switching control scheme using PID controllers [46]. By comparing different switching schemes, it shows that switched PID controllers can improve performance, but frequent switching is unnecessary. These findings lead to a control strategy that utilizes only a small number of PID controllers in this scheduled adaptation strategy.

7.2   Introduction to PID Controller:

In the control of any dynamic system, no controller has better reliability than that of the PID controller. Out of all the control design techniques, the PID controller becomes the most widely known and used one. There are many different types and design methods for the PID controller. Since many control systems using PID controller have proven satisfactory, it still has a wide range of applications in industrial control [48]. According to a survey for process control

systems conducted in 1989, more than 90% of the control loops were of the PID type [49]. PID controller popularity comes from its simplicity and its ability to be used in a wide variety of processes. PID controller has been an active research topic for many years.

The term PID stands for **P**roportional, **I**ntegral and **D**erivative. Each one of these letters (**P, I, D)** is term in a control algorithm, and each has a special purpose. It is possible to a PI controller, PD controller or P controller. It has been found from the experimental point of view that the structure of the PID controller has sufficient flexibility to yield excellent results in many dynamic applications [50].

7.3   PID Controller Configuration:

A typical structure of a PID control system is shown in figure 7.1. The basic term is the proportional term, **P**, which causes a corrective control actuation proportional to the error. The integral term, **I**, gives a correction proportional to the integral of the error. This has the positive feature of ultimately ensuring that sufficient control effort is applied to reduce the tracking error to zero. However, integral action tends to have a destabilizing effect due to the increased phase shift. The derivative term, **D**, gives a predictive capability yielding a control action proportional to the rate of change of the error. This tends to have a stabilizing effect but often leads to large control movements due to the amplification of noise by the derivative action. Various empirical tuning methods can be used to determine the PID parameters for a given application. They should be considered as a first guess in a search procedure. Attention should also be paid to the PID structure [50].
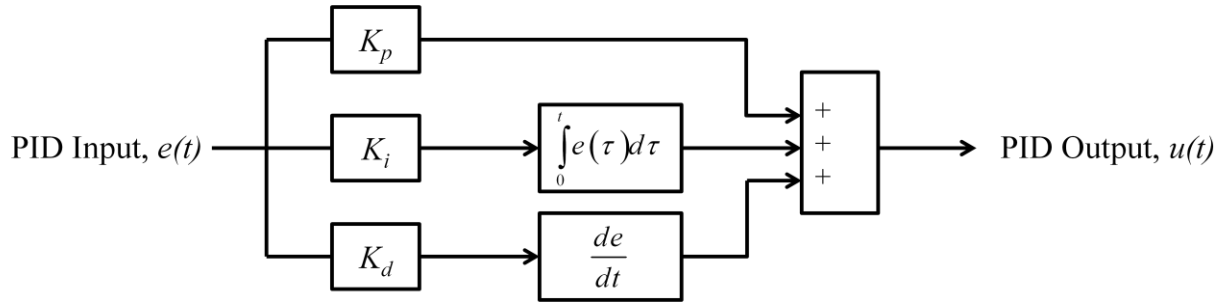
Figure 7.1 PID controller structure

From the above figure, it can be clearly seen that in a PID controller, the error signal $e(t)$ is used to generate the proportional, integral, and derivative actions, with the resulting signals weighted and summed to form the control signal $u(t)$ applied to the plant model. A mathematical description of the continuous time linear PID controller is

$$u(t) = K_p e(t) + K_i \int_0^t e(\tau)d\tau + K_d \frac{de(t)}{dt} \tag{7.1}$$

where, K_p, K_i, K_d, e, and u are proportion gain, integral gain, derivative gain, error, and output of the PID controller respectively [51].

7.4 The Characteristics of PID Controller:

A proportional controller (K_p) will have the effect of reducing the rise time and will reduce but never eliminate the steady-state error. An integral control (K_i) will have the effect of eliminating the steady state-error, but it may make the transient response worse. A derivative control (K_d) will have the effect of increasing the stability of the system, reducing the overshoot, and improving the transient response. Effects of each of controllers K_p, K_i and K_d on a closed-loop system are summarized in Table 7.1 [51-53].

Performance Specifications				
Closed-Loop Response	**Rise Time**	**Overshoot**	**Settling Time**	**Steady-State Error**
K_p	Decrease	Increase	Small Change	Decrease
K_i	Decrease	Increase	Increase	Eliminate
K_d	Small Change	Decrease	Decrease	Small Change

Table 7.1 PID performance measurement tuning table

Note that these correlations may not be exactly accurate, because K_p, K_i, and K_d are dependent of each other. In fact, changing one of these variables can change the effect of the other two. For this reason, the table should only be used as a reference when you are determining the values for K_p, K_i and K_d.

The transfer function, Gc(s), of the PID controller can be calculated by taking the laplace transform of equation (7.1) which is expressed in the time domain. The following table shows the laplace transform of the PID controller terms

$f(t)$	$F(s)$
$u(t)$	$U(s)$
$e(t)$	$E(s)$
$\int_0^t e(\tau)d\tau$	$\dfrac{1}{s}E(s)$
$\dfrac{de(t)}{dt}$	$s.E(s)$

Table 7.2 Laplace transform of PID controller terms

Equation (7.1) can be written in the s-domain as

$$U(s) = K_p E(s) + K_i \frac{1}{s} E(s) + K_d s E(s) \tag{7.2}$$

Rearranging equation (7.2) yield

$$U(s) = \left(K_p + K_i \frac{1}{s}(s) + K_d s \right) E(s) \tag{7.3}$$

The transfer function of the PID controller is

$$Gc(s) = \frac{U(s)}{E(s)} = K_p + \frac{K_i}{s} + K_d s \tag{7.4}$$

The gain K_p is the control action that is proportional to the actuating error signal, which is the difference between the reference input and the feedback signal or the output. The gain K_i is the control action which is proportional to the integral of the actuating error signal. Finally, the gain K_d is the control action which is proportional to the derivative of the actuating error signal. With the integration of all the three actions, the continuous PID can be designed [51].

Equation (7.4) can be rearranged as

$$Gc(s) = \frac{K_p s^2 + K_d s + K_i}{s} \tag{7.5}$$

Based in equation (7.5), the PID controller adds one pole at S=0 and two zeros wherever needed. Normally, the location of the two zeros is where the two slowest poles can be canceled to be able to get the best result.

7.5   Design of Individual PID Controllers for Diabetic Patient:

When designing a controller, the designer must define the specifications that need to be achieved by the controller. Normally, the maximum overshoot (Mp) of the system step response should be small. Commonly, a range between 10% and 20% is acceptable. Also the settling time

(t_s), is an important factor. The objective here is to design a PID controller so that the closed-loop system has the following specifications

- Small steady state error for a step input.

- Less than 10% maximum overshoot, (M_p).

- Settling time, (t_s), less than 60 minutes.

The damping ratio ζ and the natural frequency ω_n are related to the maximum overshoot and the settling time by the following relations

$$\zeta = \sqrt{\frac{\left(\dfrac{\ln\left(M_p\right)}{\pi}\right)^2}{1+\left(\dfrac{\ln\left(M_p\right)}{\pi}\right)^2}} \tag{7.6}$$

$$\omega_n = \frac{4}{\zeta t_s} \tag{7.7}$$

The patient dynamic system with the parameters shown in section 6.5 was expressed in the state space representation in equation (7.8). For an overshoot less than 10%, a damping ratio must be greater than 0.59, and a settling time less than 60 minutes implies that $\left(\zeta\omega_n\right)$ must be greater than 0.067.

$$\dot{x} = \begin{bmatrix} -P_1 - x_{20} & -x_{10} & 0 & 0 \\ 0 & -P_2 & P_3 & 0 \\ \gamma t & 0 & -n & 1 \\ 0 & 0 & 0 & -\dfrac{1}{a} \end{bmatrix} x + \begin{bmatrix} 0 \\ 0 \\ 0 \\ \dfrac{1}{a} \end{bmatrix} u$$

$$y = \begin{bmatrix} 1 & 0 & 0 & 0 \end{bmatrix} x \tag{7.8}$$

Analyzing equation (7.8), it is obvious that matrix A is time variant while B and C do not change with time, and they are fixed in all cases as

$$B = \begin{bmatrix} 0 \\ 0 \\ 0 \\ 0.5 \end{bmatrix} \text{ and } C = \begin{bmatrix} 1 & 0 & 0 & 0 \end{bmatrix}$$

The PID controllers can be designed based on the following operating points $t = 1, 20, 40, 60, 90, 120, 150$ and 182 minutes.

7.5.1 Design of PID controller at operating point $t = 1$ minute:

The control design is done by applying the root locus method and then evaluates it by using the step response. After substituting the numerical values at operating point $t = 1$ minute, the matrix A of equation (7.8) becomes

$$A_1 = \begin{bmatrix} 0 & -859.6667 & 0 & 0 \\ 0 & -0.0081 & 0.00000401 & 0 \\ 0.0024 & 0 & -0.23 & 1 \\ 0 & 0 & 0 & -0.5 \end{bmatrix}$$

The root locus plot can be generated by the following Matlab program (7.1).

MATLAB Program 7.1
Plotting the open loop system Root locus using MATLAB
[num, den] = ss2tf(A,B,C,D);
rlocus(num, den)
axis([–0.6 0.1 –0.5 0.5])
sgrid(0.59,0)
sigrid(0.067)
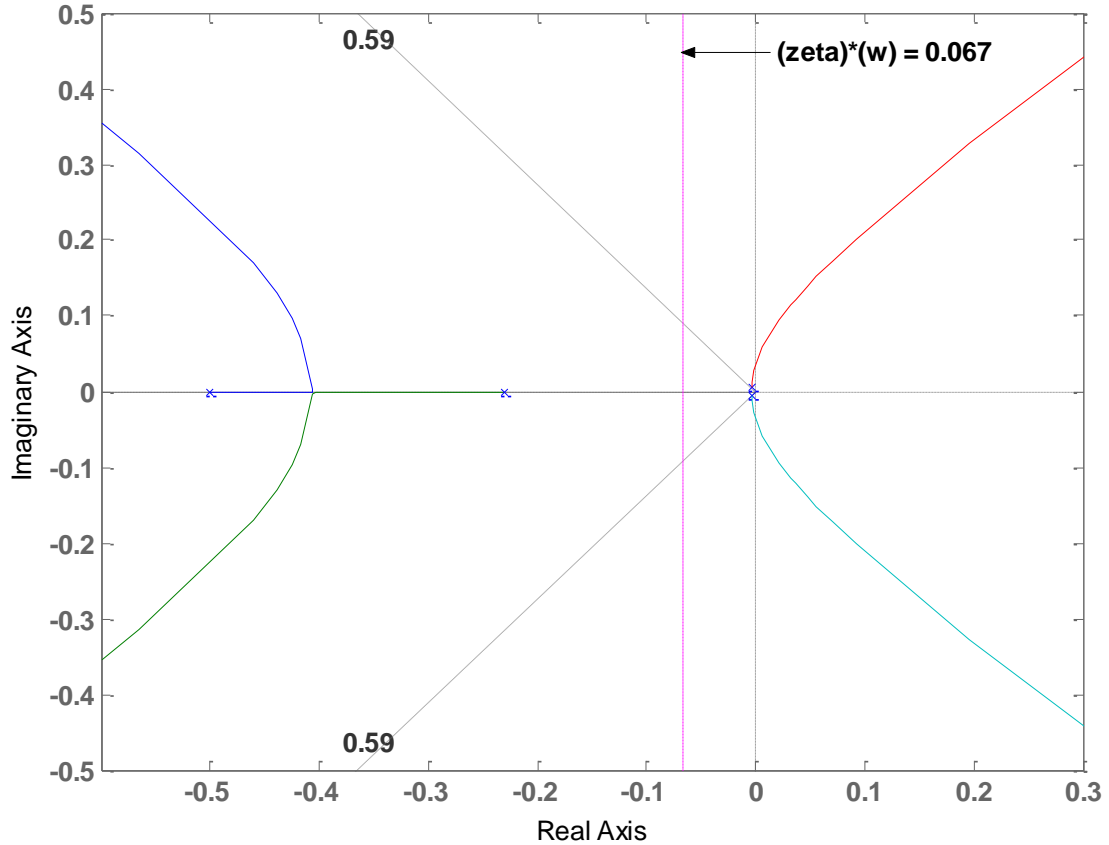
Figure 7.2 Root Locus plot at operating point $t = 1\ minute$

The open loop poles are shown in Figure 7.2. These poles are located at the following location

Pole $1 = -0.0040 + 0.0045\text{j}$

Pole $2 = -0.0040 - 0.0045\text{j}$

Pole $3 = -0.2302$

Pole $4 = -0.5$

The four poles are stable, but the first two poles are very close to the imaginary axis and hence represent the slowest dynamics. The controller takes the form

$$Gc(s) = \frac{K(s + z_1)(s + z_2)}{s} \qquad (7.9)$$

where K is the value of the gain where the root locus intersects with the line of the damping ratio.

The z_1 and z_2 represent the value of the zeros to be added and may be selected to cancel the slowest poles of the dynamic system. Hence, select

$z_1 = -0.004 + 0.0045\text{j}$

$z_2 = -0.004 - 0.0045\text{j}$

Substituting the values of z_1 and z_2 in equation (7.9) yields

$$Gc(s) = \frac{K\left(s - \left(-0.0040 + 0.0045j\right)\right)\left(s - \left(-0.0040 - 0.0045j\right)\right)}{s}$$

The above equation can be written in the following form:

$$G_c^1(s) = \frac{K\left(s^2 + 0.008s + 0.00003625\right)}{s}$$

where $G_c^1(s)$ represents the transfer function at operating point $t=1$ minute.

The design specifications of the system require the maximum overshoot to be less than 10% and the settling time to be less than 60 minutes. After inserting the PID controller in series with the patient system and connecting them in a unity feedback, it is noted that may be there are more than one value of the gain K that make the system meet the design specifications. These values are analyzed to pick up the best values. Table 7.3 shows the values of the gain K.

Gain K sorted by Maximum Overshoot		
Gain K	Maximum Overshoot %	Settling Time (min)
5.59	5.7625	47
6.59	9.4362	43

Table 7.3 PID gain K at operating *point t = 1 minute*

The value of gain $K = 5.59$ gives maximum overshoot 5.71% and the settling time 47.5 minutes (see Figure 7.3). The PID parameters are

$K_p = 0.0444$, $K_i = 2.0094 \times 10^{-4}$, $K_d = 5.59$.
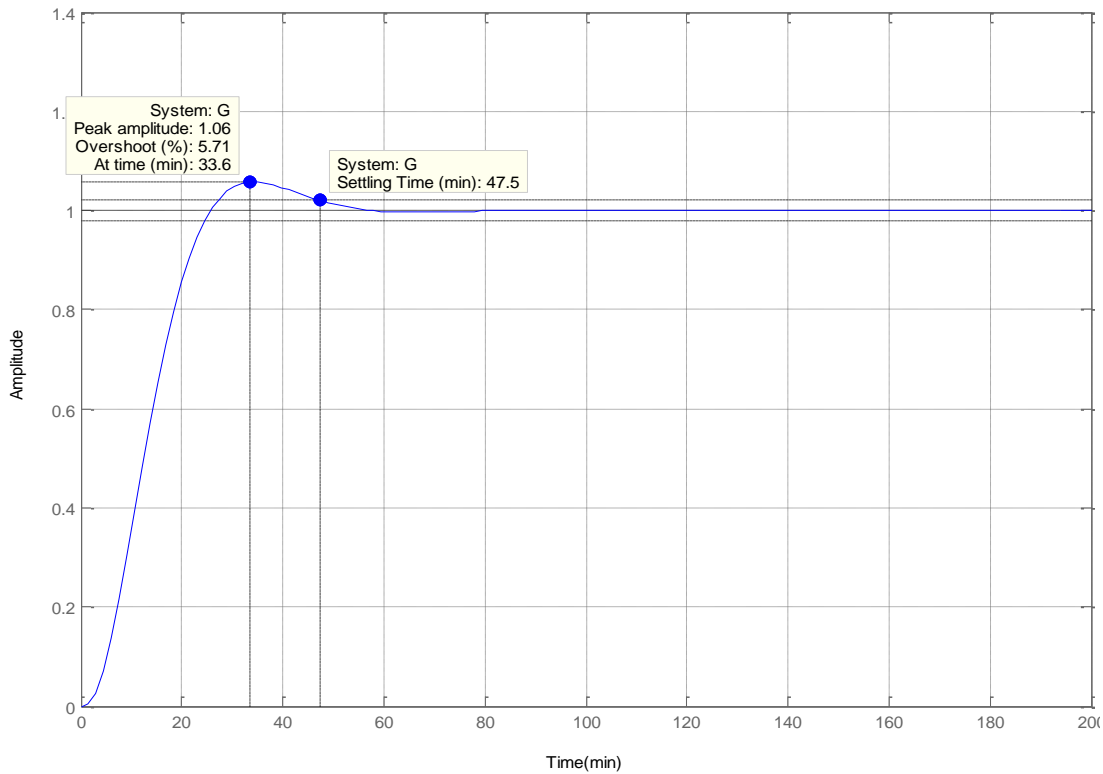
Figure 7.3 Unit step response using model at operating point $t = 1$ minute with $K=5.59$

7.5.2 Design of PID controller at operating point $t = 20$ minutes:

After substituting the numerical values at operating point $t = 20$ minutes, matrix A of equation (7.8) becomes

$$A_{20} = \begin{bmatrix} 0 & -131.33 & 0 & 0 \\ 0 & -0.0081 & 0.00000401 & 0 \\ 0.048 & 0 & -0.23 & 1 \\ 0 & 0 & 0 & -0.5 \end{bmatrix}$$

The open loop poles of the system are found by the root locus plot to be

Pole $1 = -0.0038 + 0.0098j$

Pole $2 = -0.0038 - 0.0098j$

Pole 3 = − 0.2305

Pole 4 = − 0.5

The z_1 and z_2 represent the value of the zeros to be added and may be selected to cancel the slowest poles of the dynamic system. Hence, select

$z_1 = -0.0038 + 0.0098j$

$z_2 = -0.0038 - 0.0098j$

Substituting the values of z_1 and z_2 in equation (7.9) yields

$$G_c^{20}(s) = \frac{K(s^2 + 0.0076s + 0.0001)}{s}$$

The same procedure of operating point $t = 1$ *minutes* is repeated for operating point $t = 20$ *minutes*. Table 7.4 shows the values of the gain K.

Gain K sorted by Maximum Overshoot		
Gain K	Maximum Overshoot %	Settling Time (min)
28.4	1.5633	33
29.4	1.9903	32
30.4	2.4456	48
31.4	2.9223	48
32.4	3.4279	49
33.4	3.9415	48
34.4	4.4716	48
35.4	5.0160	48
36.4	5.5662	47
37.4	6.1187	47
38.4	6.8840	46
39.4	7.2625	45
40.4	7.8303	45
41.4	8.3902	44
42.4	8.9785	44
43.4	9.5369	43

Table 7.4 PID gain K at operating *point t = 20 minutes*

The value of gain $K = 28.4$ gives maximum overshoot 1.5633% and the settling time 33 minutes.

The PID parameters are

$K_p = 0.02160$, $K_i = 0.0031$, $K_d = 28.4$.

7.5.3 Design of PID controller at operating point $t = 40$ minutes:

At operating point $t = 40$ minutes, matrix A becomes

$$A_{40} = \begin{bmatrix} 0 & -112.17 & 0 & 0 \\ 0 & -0.0081 & 0.00000401 & 0 \\ 0.096 & 0 & -0.23 & 1 \\ 0 & 0 & 0 & -0.5 \end{bmatrix}$$

The open loop poles of the system are found by the root locus plot to be

Pole $1 = -0.0036 + 0.00132j$

Pole $2 = -0.0036 - 0.00132j$

Pole $3 = -0.2308$

Pole $4 = -0.5$

The z_1 and z_2 represent the value of the zeros to be added and may be selected to cancel the slowest poles of the dynamic system. Hence, select

$z_1 = -0.0036 + 0.00132j$

$z_2 = -0.0036 - 0.00132j$

Substituting the values of z_1 and z_2 in equation (7.9) yields

$$G_c^{40}(s) = \frac{K\left(s^2 + 0.0072s + 0.0002\right)}{s}$$

The value of gain $K = 32.7$ gives maximum overshoot 1.2489% and the settling time 34 minutes.

The PID parameters are

$K_p = 0.02374,\ K_i = 0.0061,\ K_d = 32.7.$

7.5.4   Design of PID controller at operating point $t = 60$ minutes:

At operating point $t = 60$ minutes, matrix A becomes

$$A_{60} = \begin{bmatrix} 0 & -105.78 & 0 & 0 \\ 0 & -0.0081 & 0.00000401 & 0 \\ 0.144 & 0 & -0.23 & 1 \\ 0 & 0 & 0 & -0.5 \end{bmatrix}$$

The open loop poles are

Pole $1 = -0.0035 + 0.00159j$

Pole $2 = -0.0035 - 0.00159j$

Pole $3 = -0.2312$

Pole $4 = -0.5$

The PID controller is

$$G_c^{60}(s) = \frac{K\left(s^2 + 0.007s + 0.0003\right)}{s}$$

The value of gain $K = 34.9$ gives maximum overshoot 1.3898% and the settling time 34 minutes.

The PID parameters are

$K_p = 0.02483,\ K_i = 0.0095,\ K_d = 35.9.$

7.5.5   Design of PID controller at operating point $t = 90$ minutes:

At operating point $t = 90$ minutes, matrix A becomes

$$A_{90} = \begin{bmatrix} 0 & -101.52 & 0 & 0 \\ 0 & -0.0081 & 0.00000401 & 0 \\ 0.216 & 0 & -0.23 & 1 \\ 0 & 0 & 0 & -0.5 \end{bmatrix}$$

The open loop poles are

Pole $1 = -0.0032 + 0.00192j$

Pole $2 = -0.0032 - 0.00192j$

Pole $3 = -0.2317$

Pole $4 = -0.5$

The PID controller is

$$G_c^{90}(s) = \frac{K(s^2 + 0.0064s + 0.0004)}{s}$$

The value of gain $K = 36.9$ gives maximum overshoot 1.3601% and the settling time 34 minutes.

The PID parameters are

$K_P = 0.02331$, $K_i = 0.0138$, $K_d = 36.4$.

7.5.6 Design of PID controller at operating point $t = 120$ minutes:

At operating point $t = 120$ minutes, matrix A becomes

$$A_{120} = \begin{bmatrix} 0 & -99.39 & 0 & 0 \\ 0 & -0.0081 & 0.00000401 & 0 \\ 0.288 & 0 & -0.23 & 1 \\ 0 & 0 & 0 & -0.5 \end{bmatrix}$$

The open loop poles are

Pole $1 = -0.0029 + 0.022j$

Pole $2 = -0.0029 - 0.022j$

Pole 3 $= -0.2322$

Pole 4 $= -0.5$

The PID controller is

$$G_c^{120}(s) = \frac{K(s^2 + 0.0058 + 0.0005)}{s}$$

The value of gain $K = 37.9$ gives maximum overshoot 1.5325% and the settling time 33 minutes.

The PID parameters are

$K_P = 0.02234,\ K_i = 0.0187,\ K_d = 37.9.$

7.5.7 Design of PID controller at operating point $t = 150$ minutes:

At operating point $t = 150$ minutes, matrix A becomes

$$A_{150} = \begin{bmatrix} 0 & -98.11 & 0 & 0 \\ 0 & -0.0081 & 0.00000401 & 0 \\ 0.36 & 0 & -0.23 & 1 \\ 0 & 0 & 0 & -0.5 \end{bmatrix}$$

The open loop poles are

Pole 1 $= -0.0027 + 0.0245j$

Pole 2 $= -0.0027 - 0.0245j$

Pole 3 $= -0.2327$

Pole 4 $= -0.5$

The PID controller is

$$G_c^{150}(s) = \frac{K(s^2 + 0.0054 + 0.0006)}{s}$$

The value of gain $K = 37.7$ gives maximum overshoot 1.2922% and the settling time 34 minutes.

The PID parameters are

$K_P = 0.02032$, $K_i = 0.0229$, $K_d = 37.7$.

7.5.8 Design of PID controller at operating point $t = 182$ minutes:

At operating point $t = 182$ minutes, matrix A becomes

$$A_{182} = \begin{bmatrix} 0 & -97.21 & 0 & 0 \\ 0 & -0.0081 & 0.00000401 & 0 \\ 0.4368 & 0 & -0.23 & 1 \\ 0 & 0 & 0 & -0.5 \end{bmatrix}$$

The open loop poles are

Pole $1 = -0.0024 + 0.0269j$

Pole $2 = -0.0024 - 0.0269j$

Pole $3 = -0.2332$

Pole $4 = -0.5$

The PID controller is

$$G_c^{182}(s) = \frac{K\left(s^2 + 0.0048 + 0.0007\right)}{s}$$

The value of gain $K = 38.5$ gives maximum overshoot 1.3766% and the settling time 34 minutes.

The PID parameters are

$K_P = 0.0187$, $K_i = 0.0281$, $K_d = 38.5$.

Non-adaptive PID controllers use a fixed PID controller for the entire control period and rely on its robustness to maintain control performance [51, 52]. For each individual PID controller with its transfer function found in the previous subsection at operator points $t = 1, 20,$

40, 60, 90, 120, 150, and 182 minutes, the system is simulated using the simulation diagram

shown in figure 7.4. The results of *g(t)* are shown below in Figures 7.5 and 7.6.
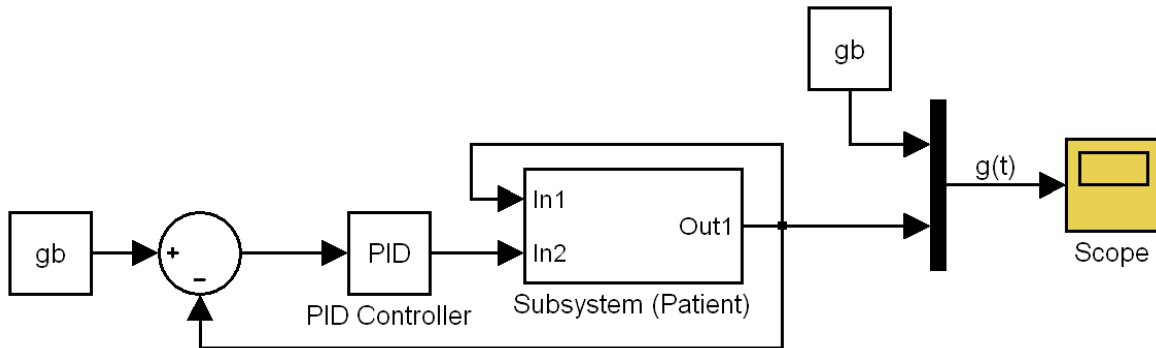
Figure 7.4 Simulation diagram of the diabetic patient with PID controller
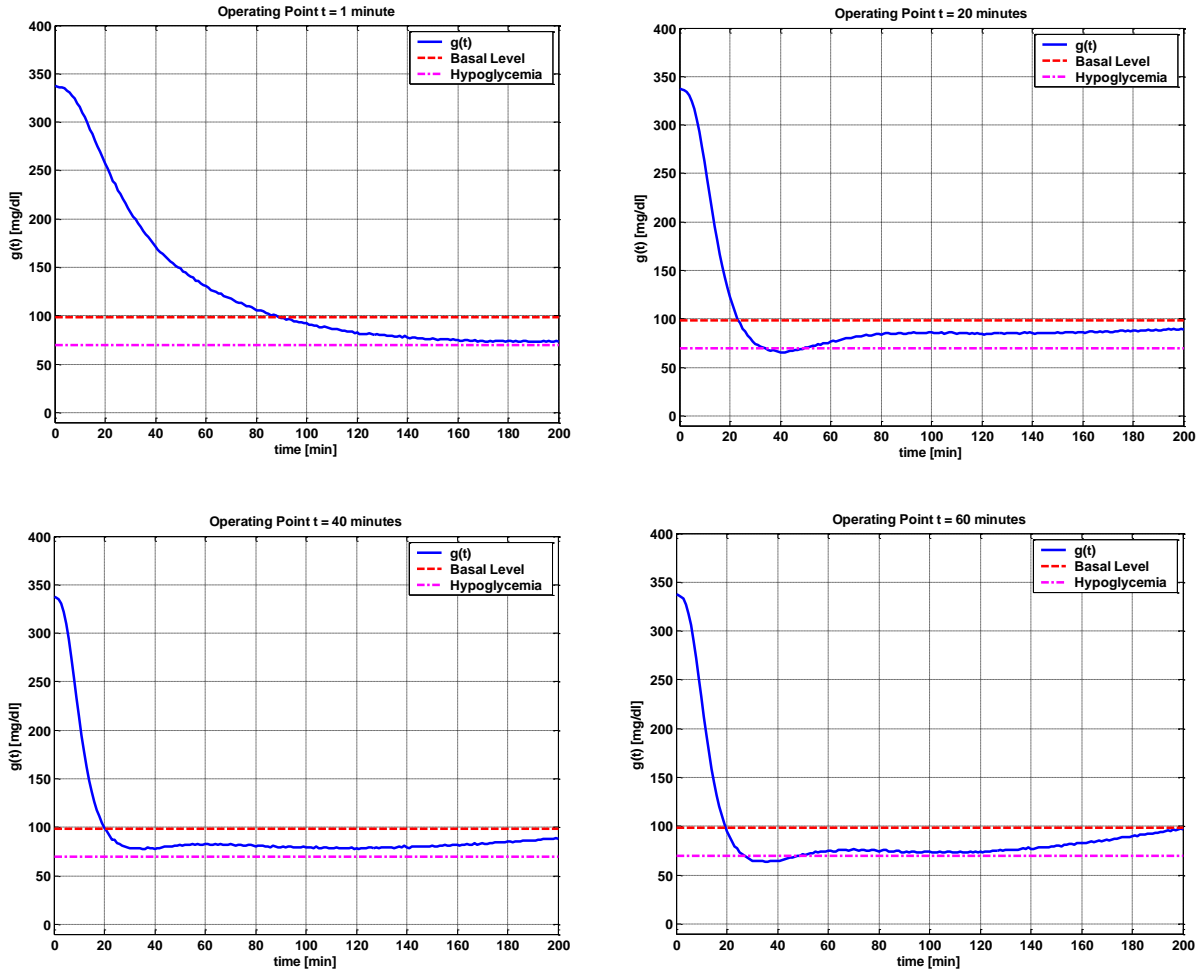
Figure 7.5 Simulation of glucose level of PID controllers
at operating points *t= 1, 20, 40, and 60 minutes*
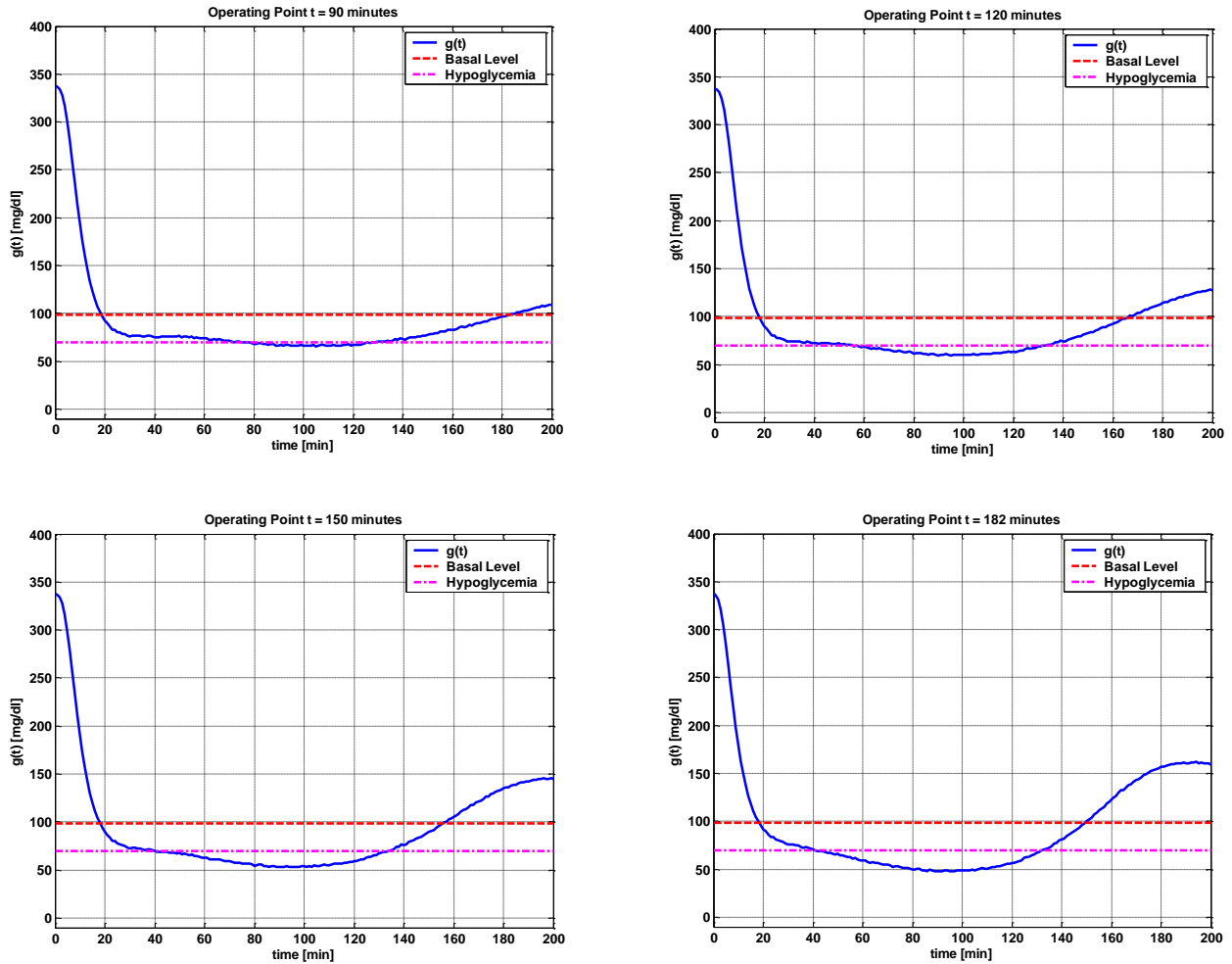
Figure 7.6 Simulation of glucose level of PID controllers
at operating points *t= 90, 120, 150, and 182 minutes*

Under the individual PID controllers, the output *g(t)*, the glucose level, did not really meet the design specification, and the glucose level is not near or at least in a small neighborhood of the glucose basal level. The overshoot of the system was too high and beyond the acceptable level. Also, the settling time was not even close to where it should be as per the design requirement. And the steady state error was not satisfactory. A new method should be

developed and implemented to meet all the design specifications. This method is explained in detail in the following section.

7.6   Regime-Switching PID Controller Scheme:

The individual PID controllers could not lower the glucose level $g(t)$ of the patient to the neighborhood of the glucose basal level. Consequently, we introduce a new Regimes-Switching control scheme that adapts controllers to meet design specifications. The control scheme consists of the following items:

- ➢ One "time clock".
- ➢ One "switch case" block.
- ➢ One "if action case" block.
- ➢ One "merge" block.
- ➢ Eight "off–on switches".

All these blocks are connected together to form the wiring diagram of the Regime-Switching control scheme. The functions of the Regime-Switching control scheme are detailed in Figures 7.7 and 7.8.
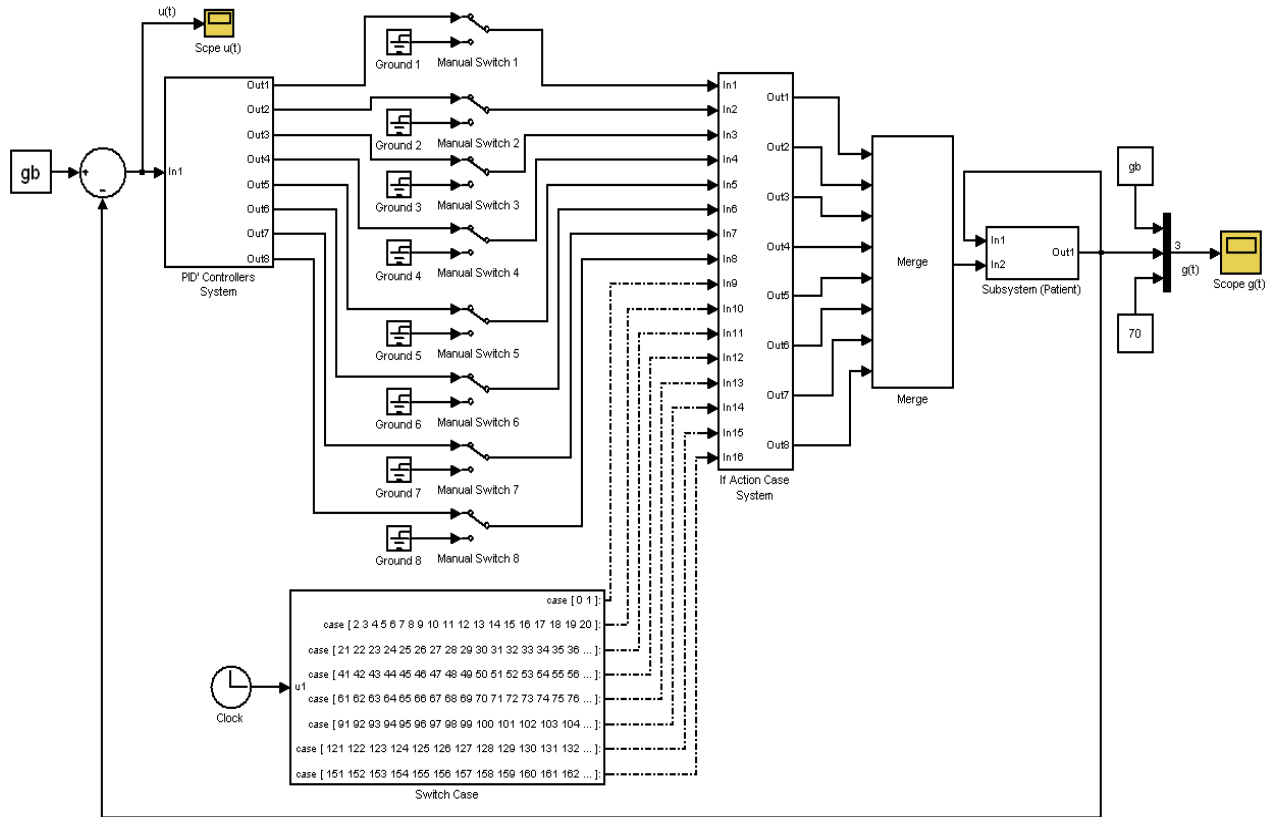
Figure 7.7 Regime-Switching Control Scheme wiring diagram
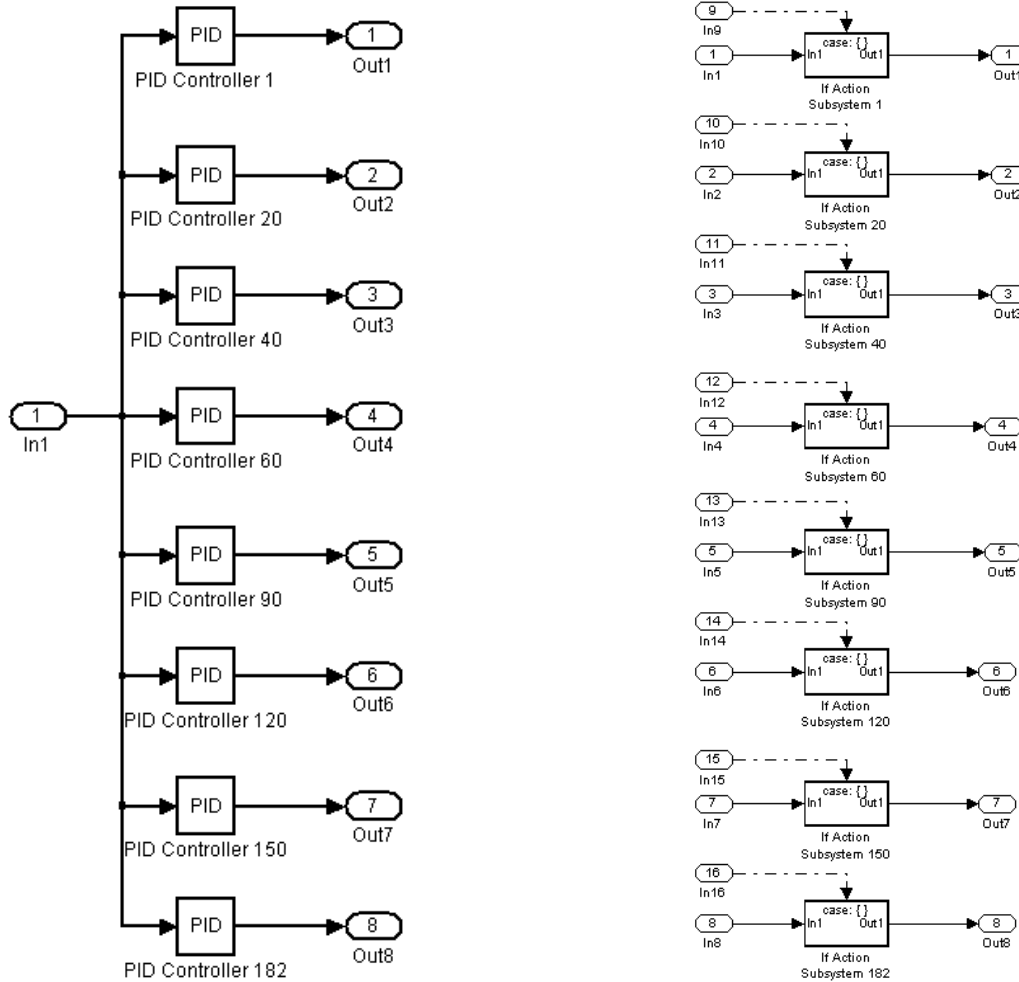
Figure 7.8 PID controller and "If-Action-Case" system switching function modules

The following is a brief explanation of each of the switching control scheme component

➢ The "Time Clock" is to provide the "Switch Case" block with time as a signal input to activate it.

➢ The "Switch Case" block receives a single input from the clock, which it uses to form case conditions that determine which subsystem to execute. Each output port case condition is attached to a "Switch Case Action" subsystem. The cases are evaluated top-down, starting with the top case. If a case value corresponds to the actual value of the

input, its "Switch Case Action" subsystem is executed. The "Switch Case" model is divided into eight time interval zones as shown in Table 7.5.

Zone number	Time Interval (minutes)
1	0 – 1
2	2 – 20
3	21 – 40
4	41 – 60
5	61 – 90
6	91 – 120
7	121 – 150
8	150 – 182

Table 7.5 Regime-Switching time interval

➤ The "If Action Case" block consists of eight "If-Action Subsystems." The "If-Action Case" implements Action Subsystems used in the "If-Statement" and switches control flow statements. Action Subsystems execute their programming in response to the conditional outputs of an "If-Statement" or "Switch Case" block. A schematic diagram of the "If Action Case" block is shown in Figure 7.8.

➤ The "Merge" block combines its inputs into a single output line whose value at any time is equal to the most recently computed output of its driving blocks. The number of inputs can be specified by setting the block's inputs parameter.

➤ The "Off-On Switches" are Cut-Off switches to turn the PID controllers OFF or ON for testing purposes.

➤ The "PID Controller System" contains eight PID at operating points *t = 1, 20, 40, 60, 90, 120, 150, and 182 minutes*.

In general, when the time clock is running, it feeds the "Switch Case" block with an input signal which in turn switches on the "If-Action Case" block as per the time interval that was specified in Table 7.5. Based on the status of the "If-Action Case", a specific PID controller will be turned on and executed to control the output of the system.

For zone 1, the time interval is between 0-1 minute. During this period of time the "Switch Case" is enabling input "In9" of the "If-Action Case". When input "In9" is enabled, it will only execute the input "In1" to the output "Out1". The input "In1" is connected to the first PID Controller. That means only the first PID Controller (PID Controller 1) is working. At the end of the first minute, the "Switch Case" will switch to zone 2 which runs from the beginning of the minute number 2 and will last until the end of the minute number 20. During this period of time, the "Switch Case" is enabling input "In10" of the "If-Action Case". When input "In10" is enabled, it will only execute the input "In2" to the output "Out2". The input "In2" is connected to the second PID Controller. That means only the second PID Controller (PID Controller 20) is working. The same procedure will be followed until the "Switch Case" switches between the eight time zones that were specified in Table 7.5. In turn, the PID Controllers will be executed based on the status of the "If-Action Case".

The Regime-Switching Control Scheme shown in Figure 7.7 was simulated with all the PID controllers executed (connected to the circuit). The output $g(t)$ of the system is shown in Figure 7.9. It can be clearly seen that the PID controllers are able to bring the glucose level from 337 mg/dl to the basal level (99 mg/dl) within 40 minutes. But in about 70 minutes, the value of the glucose starts going below the basal level, and it went further below the minimum value of the glucose level. In this case, the person will be classified as a patient with hypoglycemia (low sugar), and that is not acceptable.
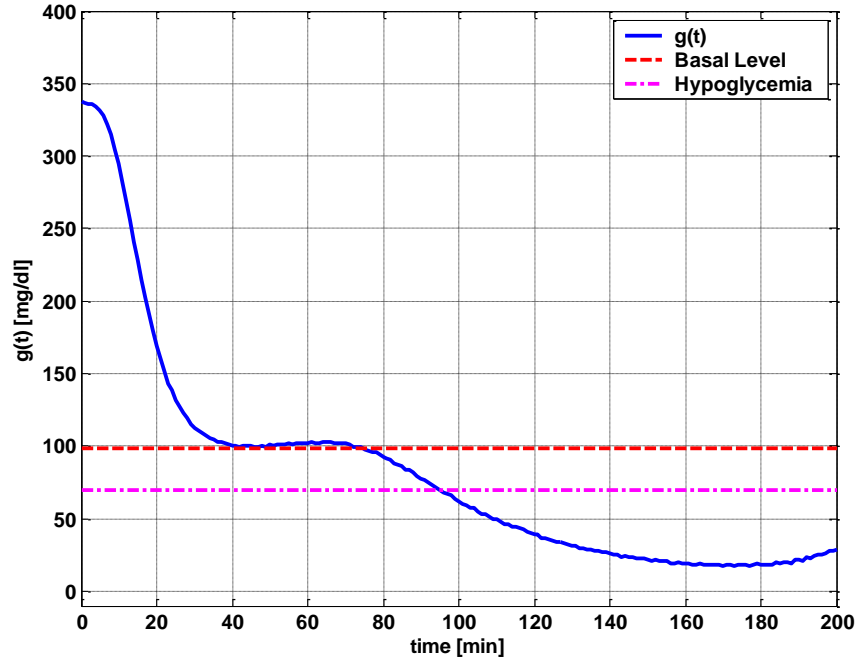
Figure 7.9 Plot of glucose level *g(t)* when all PID controllers are executed

The Regime-Switching Control Scheme was simulated in which all the PID controllers are executed except the eighth PID controller G_C^{182}. The graph of the output *g(t)* of the system is shown in Figure 7.10. It can be seen that the same problem still exists. Again in this case, the person will be classified as a patient with hypoglycemia.
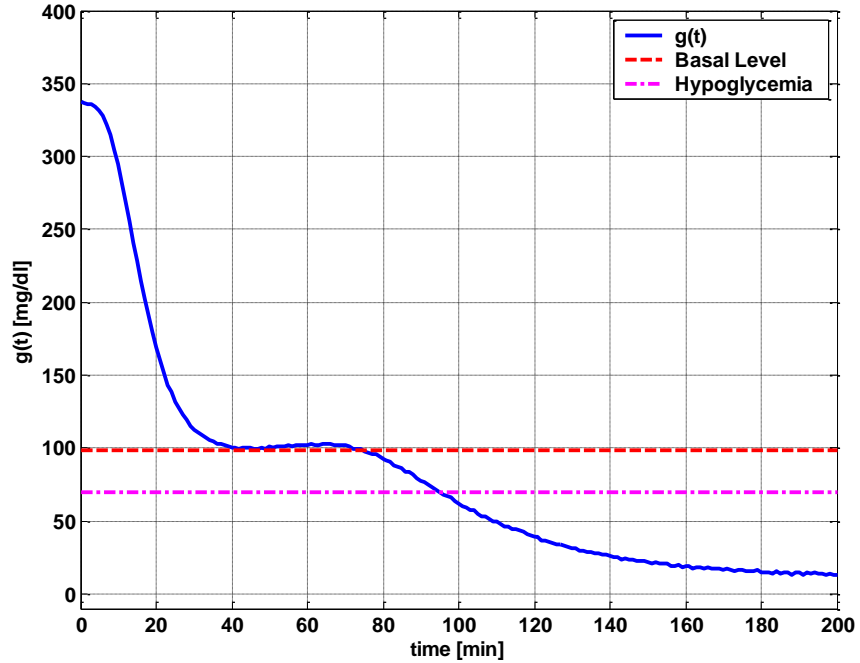
Figure 7.10 Plot of glucose level *g(t)* when all PID controllers except
controller G_c^{182} are executed

The same procedure was repeated but with all the PID controllers executed except the PID controllers G_C^{150} and G_C^{182} with the graph of the output *g(t)* shown in Figure 7.11; and excluding G_C^{120}, G_C^{150}, and G_C^{182} with the simulation result of the output *g(t)* shown Figure 7.12. Again, the glucose levels are still below the minimum value and in both cases, the person will be classified as a patient with hypoglycemia.
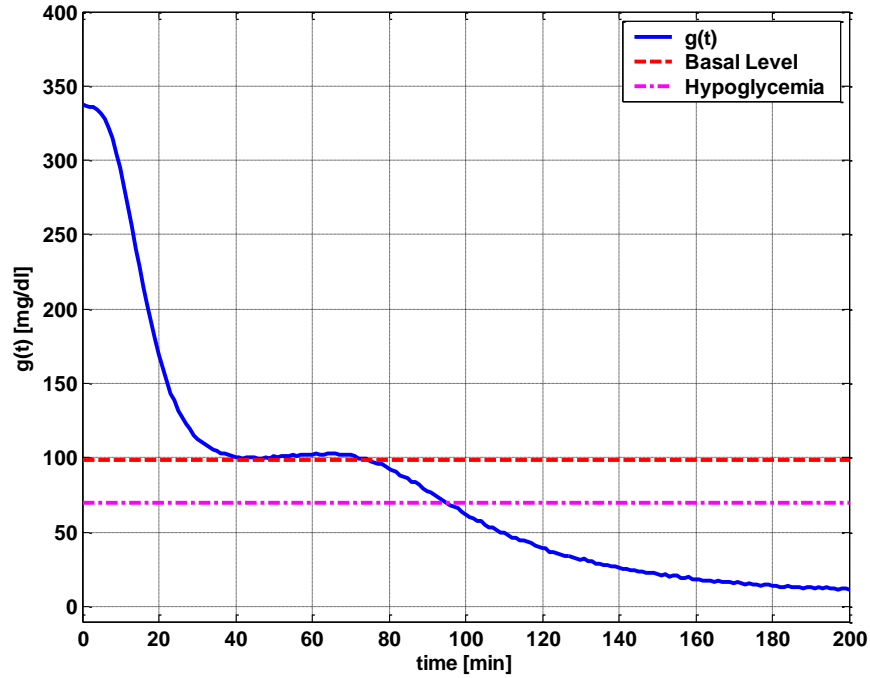
Figure 7.11 Plot of glucose level *g(t)* when all PID Controllers except controllers G_c^{150} and G_c^{182} are executed
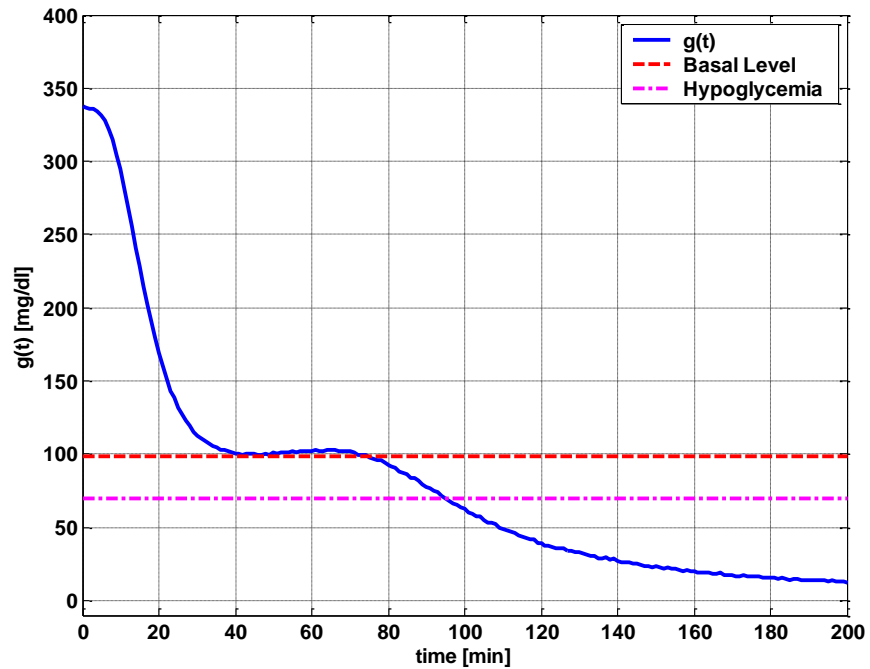
Figure 7.12 Plot of glucose level *g(t)* when all PID controllers except controllers G_c^{120}, G_c^{150} and G_c^{182} are executed

When we exclude controllers G_C^{90}, G_C^{120}, G_C^{150}, and G_C^{182} and run the simulation of the system, the output $g(t)$ of the system, shown in Figure 7.13, reaches the glucose basal level (99 mg/dl) within 40 minutes, and it stays in that neighborhood.
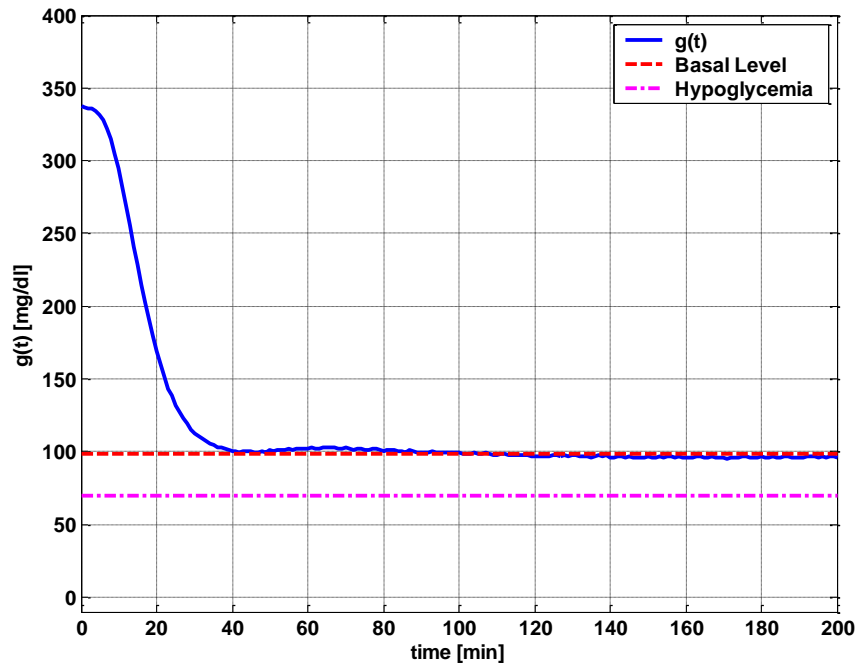
Figure 7.13 Plot of glucose level $g(t)$ when all PID controllers except controllers G_c^{90}, G_c^{120}, G_c^{150} and G_c^{182} are executed

For verification, the same control strategy is evaluated on diabetic patient #2. Following the same modeling procedure that was performed for the diabetic patient #1, the model parameters are identified [27-29] as

$P1 = 0$

$P2 = 0.42/100$

$P3 = 2.56/1000000$

$i_0 = 209$

$g_0 = 297$

$\gamma = 3.72/1000$

$h = 154$

$n = 0.22$

$a = 2$

$g_b = 100$

$i_b = 8$

Without the Regime-Switching Control Scheme, the above data was implemented in model simulation. The output of the simulation diagram is shown in Figure 7.14, which shows that without proper control, the glucose level does not come down to the basal level after injecting an amount of 297 mg/dl of glucose inside a diabetic patient. The level of the glucose inside a diabetic patient decreases for the first 120 minutes and starts increasing afterward where it reaches the value of about 270 mg/dl after 3 hours from the time the glucose was injected.
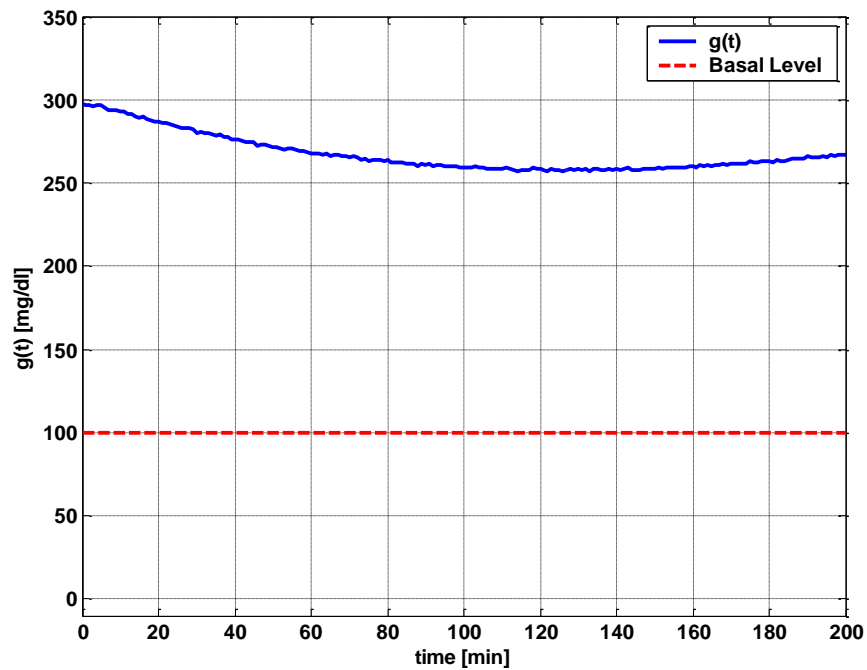
Figure 7.14 Plot of glucose level *g(t)* of diabetic patient #2
without control scheme

The same control switching scheme that was performed for diabetic patient #1 is repeated for diabetic patient #2. The values of the parameters for the first four PID controllers at operating point *t = 1, 20, 40 and 60 minutes* are summarized in Table 7.6.

PID Controllers Parameters				
Gain	PID at t = 1 min	PID at t = 20 min	PID at t = 40 min	PID at t = 60 min
K_p	0.0412	0.1069	0.0868	0.0768
K_i	$2.7402*10^{-4}$	0.0047	0.0086	0.014
K_d	10.1	30.6	33.1	33.6

Table 7.6 Paramters of PID controller for diabetic patient #2

The Regime-Switching Control Scheme was simulated for diabetic patient #2 by using only the first four PID controllers. The graph of the output of the system is shown in Figure 7.15. The output *g(t)* reaches the glucose basal level (100 mg/dl) within 60 minutes, and it stays in that neighborhood.
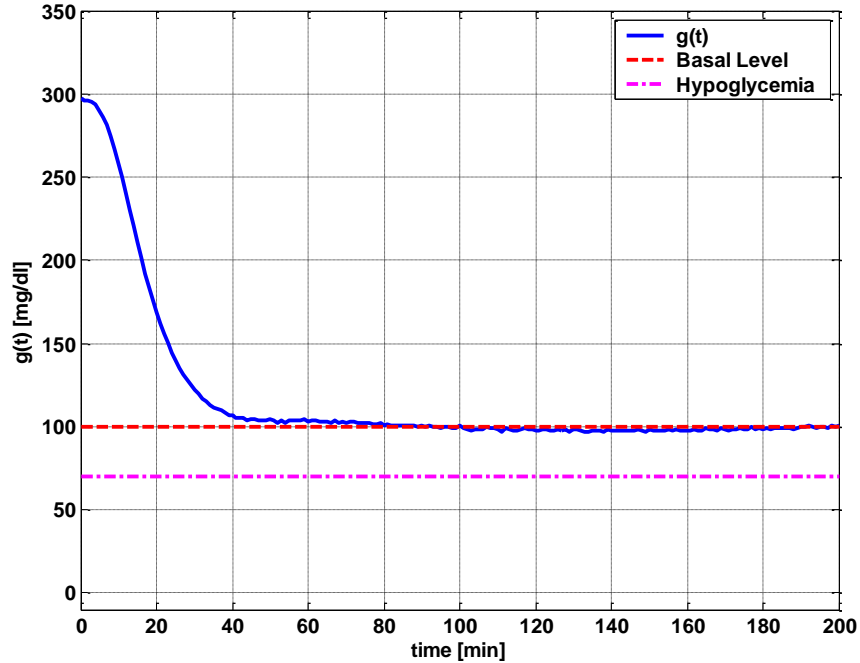
Figure 7.15 Plot of glucose level *g(t)* of diabetic patient #2 when all PID controllers except controllers G_c^{90}, G_c^{120}, G_c^{150} and G_c^{182} are executed

7.7   Conclusion:

Based on the simulation results, although adaptive control can potentially improve control performance, it is sometimes unnecessary, or even harmful, when switching overly frequently. Our results show that when the Regime-Switching Control Scheme is limited to the first four PID controllers, the performance is, in fact, enhanced. This may be related to the fact that some PID controllers are more robust with respect to the model variations. On the other hand, in comparison to individual controllers, the Regime-Switching Control Scheme achieves design specification while all individual controllers fail to deliver the required performance.

CHAPTER 8

OBSERVER-BASED STATE FEEDBACK DESIGN

8.1   Introduction:

During the past few decades, biomedical modeling techniques have been applied to improve performance of diabetes that requires monitoring and control. This research focuses on designing a state feedback controller with an observer to improve the performance of the insulin control for type 'I' diabetic patients [54]. The dynamic model of glucose levels in diabetic patients is a nonlinear model. Using a linear time invariant controller based on an operating condition is a common method to simplify control design. This research investigates patient models and presents a simplified control scheme using observer-based feedback controller.

8.2   Introduction to State Feedback Controller:

The design of the state feedback controller is based on the pole placement method using the Ackermann's Formula, with the assumption that all the state variables are measurable and are available for feedback. If the system is completely state controllable, then the poles of the closed loop system may be placed at any desired locations by means of state feedback through an appropriate state feedback gain matrix. By choosing the gain matrix for the state feedback, it is possible to force the system to have closed loop poles at the desired location, provided that the original system is completely state controllable [51].

8.3   Design of State Feedback Controller:

The state feedback design can be designed on the basis of the pole placement method. In the pole placement method, the closed loop poles will be placed at desired locations. While this is similar to root-locus method used in the PID design, the main difference is that in the root-locus method, only the dominant closed loop poles will be placed at the desired locations. When designing a controller by the pole placement method, the designer must define the specifications that need to be achieved by the controller [51, 53]. The objective is to design a state feedback controller so that the closed-loop system has the following specifications: a small steady-state error under a step input; less than 10% overshoot; and a settling time less than 60 minutes [54]. We shall choose the control signal to be [51]

$$u = -Kx \tag{8.1}$$

That means that the control signal u is determined by an instantaneous state feedback. Such a scheme is well known as state feedback. The $1 \times n$ matrix K is the state feedback gain matrix.

Substituting equation (8.1) into the state space equation $\dot{x} = Ax + Bu$, it becomes

$$\dot{x} = (A - BK)x \tag{8.2}$$

The stability and the transient response characteristics are determined by the eigenvalues of matrix $A - BK$. The eigenvalues of matrix $A - BK$ are called the regular poles. If these poles are placed in the left half s plane, then $x(t)$ approaches zero as t approaches infinity [55-57]. The well known Ackermann's Formula is used to determine the value of the matrix K [51]. Let the desired closed loop poles be

$$s = \mu_1, \ s = \mu_2, \ s = \mu_3, \ and \ s = \mu_4$$

The desired characteristic equation is

$$\left|sI - A + BK\right| = (s-\mu_1)(s-\mu_2)(s-\mu_3)(s-\mu_4)$$
$$= s^4 + \alpha_1 s^3 + \alpha_2 s^2 + \alpha_3 s + \alpha_4 = 0 \tag{8.3}$$

Let $\tilde{A} = A - BK$ and substituting it in equation (8.3)

$$\left|sI - \tilde{A}\right| = s^4 + \alpha_1 s^3 + \alpha_2 s^2 + \alpha_3 s + \alpha_4 = 0 \tag{8.4}$$

The Cayley-Hamilton theorem states that $\tilde{A}$ satisfies its characteristic equation as

$$\phi(\tilde{A}) = \tilde{A}^4 + \alpha_1 \tilde{A}^3 + \alpha_2 \tilde{A}^2 + \alpha_3 \tilde{A} + \alpha_4 I = 0 \tag{8.5}$$

The following matrix identities are used to derive Ackermann's Formula

$$I = I$$
$$\tilde{A} = A - BK$$
$$\tilde{A}^2 = (A - BK)^2 = A^2 - ABK - BK\tilde{A}$$
$$\tilde{A}^3 = (A - BK)^3 = A^3 - A^2 BK - ABK\tilde{A} - BK\tilde{A}^2 \tag{8.6}$$
$$\tilde{A}^4 = (A - BK)^4 = A^4 - A^3 BK - A^2 BK - ABK\tilde{A} - BK\tilde{A}^2 - BK\tilde{A}^3$$

Now substituting equation (8.6) in equation (8.5)

$$\phi(\tilde{A}) = A^4 - A^3 BK - A^2 BK - ABK\tilde{A} - BK\tilde{A}^2 - BK\tilde{A}^3 +$$
$$\alpha_1\left(A^3 - A^2 BK - ABK\tilde{A} - BK\tilde{A}^2\right) +$$
$$\alpha_2\left(A^2 - ABK - BK\tilde{A}\right) + \alpha_3\left(A - BK\right) + \alpha_4 I$$

$$= A^4 - A^3 BK - A^2 BK - ABK\tilde{A} - BK\tilde{A}^2 - BK\tilde{A}^3 +$$
$$\alpha_1 A^3 - \alpha_1 A^2 BK - \alpha_1 ABK\tilde{A} - \alpha_1 BK\tilde{A}^2$$
$$\alpha_2 A^2 - \alpha_2 ABK - \alpha_2 BK\tilde{A} + \alpha_3 A - \alpha_3 BK + \alpha_4 I \tag{8.7}$$

$$= A^4 + \alpha_1 A^3 + \alpha_2 A^2 + \alpha_3 A + \alpha_4 I$$
$$- A^3 BK - A^2 BK - ABK\tilde{A} - BK\tilde{A}^2$$
$$- BK\tilde{A}^3 - \alpha_1 A^2 BK - \alpha_1 ABK\tilde{A} - \alpha_1 BK\tilde{A}^2$$
$$- \alpha_2 ABK - \alpha_2 BK\tilde{A} - \alpha_3 BK$$

The minimal polynomial of the matrix A is defined in the equation below

$$\phi(A) = A^4 + \alpha_1 A^3 + \alpha_2 A^2 + \alpha_3 A + \alpha_4 I \tag{8.8}$$

After substituting equation (8.8) in equation (8.7) and rearranging its terms as

$$
\begin{aligned}
\phi(\tilde{A}) &= \phi(A) - A^3 BK - A^2 BK - ABK\tilde{A} - BK\tilde{A}^2 \\
&\quad - BK\tilde{A}^3 - \alpha_1 A^2 BK - \alpha_1 ABK\tilde{A} - \alpha_1 BK\tilde{A}^2 \\
&\quad - \alpha_2 ABK - \alpha_2 BK\tilde{A} - \alpha_3 BK
\end{aligned}
\tag{8.9}
$$

Since $\phi(\tilde{A}) = 0$, equation (8.9) can be written as

$$
\begin{aligned}
\phi(A) &= B\left(K\tilde{A}^3 + K\tilde{A}^2 + \alpha_1 K\tilde{A}^2 + \alpha_2 K\tilde{A} + \alpha_3 K\right) + \\
&\quad AB\left(\alpha_1 K\tilde{A} + \alpha_2 K + K\tilde{A}\right) + A^2 B\left(K + \alpha_1 K\right) + A^3 B\left(K\right)
\end{aligned}
\tag{8.10}
$$

Equation (8.10) can be rearranged as

$$\phi(A) = \begin{bmatrix} B & AB & A^2 B & A^3 B \end{bmatrix} \times \begin{bmatrix} K\tilde{A}^3 + K\tilde{A}^2 + \alpha_1 K\tilde{A}^2 + \alpha_2 K\tilde{A} + \alpha_3 K \\ \alpha_1 K\tilde{A} + \alpha_2 K + K\tilde{A} \\ K + \alpha_1 K \\ K \end{bmatrix} \tag{8.11}$$

Multiplying both sides of equation (8.11) by $\begin{bmatrix} B & AB & A^2 B & A^3 B \end{bmatrix}^{-1}$ yields

$$\begin{bmatrix} B & AB & A^2 B & A^3 B \end{bmatrix}^{-1} \phi(A) = \begin{bmatrix} K\tilde{A}^3 + K\tilde{A}^2 + \alpha_1 K\tilde{A}^2 + \alpha_2 K\tilde{A} + \alpha_3 K \\ \alpha_1 K\tilde{A} + \alpha_2 K + K\tilde{A} \\ K + \alpha_1 K \\ K \end{bmatrix} \tag{8.12}$$

After multiply both sides of equation (8.12) by $\begin{bmatrix} 0 & 0 & 0 & 1 \end{bmatrix}$, we obtain

$$[0\ 0\ 0\ 1]\begin{bmatrix} B & AB & A^2B & A^3B \end{bmatrix}^{-1}\phi(A)=[0\ 0\ 0\ 1]\begin{bmatrix} K\tilde{A}^3 + K\tilde{A}^2 + \alpha_1 K\tilde{A}^2 + \alpha_2 K\tilde{A} + \alpha_3 K \\ \alpha_1 K\tilde{A} + \alpha_2 K + K\tilde{A} \\ K + \alpha_1 K \\ K \end{bmatrix} \quad (8.13)$$

Equation (8.13) can be written as

$$K =[0\ 0\ 0\ 1]\begin{bmatrix} B & AB & A^2B & A^3B \end{bmatrix}^{-1}\phi(A) \quad (8.14)$$

where the matrix $K =[K_1\ K_2\ K_3\ K_4]$.

Equation (8.14) is Ackermann's Formula used to find the value of the gain K. The desired poles of the controller can be determined based on the damping ratio ζ and natural frequency ω_n. The damping ratio and the natural frequency are related to the maximum overshoot, M_p, and the settling time, t_s, with the following relations [51]

$$M_p = e^{-\dfrac{\pi\zeta}{\sqrt{1-\zeta^2}}} \quad \text{and } t_s = \dfrac{4}{\zeta\omega_n} \quad (8.15)$$

Equation (8.15) can be rearranged to obtain the values of the damping ratio ζ and the natural frequency ω_n

$$\zeta = \sqrt{\dfrac{\left(\dfrac{\ln\left(M_p\right)}{\pi}\right)^2}{1+\left(\dfrac{\ln\left(M_p\right)}{\pi}\right)^2}} \quad , \text{and } \omega_n = \dfrac{4}{\zeta t_s} \quad (8.16)$$

The dominant poles are calculated by

$$P_{1,2} = -\omega_n\zeta \pm j\omega_n\sqrt{1-\zeta^2} \quad (8.17)$$

and the remaining two poles are chosen as

$$P_{3,4} = 2P_{1,2} \quad (8.18)$$

By using the data given in section 6.5 for a diabetic patient with maximum overshoot at 10%, and settling time at 60 minutes, the damping ratio ζ and the natural frequency ω_n are calculated by using equation (8.16) as [54, 58]

$$\zeta = 0.5912, \text{ and } \omega_n = 0.1128.$$

The values of the desired poles can be calculated using equations (8.17) and (8.18)

$$P_1 = -(0.1128)(0.5912) + j(0.1128)\sqrt{1 - (0.5912)^2} = -0.0667 + j0.091$$

$$P_2 = -(0.1128)(0.5912) - j(0.1128)\sqrt{1 - (0.5912)^2} = -0.0667 - j0.091$$

$$P_3 = 2(-0.0667 + j0.091) = -0.1333 + j0.1819$$

$$P_4 = 2(-0.0667 - j0.091) = -0.1333 - j0.1819$$

Using Ackermann's Formula (8.14), the state feedback controllers can be designed based on the models at different operating points. The following are the models at t = *1, 20, 40, 60, 90, 120, 150* and *182* minutes, and the corresponding feedback controllers. Since *B* and *C* do not change with time, they are fixed in all cases as

$$B = \begin{bmatrix} 0 \\ 0 \\ 0 \\ 0 \\ 0.5 \end{bmatrix}, \text{ and } C = \begin{bmatrix} 1 & 0 & 0 & 0 \end{bmatrix}$$

The following are the matrix *A* and corresponding matrix *K* at certain operating points

t = 1 minute:

$$A_1 = \begin{bmatrix} 0 & -859.6667 & 0 & 0 \\ 0 & -0.0081 & 0.00000401 & 0 \\ 0.0024 & 0 & -0.23 & 1 \\ 0 & 0 & 0 & -0.5 \end{bmatrix}$$

$$K_1 = \begin{bmatrix} -0.4 & 4702.2 & 0.1 & -0.7 \end{bmatrix}$$

t = 20 minutes:

$$A_{20} = \begin{bmatrix} 0 & -131.33 & 0 & 0 \\ 0 & -0.0081 & 0.000004010 & 0 \\ 0.048 & 0 & -0.23 & 1 \\ 0 & 0 & 0 & -0.5 \end{bmatrix}$$

$$K_{20} = \begin{bmatrix} -2.5 & 4693.8 & 0.1 & -0.7 \end{bmatrix}$$

t = 40 minutes:

$$A_{40} = \begin{bmatrix} 0 & -112.17 & 0 & 0 \\ 0 & -0.0081 & 0.00000401 & 0 \\ 0.096 & 0 & -0.23 & 1 \\ 0 & 0 & 0 & -0.5 \end{bmatrix}$$

$$K_{40} = \begin{bmatrix} -2.9 & 4684.8 & 0.1 & -0.7 \end{bmatrix}$$

t = 60 minutes:

$$A_{60} = \begin{bmatrix} 0 & -105.78 & 0 & 0 \\ 0 & -0.0081 & 0.00000401 & 0 \\ 0.1440 & 0 & -0.23 & 1 \\ 0 & 0 & 0 & -0.5 \end{bmatrix}$$

$$K_{60} = \begin{bmatrix} -3.0 & 4675.9 & 0.1 & -0.7 \end{bmatrix}$$

t = 90 minutes:

$$A_{90} = \begin{bmatrix} 0 & -101.52 & 0 & 0 \\ 0 & -0.0081 & 0.00000401 & 0 \\ 0.2160 & 0 & -0.23 & 1 \\ 0 & 0 & 0 & -0.5 \end{bmatrix}$$

$$K_{90} = \begin{bmatrix} -3.1 & 4662.5 & 0.1 & -0.7 \end{bmatrix}$$

t = 120 minutes:

$$A_{120} = \begin{bmatrix} 0 & -99.39 & 0 & 0 \\ 0 & -0.0081 & 0.00000401 & 0 \\ 0.288 & 0 & -0.23 & 1 \\ 0 & 0 & 0 & -0.5 \end{bmatrix}$$

$$K_{120} = \begin{bmatrix} -3.2 & 4649.1 & 0.1 & -0.7 \end{bmatrix}$$

t = 150 minute:

$$A_{150} = \begin{bmatrix} 0 & -98.11 & 0 & 0 \\ 0 & -0.0081 & 0.00000401 & 0 \\ 0.36 & 0 & -0.23 & 1 \\ 0 & 0 & 0 & -0.5 \end{bmatrix}$$

$$K_{150} = \begin{bmatrix} -3.2 & 4635.7 & 0.1 & -0.7 \end{bmatrix}$$

t = 182 minute:

$$A_{182} = \begin{bmatrix} 0 & -97.21 & 0 & 0 \\ 0 & -0.0081 & 0.00000401 & 0 \\ 0.4368 & 0 & -0.23 & 1 \\ 0 & 0 & 0 & -0.5 \end{bmatrix}$$

$$K_{182} = \begin{bmatrix} -3.2 & 4621.4 & 0.1 & -0.7 \end{bmatrix}$$

As mentioned above, the response of the system to the initial condition should approach zero as the time *t* approaches infinity. After plotting the responses to initial condition at time *t = 1, 20, 40, 60, 90, 120, 150* and *182* minutes, it was noted that the graphs are very close to each other, and for that reason, only four graphs (randomly selected) are shown in Figure 8.1.
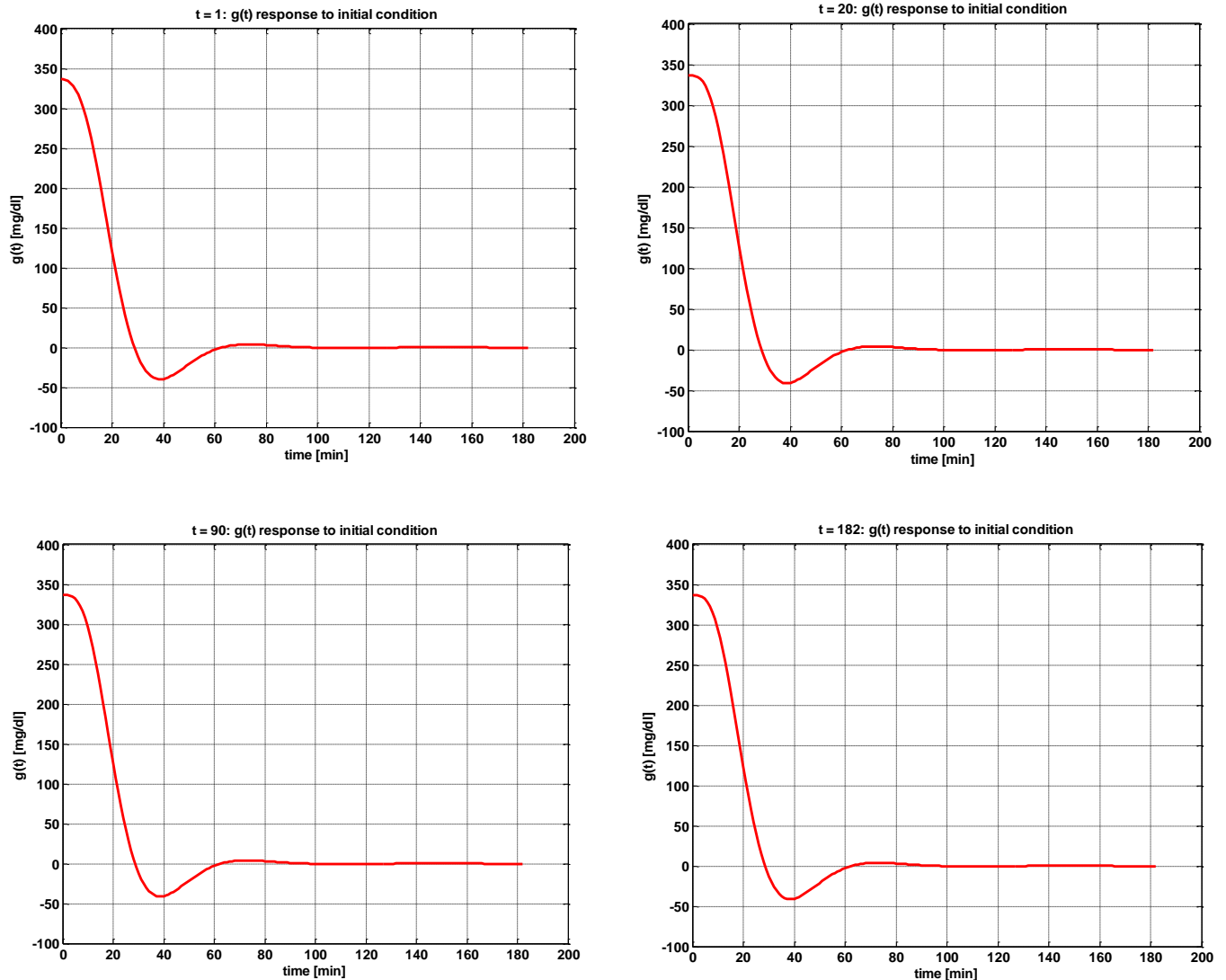
Figure 8.1 Response curves to initial conditions at operating points *t = 1, 20, 90 and 182 minutes*

8.4   Design of State Observer for Linear System:

When designing a state feedback controller by the pole placement method, it is assumed that all the state variables are available for feedback. In practice, the state variables may not be available for feedback. Then we need to estimate the unavailable state variables. The process of estimating the unmeasured state variables is commonly known as observation. The device that observes the estimation of the unmeasured state variables is called a state observer. The state

observer estimates the state variables based on the measurements of the output and control variables. The concept of observability is an important factor in the design of the state observer. The observability condition must be satisfied before a state observer can be designed [51]. The notation $\tilde{x}(t)$ is used to denote the observed state vector [59, 60]. The mathematical model of the observer is basically the same as the plant, except that we include the estimation error to compensate for inaccuracies in the initial state errors. The mathematical model of the observer is defined as

$$\dot{\tilde{x}} = A\tilde{x} + Bu + K_e\left(y - C\tilde{x}\right) \tag{8.19}$$

and the control signal to be

$$u = -K\tilde{x} \tag{8.20}$$

where $\tilde{x}$ is the estimated state, $C\tilde{x}$ is the estimated output and K_e is the observer gain matrix [51]. Substituting equation (8.20) into equation (8.19) gives

$$\dot{\tilde{x}} = \left(A - K_e C - BK\right)\tilde{x} + K_e y \tag{8.21}$$

The observed state variable $\tilde{x}(t)$ can be used to compute the feedback to the system. Figure 8.2 shows the block diagram of the observer-based state feedback control system.
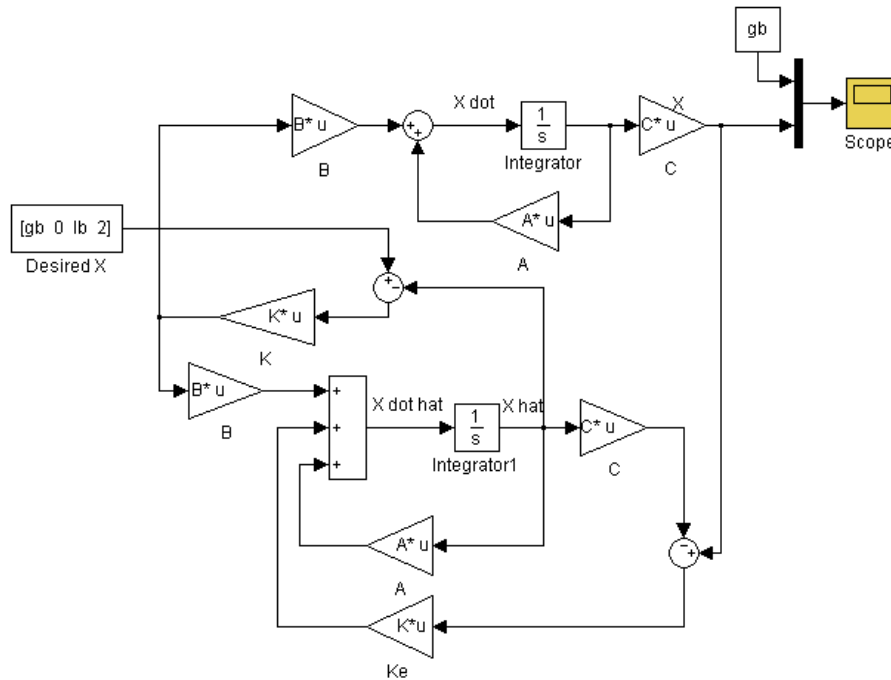
Figure 8.2 Observer-based state feedback control wiring diagram

The design process will be done in two phases. The first phase is to calculate the value of the feedback gain matrix K, and the second phase is to determine the observer gain matrix K_e. The value of the matrix K_e is calculated by Ackermann's Formula for observers as

$$K_e = \phi(A) \begin{bmatrix} C \\ CA \\ CA^2 \\ CA^3 \end{bmatrix}^{-1} \begin{bmatrix} 0 \\ 0 \\ 0 \\ 1 \end{bmatrix} \qquad (8.22)$$

where the matrix $K_e = \begin{bmatrix} K_{e1} & K_{e2} & K_{e3} & K_{e4} \end{bmatrix}^T$.

Now we need to choose the observer gain K_e. Since we want the dynamics of the observer to be much faster than the system itself, we need to place the poles at least five times farther to the left than the dominant poles of the system. The values of the desired poles of the observer are selected as

$$P_{o1} = -0.3333 + j0.4548$$

$$P_{o2} = -0.3333 - j0.4548$$

$$P_{o3} = -0.6667 + j0.9096$$

$$P_{o4} = -0.6667 - j0.9096$$

The values of matrices K and K_e at certain operating points are calculated by Ackermann's Formula. The values of matrix K were found in the previous section, and the values of matrix K_e are shown below

t = 1 minute:

$$K_{e1} = \begin{bmatrix} 1.2620 \\ -0.0017 \\ -22.4977 \\ -58.8582 \end{bmatrix}$$

t = 20 minutes:

$$K_{e20} = \begin{bmatrix} 1.2620 \\ -0.0109 \\ -147.2340 \\ -385.2770 \end{bmatrix}$$

t = 40 minutes:

$$K_{e40} = \begin{bmatrix} 1.2620 \\ -0.0128 \\ -172.3436 \\ -451.0869 \end{bmatrix}$$

t = 60 minutes:

$$K_{e60} = \begin{bmatrix} 1.2620 \\ -0.0135 \\ -182.7124 \\ -478.3364 \end{bmatrix}$$

t = 90 minutes:

$$K_{e90} = \begin{bmatrix} 1.2620 \\ -0.0141 \\ -190.3134 \\ -498.4084 \end{bmatrix}$$

t = 120 minutes:

$$K_{e120} = \begin{bmatrix} 1.2620 \\ -0.0144 \\ -194.3246 \\ -509.0897 \end{bmatrix}$$

t = 150 minutes:

$$K_{e150} = \begin{bmatrix} 1.2620 \\ -0.0146 \\ -196.7916 \\ -515.7316 \end{bmatrix}$$

t = 182 minutes:

$$K_{e182} = \begin{bmatrix} 1.2620 \\ -0.0147 \\ -198.5401 \\ -520.5064 \end{bmatrix}$$

8.5   Individual Observer-Based State Feedback Controllers:

Non-adaptive observer-based state feedback controllers use a fixed controller for the entire control period and rely on its robustness to maintain control performance. For each individual observer-based state feedback controller with its gain matrices K and K_e found in the previous sections at operating points $t = 1, 20, 40, 60, 90, 120, 150$ and 182 minutes, the simulation was performed, and the glucose level for each patient was plotted. Based on the simulation results, it can be seen that under the individual observer-based state feedback controllers, the glucose level $g(t)$ reaches the basal level within 60 minutes and stays at that level. By carefully analyzing the plots of the output, it is clear that the optimal graph is when the observer-based state feedback controller at operating point $t = 20$ minutes is used. It was noted that the graphs are very close to each other, and for that reason, only four graphs (randomly selected) are shown in Figure 8.3.
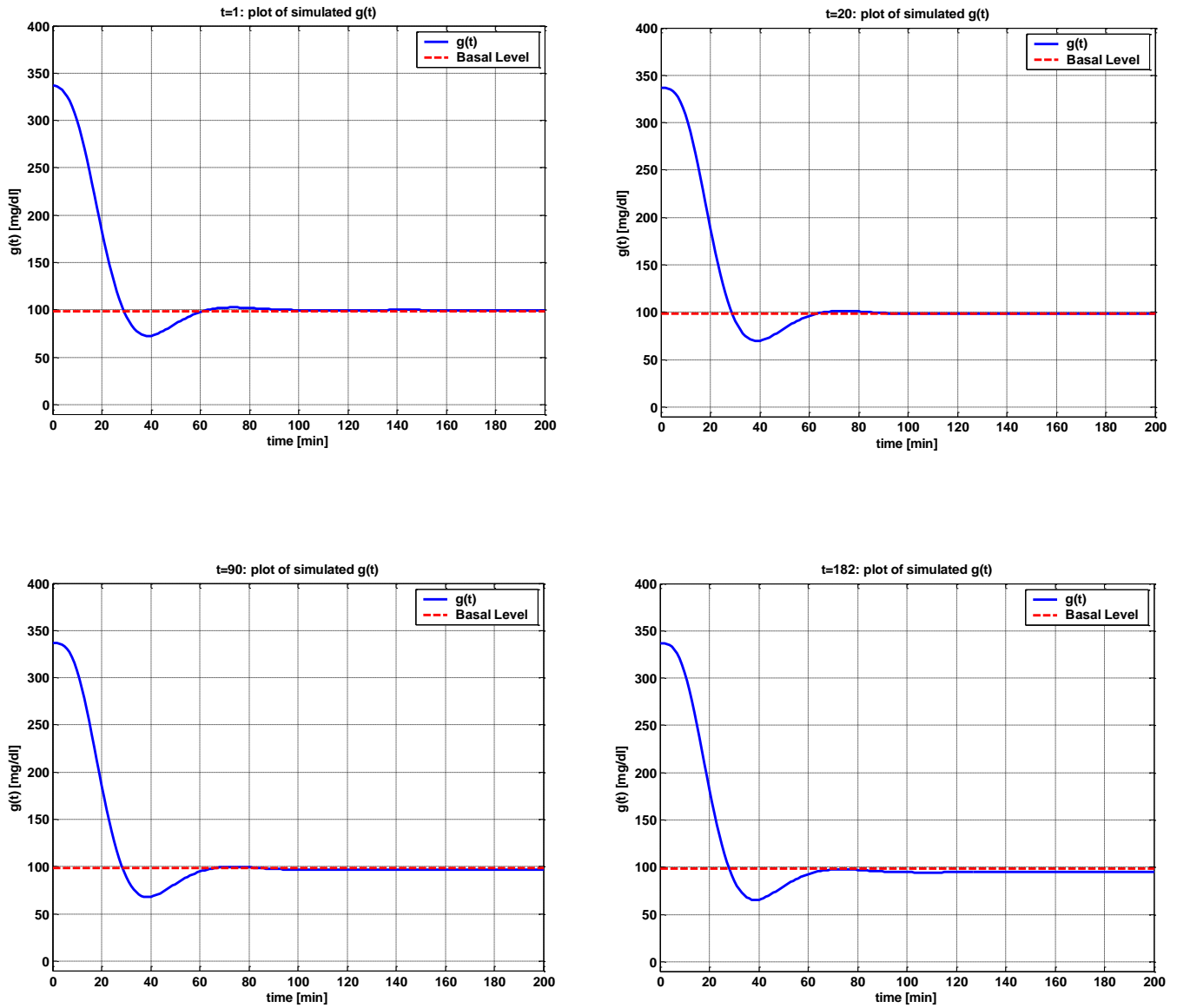
Figure 8.3 Observer-based state feedback controller output, glucose level *g(t)*
at operating points *t = 1, 20, 90 and 182 minutes*

8.6   Observer-Based State Feedback Controller for Nonlinear System:

The design for the linear system that was calculated in sections 8.4 and 8.5 is applied to

the nonlinear system at operating point *t = 20* minutes. The simulation diagram of the nonlinear

system that defines the dynamics of the diabetic patient with the observer-based state feedback is

shown in Figure 8.4. The box labeled "subsystem (patient) 1" contains the nonlinear system of the diabetic patient. The simulation is performed, and the glucose level $g(t)$ is plotted and shown in Figure 8.5. It is clear that the glucose level for the nonlinear system has the same high performance as that of the linear system.

Figure 8.4 Observer-based state feedback control wiring diagram for nonlinear system

Figure 8.5 Observer-based state feedback control output, glucose level *g(t)*,
for nonlinear system at operating point *t =20 minutes*

8.7   Test and Verification:

For verification, the same control strategy that was stated in the previous sections is
evaluated on two diabetic patients. The parameters values are shown in Table 8.1[27-29].

Parameters	Diabetic Patient #2	Diabetic Patient #3
P_1	0	0
P_2	0.0038	0.0042
P_3	3.61×10^{-6}	2.56×10^{-6}
i_0	73	209
g_0	329	297
γ	1.69×10^{-3}	3.72×10^{-3}
h	119	154
n	0.13	0.22
g_b	93	100
i_b	11	8

Table 8.1 Diabetic patients #2 and #3 parameters values

The simulation results of the two diabetic patients without the control system are shown in Figures 8.6 and 8.7 respectively.
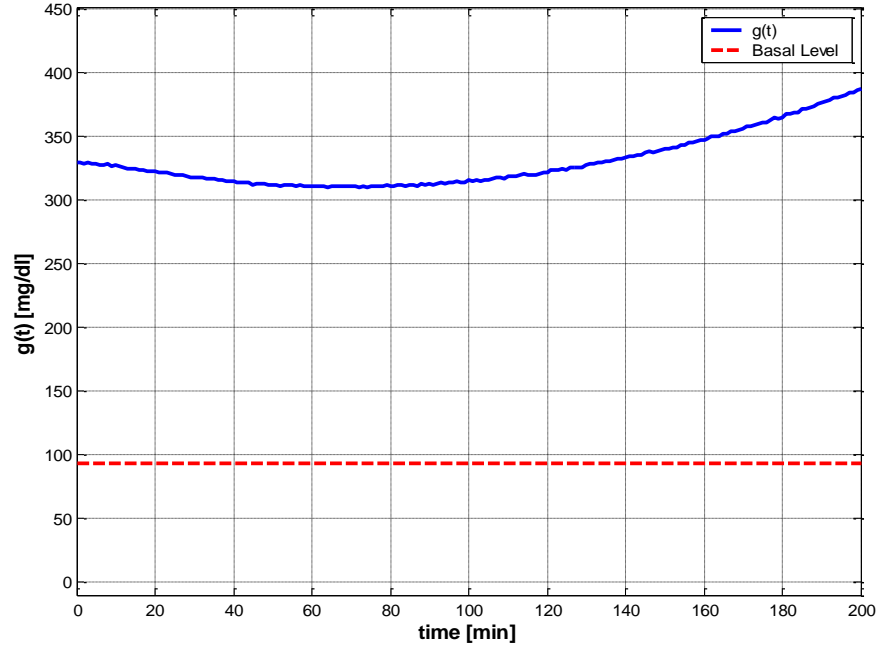
Figure 8.6 Output of the simulated system for diabetic patient #2
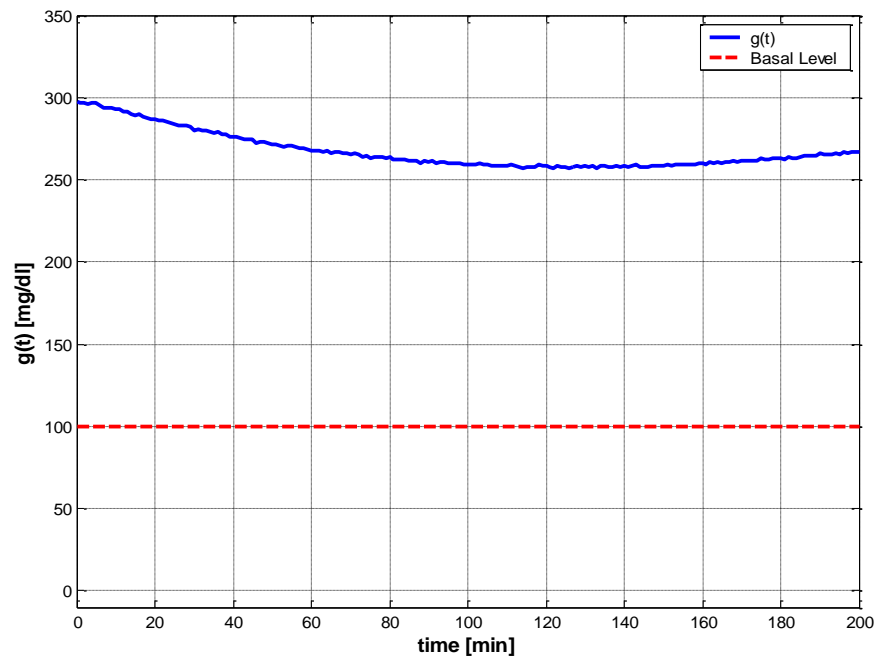
Figure 8.7 Output of the simulated system for diabetic patient #3

After injecting an amount of glucose in the two patient, the graphs of the figures 8.6 and 8.7 show that the glucose levels of diabetic patients #2 and #3 go down for a short period of time and then start going up. The glucose levels suppose to come down to the basal level within two to three hours, but that did not happen. Thus the two persons are classified as diabetic patients. The control designs that were developed in the previous sections are applied here. The values of matrices K and K_e for diabetic patients #2 and #3 at certain operating points are calculated by Ackermann's Formula. The values are shown in Tables 8.2, and 8.3.

Gain, K	Diabetic Patient #2	Diabetic Patient #3
K_1	[−0.37 5450 0.12 − 0.46]	[−0.81 7655 0.11 − 0.64]
K_{20}	[−2.22 5442 0.12 − 0.46]	[−2.84 7633 0.11 − 0.64]
K_{40}	[−2.55 5443 0.12 − 0.46]	[−3.02 7611 0.11 − 0.64]
K_{60}	[−2.66 5426 0.12 − 0.46]	[−3.07 7588 0.11 − 0.64]
K_{90}	[−2.73 5414 0.12 − 0.46]	[−3.08 7554 0.11 − 0.64]
K_{120}	[−2.75 5402 0.12 − 0.46]	[−3.07 7519 0.11 − 0.64]
K_{150}	[−2.75 5390 0.12 − 0.46]	[−3.04 7484 0.11 − 0.64]
K_{182}	[−2.75 5377 0.12 − 0.46]	[−3.01 7448 0.11 − 0.64]

Table 8.2 Controller gain matrix *K* at different operating points

Gain, K_e	Patient #2	Patient #3
K_{e1}	$\begin{bmatrix} 1.3663 \\ -0.0016 \\ -59.4194 \\ -58.2341 \end{bmatrix}$	$\begin{bmatrix} 1.2759 \\ -0.0023 \\ -55.8586 \\ -126.3840 \end{bmatrix}$
K_{e20}	$\begin{bmatrix} 1.3663 \\ -0.0096 \\ -355.5025 \\ -348.4343 \end{bmatrix}$	$\begin{bmatrix} 1.2759 \\ -0.0081 \\ -197.1173 \\ -446.1300 \end{bmatrix}$
K_{e40}	$\begin{bmatrix} 1.3663 \\ -0.0111 \\ -409.1316 \\ -401.0253 \end{bmatrix}$	$\begin{bmatrix} 1.2759 \\ -0.0087 \\ -211.1101 \\ -477.9540 \end{bmatrix}$
K_{e60}	$\begin{bmatrix} 1.3663 \\ -0.0117 \\ -430.7749 \\ -422.2694 \end{bmatrix}$	$\begin{bmatrix} 1.2759 \\ -0.0089 \\ -216.1793 \\ -489.5925 \end{bmatrix}$
K_{e90}	$\begin{bmatrix} 1.3663 \\ -0.0121 \\ -446.4994 \\ -437.7294 \end{bmatrix}$	$\begin{bmatrix} 1.2759 \\ -0.0090 \\ -219.6407 \\ -497.6747 \end{bmatrix}$
K_{e120}	$\begin{bmatrix} 1.3663 \\ -0.0123 \\ -454.7757 \\ -445.8901 \end{bmatrix}$	$\begin{bmatrix} 1.2759 \\ -0.0091 \\ -221.3588 \\ -501.8151 \end{bmatrix}$
K_{e150}	$\begin{bmatrix} 1.3663 \\ -0.0124 \\ -459.9226 \\ -450.9343 \end{bmatrix}$	$\begin{bmatrix} 1.2759 \\ -0.0092 \\ -222.3589 \\ -504.3313 \end{bmatrix}$
K_{e182}	$\begin{bmatrix} 1.3663 \\ -0.0125 \\ -463.5094 \\ -454.5520 \end{bmatrix}$	$\begin{bmatrix} 1.2759 \\ -0.0092 \\ -223.0300 \\ -506.1187 \end{bmatrix}$

Table 8.3 Observer gain matrix K_e at different operating points

As in the previous sections, for each individual observer-based state feedback controller with its gain matrices K and K_e at $t = 1, 20, 40, 60, 90, 120, 150$ and 182 min, the simulation was

performed on the nonlinear systems that describe the dynamics of both diabetic patients #2 and
#3. The graphs of the glucose levels are shown in Figures 8.8 and 8.9 respectively.
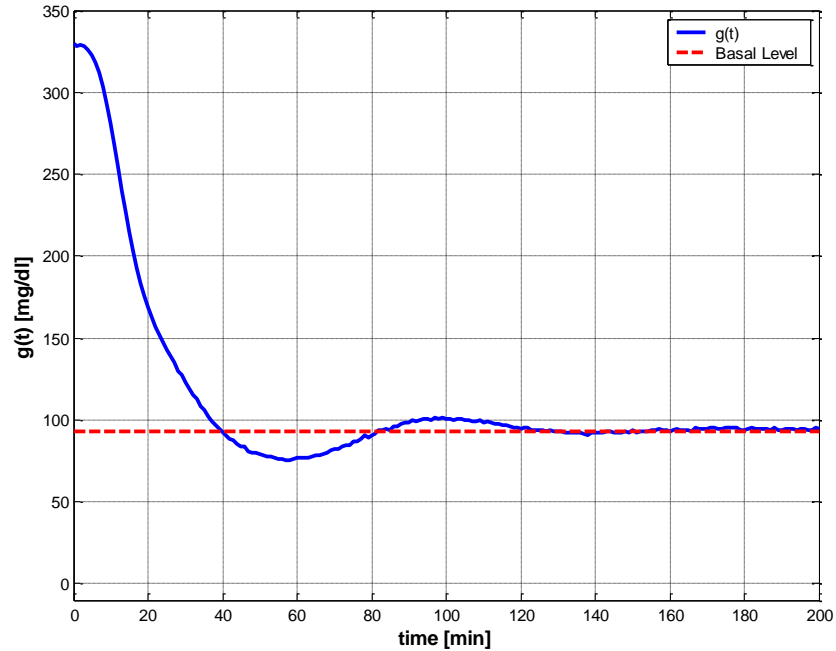
Figure 8.8 Observer-based state feedback control for nonlinear system patient #2
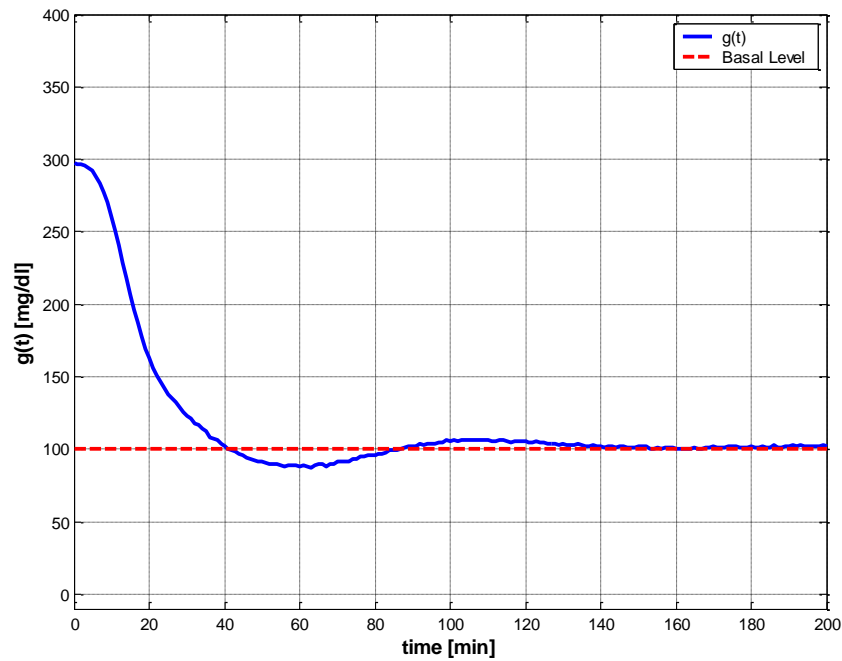
Figure 8.9 Observer-based state feedback control for nonlinear system patient #3

8.8   Control Design Investigation and Analysis:

The control design that was applied to the nonlinear system at maximum overshoot rate of 10% is repeated here but at various rates. The following maximum overshoot rates of 1%, 2%, 3%, 5%, and 8% are analyzed and investigated. The poles of the controllers and observers at operating points $t = 1, 20, 40, 60, 90, 120, 150$ and 182 minutes were calculated for each maximum overshoot, and the glucose levels were plotted. The graphs show that the best result is when using the observer-based state feedback controller at operating point $t = 20$ minutes, which was the same result that was concluded in section 8.5. The graphs of the glucose levels, $g(t)$, and the steady state zone at operating point $t = 20$ minutes at various maximum overshoot values are shown in Figure 8.10. The steady state zone is defined to be within 5% of the basal level, (94 mg/dl to 104 mg/dl). The graphs were compared to each other to determine the time it takes the glucose level $g(t)$ to enter the steady state zone, and the results are listed in Table 8.4.

Percentage Maximum Overshoot	Time to enter steady state zone (min)	Time to reach steady state (min)
1	95	110
2	82	100
3	75	80
5	61	72
8	49	55
10	44	47

Table 8.4 Steady state zone settling times
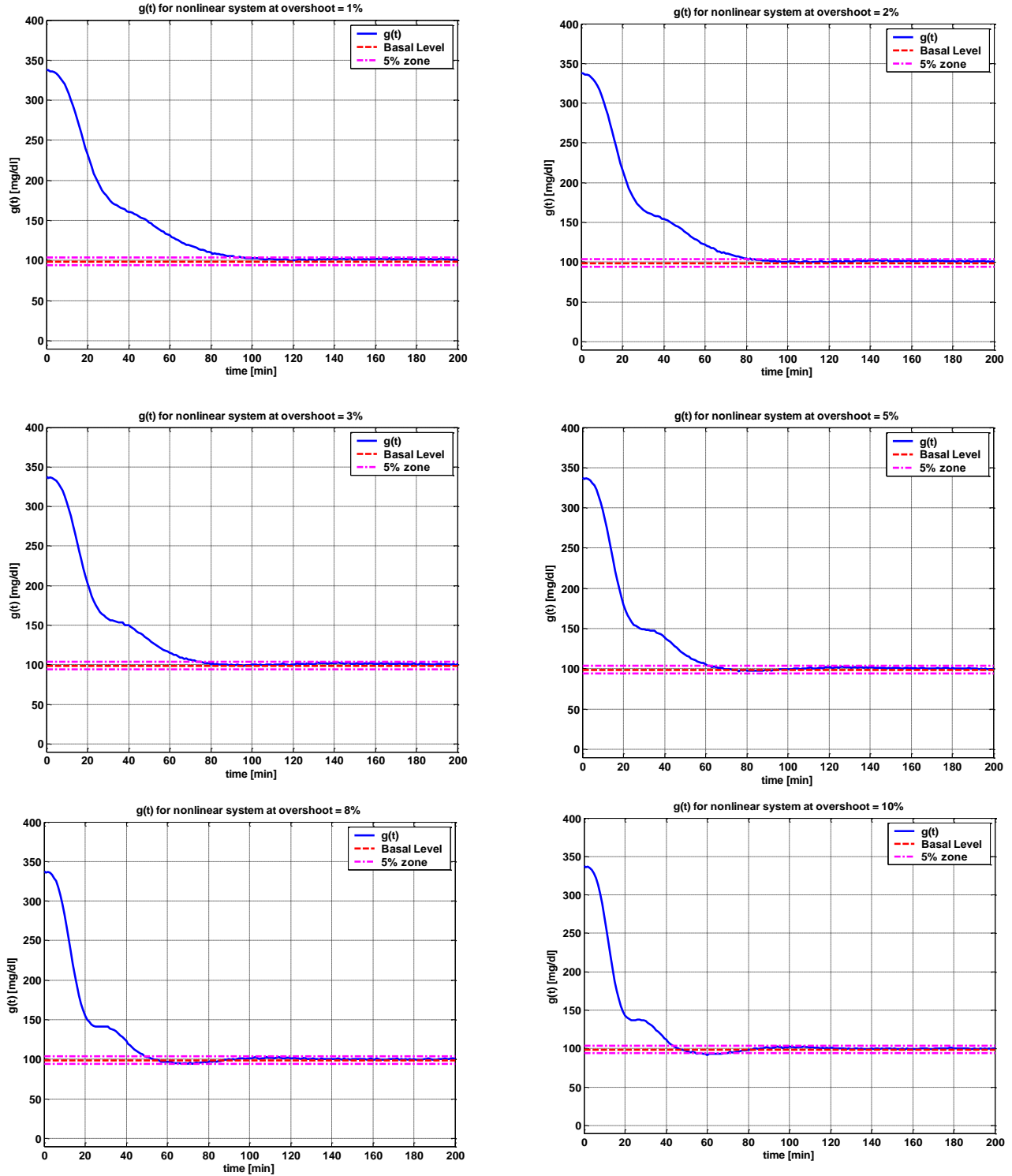
Figure 8.10 Observer-based state feedback control output, glucose level *g(t)*, for nonlinear system at operating point *t* =20 minutes for various maximum overshoots

By comparing the result of Table 8.4 and the graphs of Figure 8.10, it is obvious to conclude when the maximum overshoot is small, the settling time (the time it takes the glucose level to enter the steady state zone and stay inside that zone) is long. But when the maximum overshoot is large, the settling time is short.

CHAPTER 9

CONCLUSION

A detailed research has been conducted on type "I" diabetic patient to control the glucose levels and bring it down to the patient basal level. Specific solutions and design have been developed to improve performance on insulin control for type "I" diabetic patient. The following gives an executive summary of the contributions and results of this research

➢ In this research, one differential equation that represents a first order infusion pump was added to the set of the differential equations of the minimal model. The role of the pump is to inject the required amount of insulin to help the glucose level to come down to basal level within 2-3 hours after meal.

➢ The Nonlinear Least Squares Method with Levenberg-Marquardt Algorithm was used to estimate the unknown parameters of the differential equations that describe the dynamic of diabetic patient.

➢ The simulation diagram of the proposed mathematical model with the estimated parameters was constructed. The output (glucose) of the simulation diagram was monitored and recorded. The error between the simulated data and the experimental data was calculated to be very small.

➢ Typical PID controllers were not sufficient to meet the design specification of the glucose level control problems. This is mainly due to the nonlinear nature of patient dynamic models and limited robustness of the PID controllers. An adaptive control that switches controllers based on operating conditions was developed to potentially enhance the

control performance. The regime-switching control scheme was carefully designed to ensure that the control specifications were met and the number of PID controller was reduced to four controllers without jeopardizing the enhanced performance of the system.

➢ A simplified control scheme using one observer-based state feedback controller was presented. The control scheme was able to enhance the performance of the system and meet the design specifications.

➢ A comparison between the regime-switching control scheme using PID controllers and the individual observer-based state feedback controller scheme was investigated. However, the observer-based state feedback control scheme eliminated the switching strategy that was required in the PID design, and the adaptive control components such as the "switching case", the "if action case system", the "8-intput-1-output merge" block, and the eight manual cut-off switches were no longer needed. The observer-based state feedback control scheme reduced the complexity of the control circuit and reduced the cost to build up the circuit.

➢ The control design was investigated by comparing the results of the control scheme at various maximum overshoot rates. It was noted that when maximum overshoot was small, the settling time was longer. But when the maximum overshoot was large, the settling time was short.

REFERENCES

[1]   Karam, J. H., Grodsky, G.M., and Forsham, P.H., "Excessive insulin response to glucose in obese subjects as measured by immunochemical assay", Diabetes, 1963, vol. 12, pp. 196-204.

[2]   Ginsberg, H., Olefsky, J.M., and Reaven, G.M., "Further evidence that insulin resistance exists in patients with chemical diabetes", Diabetes, 1974, vol. 23, pp. 674-678.

[3]   Reaven, G. M., and Olefsky, J.M., "Relationship between heterogeneity of insulin responses and insulin resistance in normal subjects and patients with chemical diabetes", Diabetologia, 1977, vol. 13, pp. 201-206.

[4]   Lerner, R. L., and Porte, D. Jr., "Acute and steady state insulin responses to glucose in nonobese, diabetic subjects", J. Clin. Invest., 1972, vol. 51, pp. 1624-1631.

[5]   Reaven, G. M., "Insulin-independent diabetes mellitus: metabolic characteristics', Metab. Clin. Exp., 1980, vol. 29, pp. 445-454.

[6]   Bergman, R. N., and Cobelli, C., "Minimal modeling, partition analysis, and the estimation of insulin sensitivity", Fed. Proc., 1980, vol. 39, pp. 110-115.

[7]   Shen, S.W., Reaven, G.M., and Farquhar, J.W., "Comparison of impedance to insulin-mediated glucose uptake in normal and diabetic subjects", J. Clin. Invest., 1970, vol. 49, pp. 2151-2160.

[8]   Dua, P., Doyle III F.J., and Pistikopoulos E.N., "Model-based Blood Glucose Control for Type 'I' Diabetes via Parametric Programming", IEEE Trans. Biomed. Eng., 2006, vol. 53, issue , 8, pp. 1478-1491.

[9]   Hernjak N., and Doyle III F.J., "Glucose Control Design using Nonlinearity Assessment Techniques". AIChE J., 2005, vol. 51, pp.544–554.

[10]   Radomski, D., Lawrynczuk, M., Marusak, P., and Tatjewski, P., "Modeling of Glucose Concentration Dynamics for Predictive Control of Insulin Administration" Biocybernetics and Biomedical Engineering, 2010, vol. 30, number 1, pp. 41–53.

[11]   Hovorka R., Canonico V., Chassin L.J., Haueter U., Massi-Benedetti M., Orsini M. Federici M.O., Pieber T.R., Schaller H.C., Schaupp L., Vering T., and Wilinska M.E., "Nonlinear Model Predictive Control of Glucose Concentration in Subjects With Type 'I' Diabetes". Physiol. Meas., 2004, vol. 25, pp. 905–920.

[12]   Liu, E., and Yuanet, J.M., "DynamicSensitivity and Control Analyses of Metabolic Insulin Signalling Pathways" IET Systems Biology, 2010, vol. 4, issue 1, pp. 64-81.

[13]   Salsai,A., and Muriel, N. F. "A review Types 1 and 2 diabetes mellitus and their treatement with insulin", American Journal of Therapeutics, 2006, vol. 13, issue 4, pp.349-361.

[14]   Dunning, T., "Diabetic ketoacidosis – prevention, management and the benefits of kenote testing", Emdorcrinology and Diabetes Nursing Reaserch, 2006.

[15]   Eledrisi, M.S., Alshanti, M.S. Shah, M.F. Brolosy, B., and Jaha, N., "Overview of the diagnosis and management of ketoacidosis" The American Journal of Medical Sciences, 2006, vol. 331, issue 5, pp. 243-251.

[16]   "Diabetes Complication", Medline Pluse, National Institue of Health (NIH), http://www.nlm.nih.gov, Aug 2011

[17]   "Living with Diabetes", http://www.diabetes.org, Sep 2011.

[18]   "Diabetes Statistics", National Diabetes Fact Sheet, American Diabetes Association, Jan. 2011.

[19]   "Type 1 Diabetes", health conditions, htpp://usnews.com, Sep 2006.

[20]   National Diabetes Information Clearinghouse (NDIC), National Institute of Health, NIH Publication No. 11-3892, 2011.

[21]   Fabietti P.G., Canonico V., Federici M.O., Benedetti M.M., and Sarti, E., "Control Oriented Model of Insulin and Glucose Dynamics in Type 'I' Diabetics", Med. Biol. Eng. Comput., 2006, vol. 44, pp. 69–78.

[22]   Insel, P.A., Liljenquist, J.E., Tobin, J.D., Sherwin, R.S., Watkins, P., Andres, R., and Berman, M., "Insulin control of glucose metabolism in man", J. Clin. Invest., 1975, vol. 55, pp. 1057-1066.

[23]   Grodsky, G.M., "A threshold distribution hypothesis for packet storage of insulin and its mathematical modeling", J. Clin. Invest., 1972, vol. 51, pp. 2047-2059.

[24]   Sherwin, R.S., Kramer, K.J., Tobin, J.D. Insel, P.A., Liljenquist, J.E., Berman, M., and Andres, R., "A model of the kinetics of insulin in man", J. Clin. Invest., 1974, vol. 53, pp. 1481-1492.

[25]   Turner, R. C., Holman, R.R., Mathews, D., Hockaday, T.D.R., and Peto, J., "Insulin deficiency and insulin resistance interaction in diabetes: estimation of their relative contribution by feedback analysis from basal insulin and glucose concentrations", Metab. Clin. Exp., 1979, vol 28, pp. 1086-1096.

[26]   Lerner, R. L., and Porte, Jr, D., "Relationships between intravenous glucose loads, insulin responses and glucose disappearance rate", J. Clin. Endocrinol. Metab., 1971, vol 33, pp. 409–417.

[27]   Bergman, R.N, Ider, Y.Z., Bowden, C.R., and Cobelli, C., "Quantitative estimation of insulin sensitivity", Am. J. Physiol., 1979, vol. 236, pp. E667-E677.

[28]   Pacini, G., and Bergman, R.N., "MINMOD, A computer program to calculate insulin and

pancreatic responsivity from the frequently sampled intravenous glucose tolerance test",
Comput. Methods Programs Biomed., 1986, vol. 23, pp. 113-122.

[29] Bergman, R.N., Phillips, L.S., and Cobelli, C., "Physiologic Evaluation of factors controlling glucose tolerance in man, Measurement of insulin sensitivity and β–cell glucose sensitivity from the response to intravenous glucose", J. Clin. Invest., 1981, vol. 68, pp. 1456-1467.

[30] Bergman, R. N., and Urquhart, J., "The pilot gland approach to the study of insulin secretory dynamics", Recent Prog. Horm. Res., 1971, vol. 27, pp. 583-605.

[31] Nomura, M., Shichiri, M., Kawamori, R., Yamasaki, Y., Iwama, N., and Abe. H., "A mathematical insulin-secretion model and its validation in isolated rat pancreatic islets perifusion", Comput. Biomed. Res., 1984, vol. 17, pp. 570-579.

[32] Buchanan, T.A., Metzger, B. E., Freinkel, N., and Bergman, R. N., "Insulin sensitivity and B-cell responsiveness to glucose during late pregnancy in lean and moderately obese women with normal glucose tolerance or mild gestational diabetes", Am. J. Obstet. Gynecol., 1990, vol. 162, issue 4, pp. 1008-1014.

[33] Bolie, V.W., "Coefficients of normal blood glucose regulation", J. Appl. Physiol., 1961, vol. 16, pp. 783-788.

[34] Guyton, A.C., and Hall, J.E., Text book of Medical Physiology, 9th ed., Saunders, 1996.

[35] "Diabetic Conversion Factors", at http://www.diabetesexplained.com., 2006.

[36] Lynch, S.M., and Bequette, B.W., "Estimation-based Model Predictive Control of Blood Glucose in Type 'I' Diabetics: A Simulation Study", IEEE. Bio. Eng. Conf., 2001, pp. 79–80.

[37] Fisher, M. E., "A semi-closed loop algorithm for the control of blood glucose levels in

diabetes", IEEE. Trans Biomed. eng. 1991, pp. 57 – 61.

[38] Furler, S. M., Kraegen, E. W., Smallwood, R. H., and Chisholm, D. J., "Blood glucose control by intermittent loop closure in the basal mode: computer simulation studies with a diabetic model", Diabetes care, 1985, vol 8, pp. 553 – 561.

[39] Ibbini, M.S., Masadeh, M.A., and Amer, M.M.B., "A semiclosed-loop optimal control system for blood glucose level in diabetics" Journal of Medical Engineering & Technology, 2004, vol. 28, number 5, pp. 189–196.

[40] Gaetano, A.D., and Arino, O., "Mathematical modeling of the intravenous glucose tolerance test", Journal of Mathematical Biology, 2000, vol. 40, pp. 136-168.

[41] Marquardt, D. W., 1963, "An algorithm for least-squares estimation of non-linear parameters", J. Soc. Industrial Appl. Math., 1963, vol. 11. Pp. 431-441.

[42] Goodwin, C., and Payne, R.L., 1977, "Dynamic System Identification", Academic Press, Inc., New York.

[43] Lourakis, M.I.A., 2005, "A brief description of the Levenberg-Marquardt Algorithm Implemented by Levmar", Institute of Computer Science, Foundation for Research and Technology.

[44] DeGroot, M. H., and Schervish, M. J.W., 2002, "Probability and statistics", 3rd edition, Boston, MA: Addison-Wesley.

[45] Kuo, B.C., and Golnaraghi, F., 2002, "Automatic Control System" 8th edition, USA, Wiley & Sons.

[46] Hariri, A. M., and Wang, L. Y., "Identification and Low-Complexity Regime-Switching Insulin Control of Type 'I' Diabetic Patients" J. Biomedical Science and Engineering, 2011, vol. 4, number 4, pp. 297-314.

[47]   Ogata, K., 1994, "Discrete –Time Control Systems", 2nd edition, USA, Prentice Hall.

[48]   Dorf, R.C, and Bishop, R.H., 2010, "Modern Control Systems", 12th edition, USA, Prentice Hall.

[49]   Yu, Z., Tomizuka, M., Isaka, S., "Fuzzy Gain Scheduling of PID Controller", IEEE Trans. On Sys., Man, and Cyber., 1993, vol. 23, number 5, pp.1392-1398.

[50]   Franklin, G.F., Powell, J.D, and Emami-Naeini, A., 2010, "Feedback Control of Dynamic Systems", 6th edition, USA, Pearson.

[51]   Ogata, K., 2002. "Modern Control Engineering". 4th edition, USA, Prentice Hall.

[52]   Bequette, B.W., 2003, " Process Control, Modeling, Design, and Simulation", USA, Prentice Hall.

[53]   Golnaraghi, M.F., and Kuo. B.C., 2009, "Automatic Control System", USA, Wiley and Sons.

[54]   Hariri, A.M., and Wang, L.Y., " Design of State Feedback Controller and Observer for Type 'I' Diabetic Patients". Proceeding of the IASTED International Confrence on Modeling, Simulation and Identification Conference, Pittsburgh, Pennsylvania, Novemebr 2011.

[55]   Yue, D., Han, Q.L., and Peng, C., "State Feedback Controller Design of Networked Control Systems", IEE Trans. Circuits and Systems, 2004, vol. 51, issue 11, pp. 640-644.

[56]   Williams, R.L., and Lawrence, D.A, 2007, "Linear state-space control systems" New Jursey, Wiley and Sons.

[57]   Wang, J., Dong, L., and Bai, Y., "Switched State Feedback Controller for Networked Control System with Disturbance" Second International Conference on Intelligent Computation Technology and Automation, vol. 4, pp. 101-104, 2009.

[58]   Hariri, A.M. and Wang, L.Y., "Observer-Based State Feedback for Enhanced Insulin Control of Type "I" Diabetes", The Open Biomedical Engineering Journal, Dec 2011, vol. 5, pp. 98-109.

[59]   Ling, K.V., and Lim, K.W., "State Observer Design Using Deterministic Least Squares Technique", Proceedings of the 35th IEEE Conference on Decision and Control, Kobe, Japan, 1996, vol. 4, pp. 4077-4082.

[60]   Ma, Y., Zhong, X., and Zhang, Q., "Design of State Observer for a Class of Nonlinear Descriptor Large-Scale Composite Systems" International Journal of Innovative Computing, Information and Control, 2008, vol. 4, number 8, pp. 1349-4198.

ABSTRACT

IDENTIFICATION, STATE ESTIMATION, AND ADAPTIVE CONTROL OF TYPE 'I' DIABETIC PATIENTS

by

ALI MOHAMAD HARIRI

May 2012

Advisor: Dr. Le Yi Wang

Major: Electrical Engineering

Degree: Doctor of Philosophy

During the past few decades, biomedical modeling techniques have been applied to improve performance of a wide variety of medical systems that require monitoring and control. Diabetes is one of the most important medical problems. Most of the existing techniques assume the system to be time-invariant, and the original minimal model was modified by deleting some important parameters. In this research, the original minimal model that consists of three differential equations is used. A new differential equation represents a first order infusion pump is added to the set of the differential equations of the minimal model. The Nonlinear Least Squares Method with Levenberg-Marquardt Algorithm is used to estimate the unknown parameters of the differential equations. A new regime-switching control scheme using Proportional-Integral-Derivative (PID) controllers is designed to ensure that the control specifications are met. By comparing different switching schemes, we show that switched PID controllers can improve performance, but frequent switching of controllers is unnecessary. These findings lead to a control strategy that utilizes only a small number of PID controllers in this scheduled adaptation strategy. The regime-switching scheme proves that adaptive control can

potentially improve system performance. But it increases control complexity and may create further stability issues. This research investigates patient models and presents a simplified control scheme using observer-based state feedback controller that is able to enhance the performance of the system and meet the design specifications. By comparing different control schemes, it shows that a properly designed observer-based state feedback controller can eliminate the adaptation strategy that PID regime-switching control scheme needs to improve the control performance. Also, the observer-based state feedback control scheme reduces the complexity of the control circuit by eliminating the adaptive control switching components and reduces the cost to build up the circuits.

AUTOBIOGRAPHICAL STATEMENT

ALI MOHAMAD HARIRI

ACADEMIC BACKGROUND:
2000-2012:   PhD in Electrical Engineering, Wayne State University, Detroit, Michigan, USA
1997-1998:   MS in Electrical Engineering, Wayne State University, Detroit, Michigan, USA
1983-1987:   BS in Electrical Engineering, Wichita State University, Wichita, Kansas, USA

PROFESSIONAL EXPERIENCE:
2000 – Present: Supervisor Engineer, Substation Design, DTE Energy, Detroit, Michigan, USA
1996 – 2000:   Electrical Design Engineer, Ghafari Associates Inc, Dearborn, Michigan, USA
1993 – 1996   Electrical Engineer, H.A.S. & Associates Eng., Mississauga, Ontario, Canada
1989 – 1993   Distribution Engineer, Westlake Engineering, Mississauga, Ontario, Canada

PUBLICATIONS:
[1]   Hariri, A. M., and Wang, L. Y., "Identification and Low-Complexity Regime-Switching Insulin Control of Type 'I' Diabetic Patients" J. Biomedical Science and Engineering, 2011, vol. 4, number 4, pp.297-314.
[2]   Hariri, A.M., and Wang, L.Y., " Design of State Feedback Controller and Observer for Type 'I' Diabetic Patients". Proceeding of the IASTED International Confrence on Modeling, Simulation & Identification Conference, Pittsburgh, Pennsylvania, Nov. 2011.
[3]   Hariri, A.M. and Wang, L.Y., "Observer-Based State Feedback for Enhanced Insulin Control of Type "I" Diabetes", The Open Biomedical Engineering Journal, Dec. 2011, vol. 5, pp. 98-109.

PRESENTATIONS:
[1]   Hariri, A.M., and Wang, L.Y., " Design of State Feedback Controller and Observer for Type 'I' Diabetic Patients". Presentation at IASTED International Confrence on Modeling, Simulation & Identification Conference, Pittsburgh, Pennsylvania, Nov. 2011.

PROFESSIONAL SERVICES:
[1]   Hariri A.M. Chaired the Modelling in Biomedicine and Biomechanics session at the IASTED International Confrence on Modeling, Simulation and Identification Conference, Pittsburgh, Pennsylvania, Nov. 2011.

AWARDS:
[1]   Andrzej Olbrot Travel Award for Excellence in Graduate Student Research, College of Engineering, Wayne State University, year 2011-2012

PROFESSIONAL MEMBERSHIPS:
[1]   Member of the Order of Engineers and Architects of Beirut, Lebanon since 2000
[2]   Member of the Institute of Electrical and Electronics Engineers (IEEE) since year 2002